The Influence of Seasonal Light on the Circadian System

By

Michael C. Tackenberg

Dissertation
Submitted to the Faculty of the

Graduate School of Vanderbilt University

in partial fulfillment of the requirements

for the degree of

DOCTOR OF PHILOSOPHY

in

Neuroscience

May 10th, 2019

Nashville, Tennessee

Approved:

Ronald B. Emeson, Ph.D.

Carl H. Johnson, Ph.D.

Terry L. Page, Ph.D.

Mark T. Wallace, Ph.D.

Douglas G. McMahon, Ph.D.

For the family, friends, and colleagues
that have supported me

Acknowledgments

I am indebted to a countless number of individuals and groups that have supported me during my graduate studies.

I would first like to thank my mentor, Doug McMahon, for allowing me to join his lab and subsequently having to put up with me. Doug's mentorship style has allowed me to learn and grow as a scientist by simultaneously fostering my independence and offering guidance. His investment of time and resources into my training has made a world of difference in my scientific life, and I feel especially prepared for the challenges ahead thanks to his kindness.

In this same vein, I would like to thank my first scientific mentor, Fred Davis, for whom I worked during my time as an undergraduate at Northeastern University. Fred's enthusiasm for circadian biology had me hooked from my first week on campus, and that I still maintain such a heavy interest in chronobiology just shy of ten years later is a testament to his influence.

I have had the pleasure of working in neuroscience research in two other labs before beginning my time in graduate school. I would like to thank Harry Pantazopoulos and Sabina Berretta from McLean Hospital and June-Hee Park and Grigori Enikolopov at Cold Spring Harbor Laboratories for their training and support.

While working in an academic lab requires continuously seeing colleagues move on as they finish their degrees and fellowships, there is a silver lining in that you get to meet and work with a large number of people. I would like to thank all of the McMahon Lab and Johnson Lab members past and present who have provided scientific guidance and friendship along the way. In particular, I would like to thank Jeff Jones, Noah Green, Heng Dai, Maria Luísa Jabbur, and Manuel Giannoni-Guzmán.

The Vanderbilt scientific community is very open, and as such I have benefited from interactions with a number of research groups that surround ours. I would like to thank the members of the Emeson, Johnson, Wallace, Broadie, Gould, and Konradi labs for their friendship and intellectual stimulation.

Each member of my committee has gone above and beyond in assisting me during my time at Vanderbilt. Ron Emeson has provided valuable scientific and culinary mentorship, and Mark Wallace helped provide me with firsthand academic administrative experience. Carl Johnson and Terry Page were always available for the discussion of complex circadian topics, and generously allowed me to work with them alongside pioneer of the field Serge Daan in releasing and interpreting previously unpublished papers from Colin Pittendrigh. Not only have these individuals assisted me directly, but they have also provided me with a model for how to be a mentor myself in the future.

I would like to thank my family and friends for their love and support over the years. Graduate school can be a trying experience, but they consistently worked to keep me focused. It is a lot easier to face tough challenges when you know that you are trying to make a group of wonderful people proud.

Last, I would like to acknowledge my funding. I started my graduate career with funding from the National Science Foundation Graduate Research Fellowship Program, which greatly assisted me in getting my work moving. Later, I received a pre-doctoral fellowship from the National Institute of Neurological Disorders and Stroke allowing me to continue as a funded graduate student. Most recently, I have been supported by an R01 to Doug McMahon from the National Institute of General Medical Sciences. I am grateful for all of these tax-payer funded opportunities to perform scientific research.

Table of Contents

Page

List of Figures

Figure Page

List of Tables

Table Page

Chapter 1

Introduction

1.1. Light, The SCN, and Everything

About a day

Of the many external influences on evolution, from its earliest stages to the present day, gravity and the rotation of the Earth are unique in their consistency. Though its speed has decreased over the course of millions of years, the Earth's rotation has provided alternating intervals of light and dark throughout the entire history of life on this planet. This cycle, the solar day, is woven into the fabric of our society. Unlike the inch and the meter, the pound and the gram, and the many calendars of the world, the *day* is unequivocally recognized by all, and biology is no exception. The day is internalized by living things in the form of circadian rhythms, the biological reflection of the Earth's steady rotation. These rhythms are broadly found but narrowly defined, deeply embedded but often easy to observe.

The overt expression of these rhythms is so easy to observe, in fact, that the Greek naturalist Androsthenes made note of the daily opening and closing of leaves in the 4th century B.C. Despite their relatively obvious superficial expression, biological rhythms are much more complex than a simple daily response to the external environment. In 1729, Jean Jacques d'Ortous de Mairan made the first experimental foray into the world of biological rhythms by observing that these leaf opening and closing behaviors, of the same kind recorded 2 millennia earlier, persisted in the absence of light input to the plant. Though we know now that this persistence is the result of complex internal timekeeping, popular scientific thought continued to

ascribe these rhythms to some undefined exogenous “factor X” until the 1950s and 60s when the concept of an internal circadian clock began to gain traction in the scientific community.

Acceptance of circadian rhythms as a true internal biological phenomenon also required a formal definition. A biological property is said to have a rhythm if it changes in a repetitive manner with a regular period. Likewise, a rhythm is further categorized as circadian if it meets a specific set of criteria. First, the oscillation must be expressed without needing to be learned (i.e., innately) and without the need for input from environment (i.e., endogenously). As indicated by the name, the oscillations must be of a near-24-hour period, and while they must be expressed without environmental influence, they must also be able to be entrained (or synchronized) to external cycles. Lastly, in contrast to most other biological processes, the oscillation speed must be temperature compensated.

Even with these specific restrictions, circadian rhythms are one of the most ubiquitous biological phenomena known. With organisms ranging from single-celled bacteria to humans expressing these rhythms, an organism with a complete lack of a circadian oscillation is far more notable. Aside from the wide variety of lifeforms that express circadian rhythms, there is also great breadth in the biological factors that display these rhythms directly- body temperature, arousal, gene expression, cognitive function, and others are all candidates to be rhythmic. The maintenance of a circadian rhythm can benefit organisms by allowing them to segregate specific biological functions to relevant portions of the day, while also allowing some degree of anticipation of daily environmental events based on internal timekeeping. Increased fitness from functional circadian rhythms was first shown experimentally in cyanobacteria by Carl Johnson in 1998[1], followed soon after by studies in chipmunk by Patricia DeCoursey in 2000[2].

Understanding the basic functioning of these rhythms is critical, but perhaps just as important is understanding their disruption and dysfunction. This insight is of particular value to

humans, who with each passing technological advancement (gas lamps, electricity, air travel, and screen-based devices) bring new challenges to the circadian system that is long-adapted to the near-invariable rotation of the Earth. These changes in light exposure can lead to improper alignment of the internal circadian clock with the external natural light cycle through unnecessary or inappropriate phase shifts. Additionally, the insights provided by circadian research allow for a better understanding of how the system can be internally dysfunctional absent improper influence from the environment, such as is the case in genetic disorders like familial advanced sleep phase disorder and delayed sleep phase syndrome.

Light and the clock

The circadian systems of different organisms vary, but often share certain components through common ancestors or convergent evolution. One such shared mechanism is light detection. Circadian rhythms are subject to internal noise in the form of minor variations in the length and amplitude of the circadian cycle, and external noise in the form of changing seasonal light, weather, and other light exposure variations. As such, circadian systems evolved to incorporate information provided by the light cycle into their rhythms, allowing the organism to remain entrained to the environmental oscillation. All typical circadian rhythms therefore require some way to detect light or other daily stimuli (e.g., temperature) and integrate that information into the rhythm. The value of consistent integration of light information into the system is so great that circadian rhythms may have evolved to have periods of different lengths than that of the external cycle in order to maintain tighter alignment between the two.

While in single celled organisms like cyanobacteria the sensing of light and dark is likely integrated into the clock indirectly through altered redox and/or metabolic states of the cell as a result of photosynthesis[3–5], the circadian systems of multicellular organisms generally fall into

one of two organizational patterns: distributed and centralized. In distributed circadian systems, multiple tissue-specific circadian oscillators are entrained directly by light exposure. Photoreceptive molecules, such as Cryptochrome in *Drosophila*[6,7] and Phytochromes in *Arabidopsis*[8], integrate light information into the molecular clockwork locally within each tissue. In centralized circadian systems, such as in mammals, the overall rhythm of the organism, including the rhythms of peripheral tissues, are orchestrated by a master pacemaker in the brain. In this situation, even though each individual cell may have a functioning circadian clock, those clocks are governed by the master pacemaker. Because in most of these organisms the master pacemaker does not receive direct light exposure, light information is conveyed to that structure by other means.

Phase shifts and entrainment

The primary effect of light on the circadian pacemaker is to stabilize its position within the daily cycle, through shifts to its phase. As would be predicted from the molecular response to light exposure (discussed below), these phase shifts are heavily dependent on the phase of

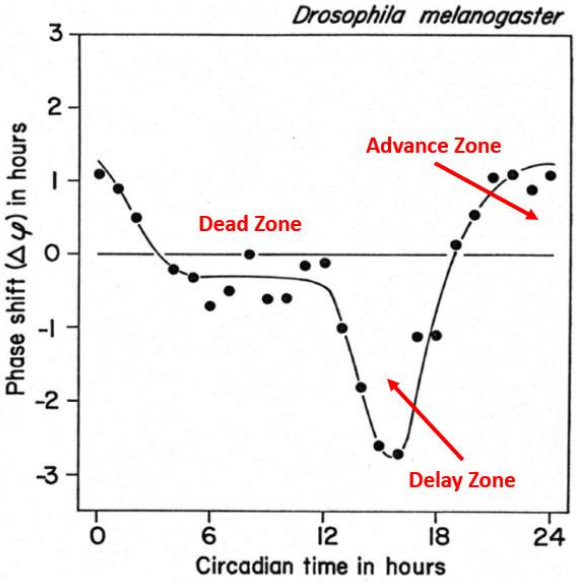

Figure 1-1. Example phase response curve. The curve shows the shift that results from a light pulse occurring at a particular circadian time. Little to no shift is caused by a pulse during the "dead zone," here shown between circadian time 6 and 12. A delay is caused by pulses falling between circadian time 12 and 20, and an advance by pulses falling between 20 and 6. Modified from Pittendrigh Paper II from Tackenberg, *et al*. 2017.

the pacemaker at the time of the shifting stimulus. The extensive study of phase shifts, however, predates the molecular understanding of the clock by several decades, and formed the basis for much of the early understanding of the circadian clock. This research revealed that phase shifts vary in magnitude and direction (i.e., advance or delay) depending on the phase of the circadian cycle at the time of the shift. Graphically, the phase shift response can be plotted against the circadian time at which it occurred to produce a phase response curve (PRC, Figure 1-1). A PRC is defined for a specific case – a particular organism, of a particular age and sex, under particular conditions – and as such its exact shape and scale will vary. The general shape, however, with a phase advance region in the late subjective night, a dead zone during the subjective day (the time of day where an organism typically is exposed to light in as 12:12 light/dark cycle), and a delay zone in the early subjective night, is largely preserved across organisms and circumstances. This stereotype provides useful clues for examining the mechanisms of circadian light responses. Despite being one of the oldest circadian properties examined, phase shifts are a pertinent and common part of current circadian studies.

The most important consequences of the phase shifting capacity of the pacemaker is its ability to entrain to light/dark cycles. Because of the phase-dependence of the phase shift response, some light exposure produces a negligible phase response (e.g., light within the dead zone) while other light exposure can result in a sizeable shift (e.g., light within the delay zone). As a result, repeated light exposure (such as in a light/dark cycle) can produce daily phase shifts that reach entrainment, a stable steady-state in which the endogenous circadian rhythm and the external light cycle maintain a consistent phase relationship. While entrained, the pacemaker with a free-running period of τ hours locks onto an external light cycle with a period of T hours by undergoing a daily phase shift of $\tau - T$ hours.

Understanding that the clock must undergo a daily phase shift of $\tau - T$ hours in order to maintain stable entrainment leads to an important question: how exactly is that daily phase shift

induced? This question was the focus of intense experimental and computational work for over a decade during the 1960s through 1980s. The debate over the mechanism of entrainment was formed over two prevailing theories: parametric and non-parametric entrainment. In the parametric (continuous) model, the required daily phase shift was realized through a continuous modulating effect of a full light cycle. As the light phase progressed each cycle, the light would induce changes to the pacemaker, altering its angular velocity and upon termination, leave the pacemaker in a shifted state compared to its original trajectory. In the non-parametric (discrete) view, the onset and offset of light each exerted a near-instantaneous phase shifting effect, balancing together to form the necessary daily shift.

Though the parametric model was shown to be explain some aspects of entrainment (see **Appendix A**), work by Colin Pittendrigh and Dorothea Minis[9] using skeleton photoperiods (light cycles in which a full duration of light is replaced by 15 minute pulses of light at the time of onset or offset) demonstrated that full light cycles were not always necessary for stable entrainment. Entrainment to skeleton photoperiods up to 14:10 LD mimicked entrainment to their complete photoperiod counterparts. Entrainment to longer skeleton photoperiods, however, resulted in a “phase angle jump” in which the pacemaker aligned with the shorter interval between light pulses, mimicking a short skeleton photoperiod. These experiments showed that when the identity of two pulses as morning or evening was relatively unambiguous, photoperiod-like phase angle encoding could be achieved without continuous light exposure during the day phase. As such, the discrete non-parametric model explained the phenomenon more completely. The presence of the phase angle jump in longer skeleton photoperiods and the lack thereof in night interruption experiments demonstrated the parametric influence of light in determining the phase angle interpretation of the two entraining light pulses. Later experiments have shown that, even for photoperiods longer than 14:10 LD, slow expansion of the skeleton

photoperiod can produce stable photoperiodic entrainment, with associated activity duration and phase angle changes, with skeletons of 16:8 LD (**Chapter 2.2**).

While the skeleton photoperiods employed by Pittendrigh and Minis gave great credence to the argument that entrainment was largely achieved non-parametrically, Pittendrigh aimed to solidify the argument further using a combination of theoretical modeling and experimental validation. One of the foundational pieces of this supplemental evidence came in the form of twin-pulse experiments conducted independently by both Chandrashekaran and Pittendrigh. In these experiments, two light pulses separated by at least one hour were presented to *Drosophila* and the resulting phase shift was measured. The experiments intended to test whether phase shifts were nominally instantaneous, or if they took an extended amount of time to be effected. Using quick but separable pulses allowed for the formation of a simple hypothesis: if the phase shift induced by the first pulse was instantaneous, the phase response curve itself would shift as well, making the final phase after the second pulse predictable from the assumed phase response curves for the first and second pulses. If any other final phase was achieved, that result would support the interpretation that phase shifting is non-instantaneous. Both Chandrashekaran[10] and Pittendrigh[11] found in these experiments that phase shifts took at most 1 hour (the minimum interval used) to be effected.

Pittendrigh began further development of his argument using an alternative plotting of the phase response curve called the phase transition curve (PTC, Figure 1-2). Unlike the phase response curve, which plots the phase shift magnitude and direction against the timing of the phase shifting pulse, the PTC plots the resulting phase of the pacemaker against the timing of the phase shifting pulse. In this way, the PTC can be considered a second-order PRC. These plots are two different ways of displaying the same information. An example of a similar situation would be plotting a commute length against departure time, and arrival time against departure time. In the first plot, commute length is directly visualized and arrival time can be calculated

using the departure time and the commute time. In the second plot, arrival time is directly visualized, and commute length can be calculated using the departure time and arrival time. This distinction is the same for PRCs and PTCs- in a PRC, the phase shift magnitude is directly visualized, and the resulting phase can be calculated using the initial phase and the phase shift magnitude. In the PTC, the resulting phase is directly visualized, and the phase shift magnitude can be calculated using the resulting phase and the initial phase.

One useful function of the PTC is that the y-axis value, the resulting phase, can act as a rotated x-axis value, the initial phase, for a future phase-shifting light pulse. As a result, two PTCs can be overlaid (with one rotated) onto a single graph to build expectations about how two repeated pulses will interact over the course of several circadian days. Given the earlier results that phase shifts were nominally instantaneous, Pittendrigh applied PTCs in this way to each pulse of a skeleton photoperiod, using those curves to predict stable phase angles which could then be tested experimentally. The results of these models and experiments are discussed in **Appendix A**.

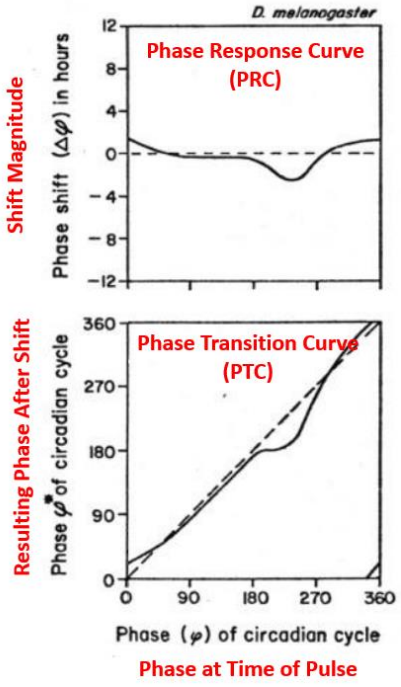

Figure 1-2. Phase response curve and phase transition curve. A side-by-side comparison of a phase response curve (top) and phase transition curve (bottom). In both graphs, the x-axis is the time of the phase-shifting light pulse in circadian degrees. In the PRC (top), the y-axis is the size of the phase shift. In the PTC (bottom), the y-axis is the resulting phase after the shift (original phase + size of phase shift). Modified from Pittendrigh Paper II from Tackenberg, et al. 2017.

The SCN

An important focus of mammalian circadian rhythms research throughout the 1970s and 80s was the locus of circadian rhythm control within the brain. The evidence converged upon the suprachiasmatic nucleus (SCN) of the hypothalamus, and was conclusively confirmed to be the anatomical site of circadian control by Martin Ralph, Russell Foster, Fred Davis, and Michael Menaker in 1990[12]. In their study, they concisely summarize the five major factors underlying the hypothesis that the SCN is the mammalian master circadian clock: the SCN receives information from the retina[13] and consumes glucose rhythmically[14], its ablation eliminates behavioral rhythms[15], isolated and cultured SCN maintain rhythmicity[16,17], and arrhythmic hosts have their rhythmicity restored upon implantation of SCN cells[18]. Though these foundational points were quite convincing, the 1990 study cemented the SCN's role by transplanting the SCN of mutant hamsters with atypical free-running periods into arrhythmic hosts. Because the rhythms restored in the host matched the altered period of the donor mutant, the master orchestrator role of the SCN was confirmed.

Though the SCN as a whole has a clear function in maintaining biological time and synchronizing it with the environment, the structure itself is heterogenous. The SCN is comprised of about 20,000 neurons across two interfacing nuclei straddling the third ventricle. Historically, the SCN has been divided into two major subregions based upon anatomical position and neurochemical (specifically, neuropeptidergic) composition[19]. The ventrolateral (core) portion of the nucleus is characterized by the expression of vasoactive intestinal peptide (VIP), relatively rapid response to light input and a high number of retinal inputs, and a relatively delayed phase angle of entrainment (see below). The dorsomedial (shell) portion of the nucleus is characterized by the expression of arginine vasopressin (AVP), a higher latency to response to light input with a low number of retinal inputs, and a more advanced phase angle of entrainment[20]. The presence and function of many other neuropeptides, including gastrin

releasing peptide (GRP), calcineurin (CN), and neuropeptide Y (NPY) have led to further refinements to the traditional two-region subdivisions, but full functional anatomical characterization has not been realized.

Despite some uncertainties about the specifics of the cellular network, the two-region model of the SCN helps explain the structure's combination of flexibility and robustness. With one region that rapidly responds to light input but does not correlate well with downstream behavioral outputs, and another that remains more firmly fixed in its phase which is slowly influenced by the other half and heavily correlated with downstream outputs, the clock seems able to handle both permanent and temporary changes in the LD cycle appropriately. It is therefore of great scientific interest to determine the exact method of communication between (and within) the two regions to determine how, specifically, the SCN responds to perturbation. Changes to the clock by external influences are, as described above, one the core properties of a circadian rhythm (i.e., the rhythm is entrainable to external cycles). Understanding the response of the circadian system to light input, from the level of the genes downstream to the overt behavioral response, is a critical question of circadian rhythms.

Far from the exterior of the body where direct light exposure can occur, the SCN receives light information indirectly from the retina. There, light is transduced into electrical signals by photoreceptor cells expressing specialized light-responsive G-protein coupled receptors (opsins). The majority of light detection, such as image-forming vision, is mediated by the rods (via rhodopsin) and cones (via conopsin) of the retina. In 1999, however, Russell Foster and colleagues discovered that mice lacking rods and cones entirely were still able to entrain their circadian rhythms to light/dark cycles[21]. Further examination over the following years revealed that circadian entrainment was mediated predominantly by a special set of intrinsically photosensitive retinal ganglion cells (ipRGCs) that expressed a then-recently described opsin, melanopsin[22–24]. As their name describes, these cells are directly activated by

light and transmit that information along the retinohypothalamic tract (RHT) to a subset of SCN neurons[24]. The influence of activated RHT neurons on these retinorecipient SCN neurons is excitatory, leading to an induction of action potentials. To understand how light influences the mammalian circadian clock through this signaling, we must examine the molecular basis of circadian oscillations and the cellular network that underlies the overall behavioral response.

The molecular clock

As described above, circadian rhythms are endogenously generated, and the molecular basis for that internal oscillation in mammals is found at the genetic level in the form of the transcription-translation feedback loop (TTFL). During each cycle, the circadian clock genes *Period 1* (*Per1*), *Period 2* (*Per2*), *Cryptochrome 1* (*Cry1*), and *Cryptochrome 2* (*Cry2*) are activated by the binding of the BMAL1::CLOCK complex to their E-Box promotor region, inducing their transcription. After translation, the PER1/2 and CRY1/2 proteins exit the nucleus and heterodimerize, accumulating in the cytoplasm and eventually re-entering the nucleus where they act on the BMAL1::CLOCK complex to inhibit further *Per1/2* and *Cry1/2* transcription. The *Per/Cry* heterodimers are then slowly degraded, eliminating the inhibitory effect on their transcription and beginning the cycle anew. This process takes about 24 hours, and as such forms the basis of the overall circadian rhythm of the organism[25].

While the circadian clock genes under E-Box control are generally activated during the subjective day, the molecular clock is able to initiate the expression of clock-controlled genes during the subjective night through the accessory loop of the TTFL. In this loop, *Rev-ERBα* is transcribed and translated during the subjective day, reaching higher levels of functional protein in the late subjective day/early subjective night. The REV-ERBα protein then acts upon its own set of transcriptional regulation elements referred to as REV-ERB Response Elements (RREs)

to initiate transcription of *Bmal1* and other subjective-night-transcribed clock-controlled genes. In this way, the clock is able to initiate transcription of particular genes at specific times of day[25].

This loop is stable and self-sustaining, but has particular avenues for producing output and receiving input. The TTFL projects its cyclic influence throughout the cell through a variety of circadian controlled genes (CCGs) that contain the same E-box promotor sequence as the *Per* and *Cry* genes (or RRE sequences as *Bmal1*), thus being activated in a similar fashion by the *Bmal1::Clock* complex. Circadian transcriptional control has tangible rhythmic effects on the cell. A good example of this influence is the interaction of the TTFL on the daily firing rate rhythm of SCN neurons. While there is a persistent sodium current present around the clock that provides a depolarizing influence on SCN neurons, other circadian-controlled ion channels make the subjective day phase of the SCN high firing and the subjective night phase low firing. The persistent sodium current is counteracted only during the circadian night by a leak potassium current (though the particular channel or channels responsible for this current have yet to be identified), which makes SCN neurons relatively hyperpolarized during the night. During the high firing subjective day, fast-delayed rectifier potassium channel currents reduce the duration of the falling phase of the action potentials, shortening the refractory period and allowing SCN neurons to fire more quickly. During the low firing subjective night, large-conductance potassium channels are most active, extending the hyperpolarization following each action potential and therefore working against repeated firing[26].

The TTFL can be influenced externally through cAMP response elements (CREs) on the *Per* genes. When CRE-binding protein (CREB) is activated, it binds to CREs and induces *Per* transcription. CREB is activated as a result of multiple intracellular signaling pathways triggered by a range of extracellular signaling events involving both neurotransmitters and neuropeptides. As an example, when the neuropeptide vasoactive intestinal polypeptide (VIP) binds to its

receptor, $VPAC_2R$, the $G_{\alpha S}$ subunit of the receptor is activated, leading to an upregulation of cAMP and eventually CREB activation.

Light information is integrated into the TTFL of SCN neurons in a similar fashion. Light activation of ipRGCs in the retina result in the release of glutamate and PACAP from the RHT onto retinorecipient neurons. These retinorecipient neurons respond to the excitatory input by increasing their firing rate, and the resulting calcium influx converges intracellularly on the activation of CREB. In this way, the activation of ipRGCs in the retina leads to an upregulation of *Per* in the retinorecipient regions of the SCN. That change in *Per* leads to an alteration of the phase state of the TTFL, which leads to differential firing and signaling to the rest of the SCN, finally resulting in an overall phase shift.

The inputs and outputs of the TTFL form an intricate intracellular network of rhythmic components. In this tiered system, the rhythms in gene expression, firing rate, neuropeptide signaling, and calcium have influences on and are influenced by one another. As described above, the TTFL includes the activation of CCGs, some of which encode particular ion channels that upon translation and trafficking to the membrane, cause changes in firing rate. Similarly, the firing rate from these channels can influence the TTFL through calcium influx. Release of neuropeptides can be firing-rate-dependent, and the reception of neuropeptide signals can increase or decrease firing rate. In this way, the interaction between rhythmic layers form the overall rhythmicity of the cell, the SCN, and the organism.

Seasonal light and entrainment

Through the course of study of the mechanisms of general entrainment, seasonal light was employed as a means to compare skeleton photoperiods to complete photoperiods, as seasonal light induces characteristic alignments of the circadian rhythm with the external cycle.

The study of seasonal responses, however, much like circadian rhythms as a whole, is on its own a well- and long-studied biological phenomenon. The first scientific mention of photoperiodism was made nearly 100 years ago by Garner and Allard, who observed photoperiod-dependent light responses in plants[27]. By the 1960s, biologists were interested in defining the relationship between the circadian clock and seasonal responses. The theory first proposed by Erwin Bünning in 1936[28] and updated in 1960[29] (discussed in **Chapter 1.2** and **Appendix A**) acted as a foundation for many of Pittendrigh's mechanism of entrainment experiments through the late 1960s to 1980s (**Appendix A**).

Bünning's model integrated daily and seasonal responses by placing the circadian clock at the heart of photoperiodic output. Though at the time the molecular workings of the circadian pacemaker were not defined, Bünning proposed a system in which circadian oscillations in light-requiring and dark-requiring processes allowed for recognition within an organism of relatively longer or shorter days. Pittendrigh later refined Bünning's model to take into account that light, in addition to inducing photoperiodic properties, also set the phase of the circadian pacemaker[30]. Importantly, he also drew from this theory an intriguing supplemental factor: the idea that if the clock did regulate seasonal responses in this way, then a single light pulse timed precisely would be able to induce or inhibit seasonal responses in the absence of all other light.

The adjustment of Bünning's hypothesis to incorporate the dual function of light in setting both phase and photoperiodic responses was the foundation of the skeleton photoperiod experiments described above[9]. Though those experiments were focused on discerning the parametricity of entrainment, they did so through the known interaction between photoperiodic light and corresponding circadian responses. In these experiments, the measurement was the timing of *Drosophila* eclosion after exposure to a particular light schedule. The timing of eclosion is under tight circadian control in *Drosophila*, and different prior photoperiodic exposure results in a different temporal alignment of the eclosion timing relative to the light/dark cycle. This

alignment, referred to as the phase angle of entrainment, describes the temporal relationship of any two related cyclic properties. For instance, if rhythmic blood pressure peaks three hours after dawn each day, the blood pressure peak would be described as having a phase angle of -3 hours relative to dawn. Likewise, if melatonin onset occurs two hours before dusk each night, that melatonin onset would be said to have a phase angle of +2 hours relative to dusk. In *Drosophila*, the peak time of eclosion generally has a later and later (more negative) phase angle relative to lights on as the photoperiod length increases. Pittendrigh and Minis demonstrated that entrainment to skeleton photoperiods (photoperiods in which a complete photoperiod is replaced with two brief light pulses at the onset time and offset time) resulted in virtually the same phase angle changes as entrainment to a complete photoperiod for photoperiods shorter than 14:10. These results cemented the idea that onset-offset interval, rather than the presence of continuous light between those times, was critical for determining the exact profile of entrainment.

While these results were extremely important for understanding the general mechanism of circadian entrainment, they also have additional ramifications for understanding seasonal encoding and its relationship to the circadian system. By acknowledging phase angle of entrainment in this context as not just a proxy for measuring the profile of entrainment but rather as a photoperiodic circadian property *per se*, we can see that similar experimental approaches can be used to address the mechanisms of photoperiodic encoding. To understand the significance of better characterizing how photoperiodic changes are initiated in mammals through the circadian system, we must examine how the mammalian circadian system responds to photoperiodic signals.

1.2. Photoperiodic Programming of the SCN and Its Role in Photoperiodic Output

Michael C. Tackenberg & Douglas G. McMahon

Modified from: Tackenberg, M.C., McMahon, D.G. Photoperiodic programming of the SCN and its role in photoperiodic output. *Neural Plasticity* **2018**, 1-9 (2018).

Outside of the tropics (where day length remains relatively consistent throughout the year), the changing photoperiod is a reliable and predictable seasonal signal that presents an opportunity for organisms to adapt to seasonal changes in factors such as temperature and resource availability in an anticipatory fashion. The first scientific observation that changing day length was the critical factor in seasonal responses was reported in 1920 by Garner and Allard[27]. In that study, they observed that certain plants could only attain the flowering and fruiting stages of their development when housed in particular day lengths: while some species required long days and others required short days, those light durations were the critical factors in their reproductive cycle. Since that time, seasonal responses have been described and studied in a wide variety of different organisms[31–34]. More recently, seasonal factors have been linked to human health. While we have benefitted greatly from understanding the seasonal responses of the organisms on which we rely for survival, evidence is emerging that we are also photoperiodic organisms ourselves[35]. Over the last several years, much research has been done on the relationship among photoperiods, especially extreme photoperiods, and psychiatric health, sleep, and non-communicable diseases[36–41].

The ability of organisms to exhibit daily biological time-keeping is well-established. Organisms ranging from bacteria to humans have innate, endogenous 24-hour biological oscillations that persist into constant conditions and can be entrained by the external light/dark

cycle of the Earth. These rhythms allow for a myriad of time-dependent functions, including predator avoidance[2], sun-based navigation[42–44], metabolic regulation during hibernation and torpor[45–48], and photosynthetic efficiency[49–51]. In mammals, these daily rhythms are orchestrated by a central circadian pacemaker located in the hypothalamus, the suprachiasmatic nucleus (SCN)[12]. The SCN consists of approximately 20,000 neurons, and is not a homogenous structure. It can be divided into two major subregions based on neurochemical composition, connectivity, and spatial position. These subregions are typical referred to as the dorsomedial (also referred to as the dorsal or shell SCN) and ventrolateral (ventral, or core SCN). The SCN receives input from the retina directed towards its ventrolateral subregion, while its dorsomedial region features numerous direct and indirect projections to other hypothalamic nuclei controlling homeostatic function and to the rest of the brain[19]. When considering the SCN's primary function is to integrate external light information with endogenous timekeeping and then orchestrate a wide range of behavioral and physiological responses, the structure is a prime candidate for controlling seasonal rhythms.

The first suggestion that circadian pacemakers were involved in orchestrating seasonal responses was made by Erwin Bünning in 1936[28] and refined in 1960[29]. He proposed that a portion of a plant's circadian cycle was light-requiring, or "photophilic," while the other portion was dark-requiring, or "scotophilic." In this model, when a short-day plant in its photophilic phase is exposed to dark, a short-day mechanism is successfully initiated, while a long-day plant in its scotophilic phase exposed to light will have a long-day mechanism successfully induced. This theory was accepted and further refined by Colin Pittendrigh, who suggested that it overlooked the primary function of the circadian pacemaker's response to light- to set the phase of the pacemaker[9]. This combined view, in which the master circadian pacemaker integrates information about both the time of day and the length of day, was a critical factor in the way Pittendrigh viewed the circadian clock, and its entrainment by light, for the following

thirty years[11]. The experimentation of Pittendrigh and others on entrainment theory resulted in an increased understanding how circadian pacemakers entrain, or synchronize, to the light cycle. Notably, how a circadian rhythm synchronizes to a light dark cycle to produce stable entrainment is dependent on the length of the photoperiod, with different photoperiods producing characteristic phase angles of entrainment[9].

Later, when the SCN was conclusively identified as the locus of a mammalian master clock, investigations began into the mechanisms of mammalian circadian entrainment at a cellular level. In 1995, it was established that the duration of the light sensitive phase of the SCN, measured via *c-fos* gene expression, was longer in rats housed in short photoperiods than those housed in long photoperiods[52]. When rats were switched from long to short photoperiod, the light responsive phase took as long as two weeks to reach the decompressed short photoperiod phenotype, demonstrating that there were lasting effects of photoperiod within the SCN[53]. Later, invaluable descriptions of the cellular and network properties of the SCN began to emerge, and continue through today (for review, see Colwell, 2011[26]). These findings enabled new approaches to determining the biological mechanism for mammalian photoperiodic encoding[54,55], as well as in elucidating the neurophysiological basis for seasonal outputs like depression-anxiety behavior and reproduction. A principal goal of this line of research, which continues today, is to define the neurobiological network that orchestrates photoperiodic responses. While future improvements to our understanding of this network will produce benefits for medicine and society, current research on the subject has already yielded useful applications in clinics and beyond.

The SCN as a site of photoperiodic encoding

Though the idea that the circadian pacemaker can encode seasonal information was generally accepted by the circadian field in the 1960s, at that time the mechanistic basis of seasonal encoding by the SCN was difficult to examine with the experimental tools at hand. Substantial progress on understanding of the cellular and molecular mechanisms underlying daily oscillations in the SCN provided a greatly enhanced basis to study the mechanisms of encoding the season light cycle. A key piece of the puzzle was the elucidation of the molecular mechanisms of the mammalian circadian clock-works. This provided not only critical insight into the molecular and genetic foundations of daily time-keeping, but in addition it provided a whole new generation of experimental tools. Since the clock-works was found to be a gene-based oscillator, probes and transgenes that enabled real-time gene expression analysis provided a new way to visualize and quantify circadian rhythmicity in SCN neurons and networks.

Within each SCN neuron, a genetic feedback loop known as the Transcription-Translation Feedback Loop (TTFL) was found to be the foundation of the autonomous near 24-hour rhythms in gene expression and neuronal firing rate (for reference, see Takahashi, 2008[56]). In this loop, the transcription of the *Period* (*Per1* and *Per2*) and *Cryptochrome* (*Cry1* and *Cry2*) genes is initiated through binding of the CLOCK::BMAL1 transcription factor complex to E-box enhancer elements in the promoter regions of *Per*, *Cry* (and many other circadian-regulated genes). The protein products of the *Per* and *Cry* genes then accumulate in the cytoplasm, where they heterodimerize and re-enter the nucleus to inhibit their own transcription. This process takes roughly 24 hours to complete, thus forming a self-sustaining circadian oscillation in both core clock genes and other circadian regulated genes. This feedback loop contributes to intracellular calcium rhythms and rhythmic electrical activity through daily oscillations in ion channel and receptor transcription[26]. The result of these interlocking rhythms is a particular daily profile in circadian gene expression and firing rate within individual SCN neurons and across the

SCN neuronal network, in which the degree of synchrony between individual SCN neuron gene expression or electrical activity cycles sets the overall waveform of SCN gene expression or electrophysiological activity[57–59]. These profiles have been extensively studied in equinox (12 hours light:12 hours dark) conditions. Generally, SCN neurons fire at a higher rate (approximately 6-10 Hz) during the day, and at a lower rate (approximately 1-2 Hz) during the night. This firing pattern persists into constant conditions. Light pulses during the low-firing phase at night have been shown to transiently increase firing rate and gene expression as part of a phase shifting response of the clock[60–62].

Do the cellular or network gene and electrical rhythm profiles change across different photoperiods? If so, this change could form a basis for photoperiod encoding. Reports from studies on hamsters[63], mice[64], and sheep[65] showed Per1 mRNA levels had a longer elevated phase when assayed during long days compared to short days. This result, however, could be explained by the light activation of the retina increasing neuronal activity and, as a result, *Per1* transcription. Sumová and colleagues addressed that possibility by assaying the *Per1* (as well as other clock genes) mRNA levels in the SCN of rats that had been housed in different photoperiods, but were then transferred to constant darkness, thus eliminating the proximal effect of light exposure[66,67]. In these tests, the high-expression phase of the *Per1* mRNA rhythm was found to lengthen in rats previously housed in long days when compared to short days. *Cry1* mRNA was also found to have significant differences between long- and short-photoperiod rats, but *Bmal1* and *Clock* mRNA were not significantly affected by photoperiod.

When asking a similar question about the effect of photoperiod on electrical activity within the SCN, Schaap and colleagues found that different photoperiods altered the waveform of the spike frequency rhythm of the SCN, extending the high-firing phase and contracting the low-firing phase in long days, with the opposite effect occurring in short days[68]. Simulations suggested that while SCN neurons fire individually in the same waveform regardless of

photoperiod (i.e., each individual neuron's high-firing phase duration remains unchanged across different photoperiods), changing their phase relationship can combine to produce the firing rate profile changes observed between the two photoperiods. Further investigation into the phase distribution of SCN neurons in long or short photoperiod revealed that while single SCN neurons do in fact maintain the same daily firing rate profile across short and long photoperiods, the phase relationship between the neurons does in fact change, broadening in long photoperiods[69]. Interestingly, a population of approximately 50 neurons is required before a differentiable photoperiodic profile emerges. Thus a key finding of these studies was that photoperiod was encoded in the SCN at the network, rather than at the cellular level.

Studies examining the photoperiodic response of gene expression rhythms within the SCN have found results similar to those detailing the response of rhythms in firing rate. Inagaki reported that while individual neurons maintained the same waveform of *Per1* transcriptional activity read out with *Per1::luc* expression across different photoperiods, their phase relationships to one another was more widely distributed in long photoperiods than in short[70]. Ciarleglio found similar results when examining the effect of proximal photoperiods on the *Per1* transcriptional activity rhythm read out by a *Per1::GFP* reporter[71]. Thus increasing photoperiod (long days) was found to increase the phase dispersal of both single SCN neuron gene and electrical activity. Interestingly, fitting with this trend, constant light, which can be considered the most extreme long photoperiod, can result in a complete dispersal of SCN neuron phasing, producing both behavioral and SCN tissue level arrhythmicity while essentially randomizing the phase of the still cycling individual SCN neurons[72]. Clear parallels exist between the rhythmic profiles of firing rate and circadian gene expression in the SCN across photoperiods, demonstrating that the photoperiodic response of the SCN goes beyond simple light-driven changes, including a persistent change at the network level. These results, in conjunction with

the spike frequency rhythm profile studies already discussed, provide ample evidence that phase variance of SCN neurons is an encoding mechanism for photoperiod within the SCN.

The results described above were obtained by exposing adult rodents to different photoperiods. What, then, are the effects of photoperiods experienced during development? In terms of the development of clock gene rhythms in the SCN, the effect of photoperiods on the timing and waveform of these rhythms was shown to be measurable by P10 in the rat[73] suggesting that the interval photoperiod encoding begins during the perinatal period. In addition, Cambras and colleagues showed in a series of studies that non-circadian lighting conditions (principally LL and DD) experienced by rodents during development and maturation can have lasting effects on the circadian system and its responsiveness light[74–77]. Ciarleglio *et al*. subsequently studied the impact of entrainment to different photoperiods during perinatal development on the resulting cellular and network properties of the SCN and on locomotor behavior rhythms[71], asking whether exposure to different seasonal photoperiods during development and maturation can have enduring effects on clock properties. Interestingly, in contrast to photoperiod encoding in adult animals that acts primarily at the network level altering the phase distribution of clock neurons, perinatal photoperiods induced enduring changes in the waveform of single SCN neurons to program overall SCN gene expression waveform later in life. Consonant changes were apparent in locomotor behavioral rhythms and in the phase stability of SCN entrainment to different photoperiods in adulthood. Thus, results to date suggest that while photoperiod encoding primarily resides at the network level in the mature SCN (but see Farajnia, *et al*., 2016[78]), during development photoperiod programs rhythms at the cellular level in a manner that persists into adulthood.

As mentioned previously, the SCN is a heterogenous structure, with two principal regions identified by their neuropeptide gene expression – the ventrolateral region by VIP expression and the dorsomedial region by AVP expression. Are different SCN regions differentially involved

in encoding? In terms of rhythmicity and acute responses to light, the predominantly retinorecipient ventrolateral SCN has been shown to lag behind the dorsomedial SCN in gene expression[79] (but see Quintero, *et al*. 2003[57]) by approximately 1 hour, but has also been shown to respond to phase-shifting light stimuli rapidly while the dorsomedial SCN shifts more slowly[20,61,80,81]. Because of this steady phase angle difference, as well as photoperiod-dependent differences in c-Fos rhythms in the two regions[82], differences between the phasing of the two regions of the SCN between short and long photoperiods became an experimental focus. Brown and Piggins found that the phasing of the electrical activity in the dorsal SCN was less tightly organized than the ventral SCN in slices collected from animals in equinox conditions, and that the electrical activity profile of the dorsal SCN did not change across short or long photoperiods. The overall SCN profile change in electrical activity observed in long days versus short days was found to be caused by changes within the ventral SCN alone[83]. Likewise, arginine vasopressin (AVP) mRNA profiles have been shown to be altered between long and short photoperiods, indicating a change in profile within the dorsomedial SCN[84]. Significant phase differences have also been demonstrated between the rostral/anterior and caudal/posterior SCN[85]. Those differences are enhanced in long photoperiods compared to short[86–88]. Buijink and colleagues found that phase distribution differences in PER2 expression under long day conditions were associated with changes in period stability within the dorsolateral anterior SCN[89]. Looking at the SCN along the anterior-posterior axis rather than the dorsal-ventral axis, using coronal slices, both Inagaki using *Per1::luc*[70] and Buijink using PER2::LUC[89] found that the photoperiodic differences in the phase variance of cellular gene expression rhythm profiles were emphasized in the anterior SCN versus the posterior. The functional significance of the regional differences in phase distribution remains poorly defined. One possibility is that subregions with large phase differences comprise the morning and evening (M and E) oscillators proposed by Pittendrigh and Daan[90]. Inagaki and colleagues observed a bimodal distribution of phase of anterior SCN neurons in long photoperiods,

corresponding to these M and E oscillators[70]. Recent work by Yoshikawa and colleagues used horizontal slices, as opposed to the previously-used coronal slices, to better localize putative M and E oscillators along the anterior-posterior axis[91].

Considering that the dorsal SCN is the source of many of SCN efferents, a question arises about how seasonal information encoded within the phase distribution of ventrolateral SCN neurons is relayed to the dorsomedial SCN for signaling to the rest of the brain. Neurotransmission within the SCN is a major research focus, with many signaling molecules released within the SCN. The phase difference between the dorsal and ventral SCN has been shown to increase as photoperiod length increases, with resynchronization between the two regions after transfer to constant conditions being sensitive to TTX, $GABA_A$ blockers, and vasoactive intestinal polypeptide (VIP) antagonists[92]. GABA, the predominant neurotransmitter within the SCN, was found to have a significant role in the coupling of dorsomedial and ventrolateral SCN, with the addition of the $GABA_A$ blocker bicuculline to SCN slice cultures mimicking the effect of physically disconnecting the two SCN subregions with a knife cut[93]. In that study, Albus and colleagues found that the transient response to a phase-shifting light pulse involved a bimodal distribution of electrical activity during the phase resetting. When the SCN was cut in half, separating dorsomedial from ventrolateral SCN, the electrical response to the light pulse was unimodal for each region, but the two regions were out of phase. The retinorecipient ventrolateral SCN half was more responsive to the light pulse, with the dorsomedial SCN not undergoing a significant shift. Interestingly, the blockade of $GABA_A$ receptors with bicuculline yielded similar results to the physical cut, with unimodal electrical activity in each half and a significantly smaller phase shift within the dorsomedial region as compared to the ventral region. This study provided compelling evidence that $GABA_A$ receptors were mediating dorsal-ventral SCN coupling. Later, when the spatial relationship of the photoperiodic response within the SCN became clearer, the GABA-mediated signaling results

took on new meaning. Farajnia and colleagues followed up on this line of research in 2014, showing that the dual role of GABA within the SCN (acting as both an excitatory and inhibitory neurotransmitter) may be an integral part of the SCN's photoperiodic response[94]. In that study, GABAergic activity was found to be higher during the day in a long photoperiod than at night, while in a short photoperiod GABAergic activity was found to be lower during the day than at night. Closer examination of the electrical properties of GABA signaling in these two photoperiodic conditions revealed a differential rate of excitatory and inhibitory currents. The period instability observed by Buijink and colleagues within the anterior SCN during long photoperiods can contribute to the SCN reaching the altered phase distribution among its constituent neurons[89]. This period-instability mechanism may occur in conjunction with active decoupling that was demonstrated in models described by Myung and colleagues, in which differential effects of GABA reception are used as attractive and repulsive forces within the SCN network[95].

The phase distribution found to be characteristic of a particular photoperiod is primarily driven by neurons in the ventral SCN, which is often defined by its expression of VIP, an important neuropeptide for interneuronal coupling in the clock. VIP was found to be required for the persistence of the photoperiodic electrical activity profile of the SCN into constant conditions[96]. This result suggests that the VIPergic population of the SCN, mostly within the ventral half, are necessary for encoding at least the duration of locomotor activity.

The SCN and photoperiodic response signaling through melatonin

How then does the SCN fit into a putative photoperiod response network in the brain? An important aspect of creating a map that links light input to the retina with photoperiodic outputs is the understanding of the direct neurophysiological basis of each of those outputs. Once these

neural correlates are understood, a framework can be made for how differing durations of light exert effects on those structures. While in many cases these brain structures have been defined, the enumeration of each of these cases is beyond the scope of this review. Rather, we will focus on examples of those structures and outputs that may be directly related to the SCN's photoperiodic role, particularly in conjunction with the SCN's indirect projections to the pineal gland and its role in regulating melatonin rhythms.

The release of melatonin by the pineal gland is a prime candidate for transmitting photoperiodic cues throughout the brain (for review, see Goldman, *et al*. 2001 & 1983[97,98]). Melatonin is clearly involved in seasonal control of reproductive behavior, one of the most well-studied photoperiodic outputs[99]. Seasonal reproductive behaviors have been shown to be sensitive to melatonin applications and are ablated with removal of the pineal gland, the source of melatonin in the brain[100–102]. Further upstream, those seasonal changes were found to be mediated by the periventricular nucleus (PVN) and the SCN[103,104]. This forms a photoperiodic response circuit, with the SCN projecting indirectly to the pineal gland through a chain of polysynaptic connections that include the PVN. In addition to reproductive behavior, body weight changes associated with different photoperiods (which have been shown to be influenced by melatonin[105]) have been traced to hormone and neuropeptide signaling differences within the arcuate nucleus of the hypothalamus[106]. Interestingly, while long infusions of melatonin replicate short days in Siberian hamsters and induce a reduced body weight phenotype, SCN lesions eliminate those effects, suggesting a role for the SCN both downstream and upstream of melatonin signaling in the photoperiodic signaling network[100]. Another target for indirect melatonin signaling from the pineal is the Raphe nucleus. Recent evidence shows that changes in Raphe serotonin neuron firing rate across different developmental and proximal photoperiods is melatonin-dependent, with melatonin-receptor knockout mice lacking photoperiod-specific firing rates[107].

Not all photoperiodic effects are melatonin-dependent, however. Recent work on C57BL/6 mice, which do not produce substantial amounts of melatonin, has shown that mice in long photoperiods undergo body weight increases and have altered plasma metabolic profiles[108]. Earlier work in the same mouse model and in Fischer 344 rats shows an altered corticosterone profile in long versus short days[109]. Mice with genetic defects in melatonin synthesis have been shown to have modulated locomotor behavior in different photoperiods, manifested as shorter durations of activity in long photoperiods and longer durations of activity in short photoperiods[110]. Work discussed previously demonstrating the necessity of VIP neurons in the persistence of long and short day locomotor behavior duration patterns into constant conditions were also performed in the same melatonin-deficient C57BL/6 mice, demonstrating that the persistence of this photoperiodic output is not melatonin dependent[96]. With few afferent connections, the retina may be an example of an SCN- and melatonin-independent photoperiodic system, with different day lengths altering ERG responses in a persistent manner[111].

In the retina and Raphe, as in the SCN itself, photoperiods experienced during the development and maturation of these neural circuits have been demonstrated to have enduring effects that shape sensory perception and behavior in adulthood. Within a circadian context, developmental photoperiod was shown to persistently change the waveform of circadian *Per1* promoter activation in the SCN, as read out by *Per1::GFP*, as well as the phase angle of the peak relative to dusk and the duration of the locomotor activity phase[71]. Photoperiod effects within the mouse retina are development-dependent, with animals raised on short photoperiods continuing to have reduced retinal sensitivity (short photoperiod ERG phenotype) despite being moved to long photoperiods during adulthood[111]. In the Raphe nucleus, enduring changes in serotonin neuron firing rate were found to be dependent on the developmental photoperiod, with proximal photoperiod playing a less prominent role[107]. Mice matured in long, summer-like

photoperiods exhibit increased serotonin neuron firing, increased mid-brain serotonin content and decreased depression and anxiety-like behaviors in adulthood. In the extreme of constant light, the disruption of the SCN and behavioral rhythms observed in adult mice[72] is much more dramatic and pervasive with perinatal exposure[112]. The SCN is likely to play a role in the encoding of lasting developmental photoperiod effects, with recent work demonstrating that individual SCN neurons exhibit enduringly altered *Per1::GFP* expression rhythm profiles across different developmental photoperiods[71]. In contrast to studies mentioned above where gene expression and firing rate rhythms remained consistent across photoperiods but changed their phase relationship in adult animals exposed to different photoperiod, this work focused on animals reared in particular photoperiods. Photoperiods experienced during the perinatal period had lasting effects into adulthood on the gene expression waveforms of individual SCN neurons, their phase relationships to the light cycle and their intrinsic periods[71]. Considering the influence that the SCN has on the rest of the brain, enduring changes within the SCN during development may help explain the persistent effects of early-development photoperiod observed in other tissues, such as the Raphe. The precise timing of this critical developmental window, as well as the underlying changes within the SCN neurons that lead to the altered neuronal period, remain undetermined.

It remains an open question which photoperiod-dependent behaviors and physiological responses are mediated through the SCN, regardless of how well the photoperiod may imprint onto the phase distribution of the SCN neurons. While the inputs and outputs of the SCN are a consistent subject of study, most of these connections are examined in the context of circadian timing and regulation. Moving forward, careful experimentation will be required to determine the role that the SCN, or any other structures capable of encoding seasonal light information, play in a particular photoperiodic output. Further, these studies will need to differentiate between those photoperiodic effects that are directly driven by light, those that persist for some length of time

even after photoperiodic input has ceased, and those that are imprinted developmentally and produce lasting changes to physiology.

Applications in medicine and society

Whereas the evidence for seasonality driven by photoperiodism in many animals and plant species is widespread and compelling, such evidence is less developed for humans. Still, there are dramatic examples of the impact of seasonality on human health, particularly in the developmental domain, consonant with the developmental origins of adult disease. There is also demonstrated promise of the application of circadian photobiology to address these issues. For example, in 2015, Boland *et al*. reported the results of a "SeaWAS" (Season-Wide Association Study) in which they analyzed the medical records of more than 1.7 million patients at Columbia University Medical Center for associations of medical diagnoses for 1688 diseases with season of birth[113]. They found significant associations with 55 diseases including ADHD, asthma, and 9 cardiovascular conditions. This approach, combined with PheWAS analysis of genomic data holds great promise in revealing the gene by environment interactions underlying disease risk from developmental exposures to season variables.

Therapeutic intervention based on circadian photobiology has already begun in the clinic. Circadian light therapy has long been recognized as a successful treatment for seasonal depression[114]. A salient recent example is the work of Ohta and colleagues who defined perinatal exposure to constant light as a potential risk factor for disruption of the developing mammalian biological clock in mice[112] and then applied this to the neonatal intensive care unit (NICU) where infants may be exposed to constant light. To ensure proper circadian light cycles for premature infants and the ability of medical staff to provide continuous care, Ohta and colleagues targeted stabilization of the developing clock by selective optical filtering of

wavelengths that affect clock entrainment to produce a circadian day and night while preserving the ability of the staff to provide care[115]. This resulted in enhanced day night activity rhythms and increased weight gain critical in premature infants. These initial cohorts of infants are being tracked in a longitudinal study to ascertain if there are lifetime benefits of maintaining circadian cohesion during development.

Conclusion

Our understanding of ourselves as photoperiodic organisms has given new importance to research into the neural basis for photoperiodic responses. While much progress has been made in demonstrating the ability of the mammalian master circadian clock, the SCN, to encode photoperiodic information, as well as in identifying various brain structures involved in the many types of photoperiodic outputs observed, there remains a great deal to be understood. At present, there are a myriad of day-length dependent responses in physiology that range from purely light driven, to transiently sustained, to permanent. More must be learned about the physiology that underlies the differences between these types of responses. Some may rely on the SCN, while others may act independently of the clock. Likewise, many clearly depend on melatonin but others may not require melatonin signaling to occur. We have already observed the benefits that medicine and society may see when photoperiodic research is applied, but to truly modify or medically intervene with this system, a better understanding is required.

Acknowledgments

The authors would like to thank Maria Luísa Jabbur and Terry L. Page for thoughtful discussions and assistance in the preparation of this review.

1.3. Missing Pieces in Seasonal Encoding

Despite their relevance to human health, a full understanding of the mammalian response to photoperiodic influences and their interaction with the circadian system has remained elusive. One reason for these gaps in knowledge is that research into photoperiodism is essentially an umbrella term encompassing many related questions that vary in complexity, significance, and application. Observations must be made in any organism to determine which, if any, properties vary with seasonal light. As described in detail above, any one of these properties can be further dissected to determine if it persists beyond direct seasonal light exposure and, as a result, can be said to be encoded. An encoded property can be analyzed for what physiological changes comprise the mechanism of induction or maintenance of that encoding. Other studies seek to determine how seasonal properties can be manipulated, such as those that attempt to address physiological dysfunction like Seasonal Affective Disorder. In general, these efforts to define treatment strategies will become more effective as more is learned about the physiological changes that underly a given seasonal property.

We can consider changes in mood as an example. Mood is capable of being altered by exposure to different types of seasonal light[116]. Once this response was established through observations of human populations, the next question was how light induced this change. The depression-anxiety behaviors associated with mood are also present in nocturnal mice, which have been used in this case as a model for studying this mechanism of induction. In mice, the developmental exposure was determined to be the most critical for affecting depression-anxiety behavior in adulthood[107], laying the groundwork for similar (albeit retrospective) studies in humans. Though this study narrowed the “when” of the induction of seasonal changes, there remained multiple open questions about the “how” and the “what”: how does light induce these changes, and what underlying physiological changes in the brain occur?

As described in **Chapter 1.2**, the SCN is a prime target for examining what changes occur after seasonal exposure. Earlier work on the SCN under photoperiodic conditions revealed that the overall electrical activity rhythm waveform of the SCN changed in response to photoperiod, with a broadening of the high firing phase of the waveform in long photoperiods and a contraction in short photoperiods[68]. This observation raised the question of whether individual SCN neurons each broadened or contracted their own waveforms, or if the overall change was the result of a change in phase distribution – multiple neurons with unaltered waveform shapes peaking at different times. While developmental exposure to different photoperiods does have an effect on waveform shape[71], the broadening and contracting of the waveform of SCN gene expression after exposure to a particular photoperiod is largely the result of a change in phase distribution of those neurons[69]. More recent work has expanded this work from electrical activity and clock gene expression, again showing a phase distribution change[89]. From there, research focused on the maintenance of this phase distribution, examining GABA transmission changes between excitation and inhibition as a potential mechanistic explanation for how different phase distributions can be achieved[95]. Other work focused on the plasticity of the SCN after photoperiodic exposure, as it reorganizes and re-establishes non-photoperiodic phase distribution levels[92].

A large remaining open question surrounds the way that light is able to induce seasonal changes, such as in behavioral after-effects in free-running period (tau) or activity duration (alpha), or in the change in SCN phase distribution. To answer such a question, inspiration can be drawn from some of the classic experiments described in **Chapter 1.1** and **Appendix A** in which the mechanisms of light influence on the circadian clock are explored. In the case of those experiments, the focus was the general mechanism of entrainment, but similar approaches can be taken to address the question of how clock-mediated changes in photoperiodic properties are achieved. In **Chapter 2**, the influence of distinct components of

light on the circadian clock are examined. First, through the use of repeated phase shifts (**Chapter 2.1**) and then through a combination of repeated phase shifts and light durations (**Chapter 2.2**). Additional interesting ramifications of aberrant activation of light exposure pathways is presented in **Appendix Bee**, where the interaction between light exposure and sublethal doses of the common neonicotinoid pesticides in honey bees and fruit flies is examined.

Another question surrounding photoperiodic light input surrounds the cells within the SCN that are required for propagating seasonal light information to the rest of the nucleus. Given the important role of VIP in the SCN (discussed in **Chapter 3.1**), the cells that express this peptide are a strong candidate for mediating that seasonal message. Experiments shown in **Chapter 3.2** demonstrate that artificial activation of VIPergic neurons alone is sufficient to drive locomotor behavior changes phenotypic of seasonal light exposure.

In any subfield of experimental biology, there is a need for specialized methods. **Chapter 4.1** discusses the technical challenges inherent in circadian research, including those unique to the field and those present across all of biology. Here, a case is made for the need for improved accuracy, throughput, and automation in circadian research, with **Chapter 4.2** revealing a novel method for the measurement of phase shifts in circadian data sets, **Chapter 4.3** showing an automated method for detecting activity duration, and **Chapter 4.4** concerning the fast analysis of long term SCN culture imaging.

These chapters and appendices are together intended to address the complex influence of light, particularly seasonal changes thereof, on the circadian system. The overall summary of the findings and techniques, a description of their significance, and an explanation of future directions is presented in **Chapter 5**.

Chapter 2

Examining the Distinct Components of Photoperiodic Light

2.1. Examining the Parametricity of Period and Alpha After-Effects

The effect of light on the circadian system has been investigated in the context of overt behavior and, upon the identification of the mammalian master clock, the gene expression, excitability, and network properties of the SCN. From the earliest work on acute phase shifts and stable entrainment in *Drosophila pseudoobscura*, light was found to have both continuous (parametric) and discrete (non-parametric) effects[11,117]. As such, a daily light signal influences the pacemaker in multiple ways, depending on the phase of the pacemaker at light onset and offset, the interval between those two transitions, and the duration of the light (Figure 2-1). Pittendrigh and Minis examined the question of onset-offset interval using "skeleton photoperiods," in which two 15-minute light pulses separated by darkness were substituted for

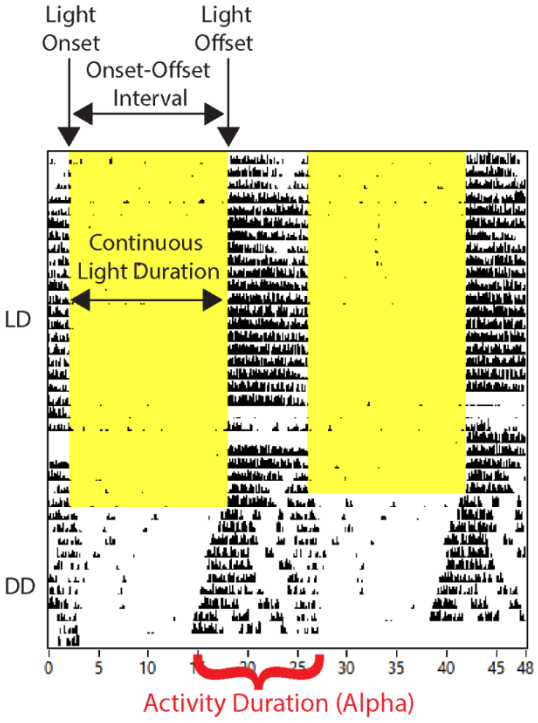

Figure 2-1. Example actogram showing the various components of a single light cycle. Each light transition (light onset, light offset) is capable of inducing a phase shift, which when entrained combine each cycle to match the required daily shift for entrainment. Parametric effects of light are exerted throughout retinal exposure to the light. Activity duration, or alpha, is visualized on the actogram as the portion of the day in which the

dark-to-light (dawn) and light-to-dark (dusk) transitions, and demonstrated that onset and offset transitions alone were sufficient to produce synchronization to most photoperiods[9]. This result implied a strong role for the non-parametric, phase-shifting effects of light at onset and offset. The duration of the light, a parametric input, also provides information to the clock: the pacemaker's phase alignment with skeleton photoperiods is for some intervals "bi-stable" (each 15-minute pulse can be aligned as either light onset or light offset), but full photoperiods produce only one stable phase alignment[9].

The approach to analyzing the parametric and non-parametric properties of photoperiodic light, described above to interrogate the mechanisms of general circadian entrainment, can also be applied to forming a better understanding of the mechanisms of photoperiodic encoding itself. Short and long photoperiods can be defined as light cycles in which the light duration is less than or greater than 50% of the total cycle length, respectively, such as 8:16 and 16:8 LD (roughly equivalent to the photoperiod at the winter and summer solstices in London, Paris, Berlin, or Vancouver). While short and long photoperiods overtly differ in light duration (8 hours vs. 16 hours), they also differ markedly in underlying non-parametric components. Based on conclusions drawn from two-pulse entrainment experiments (for review, see **Appendix A**/Tackenberg, *et al*. 2017[11]), discrete phase shifts are likely induced by the morning onset and evening offset of light.

When entrained to a particular light cycle, the circadian pacemaker undergoes a daily net phase shift, $\Delta\phi_{Eq}$, equal to the difference between the free-running period of the pacemaker, τ, and the period of the light/dark cycle, T ($\tau - T = \Delta\phi_{Eq}$). This daily net phase shift is the sum of the individual phase shifts evoked by the two light-dark transitions each cycle - phase advances caused by light onset ($\Delta\phi_{on}$) and phase delays caused by light offset ($\Delta\phi_{off;}$ $\Delta\phi_{on} + \Delta\phi_{off} = \Delta\phi_{Eq}$). Because the timing of entraining stimuli (light onset and offset) influences the magnitude and direction of resulting shifts, the difference in interval between $\Delta\phi_{on}$ and $\Delta\phi_{off}$ across photoperiods

can result in different component phase shifts, even if the net daily shift remains the same (e.g., a cycle with $\Delta\phi_{on}$ of +1 hour and $\Delta\phi_{off}$ of -1.5 hours and a cycle with $\Delta\phi_{on}$ of +0.5 hours and $\Delta\phi_{off}$ of -1 hour both have a net daily shift of $\Delta\phi_{Eq}$ = -0.5, despite different component phase shifts). The combination of component phase shifts is therefore one of the key differences between entrainment to different photoperiods.

To address the possibility that phase shifts may alter circadian properties in a similar fashion to different light durations, we combined phase-resetting light schedules with measurements of two clock properties that have been previously shown to have photoperiod-dependent after-effects: duration of locomotor activity (alpha) and free-running period (Figure 2-1). We analyzed the effects of single repeated phase delays and advances on alpha and free-running period and show that phase shifts, in particular repeated phase shifts, do induce changes to both free-running period and alpha without the introduction of asymmetric photoperiods.

Results

A single phase shift produces changes in free-running period but not alpha

Exposure to long photoperiods in nocturnal animals has been previously reported to be associated with a shortened daily duration of activity after transfer to constant darkness (DD), referred to as “after-effects”. Conversely, exposure to short photoperiods is associated with increased duration of activity. In particular circumstances, including developmental photoperiod exposure[71] and 20:4 L:D[92], prior entrainment to long photoperiods is associated with shortening of free-running period in subsequent DD, and short photoperiods with increased free-running period in subsequent DD. To test the response of the circadian system to a non-parametric light input, we exposed animals to a single one-hour phase-shifting light pulse within the advance or

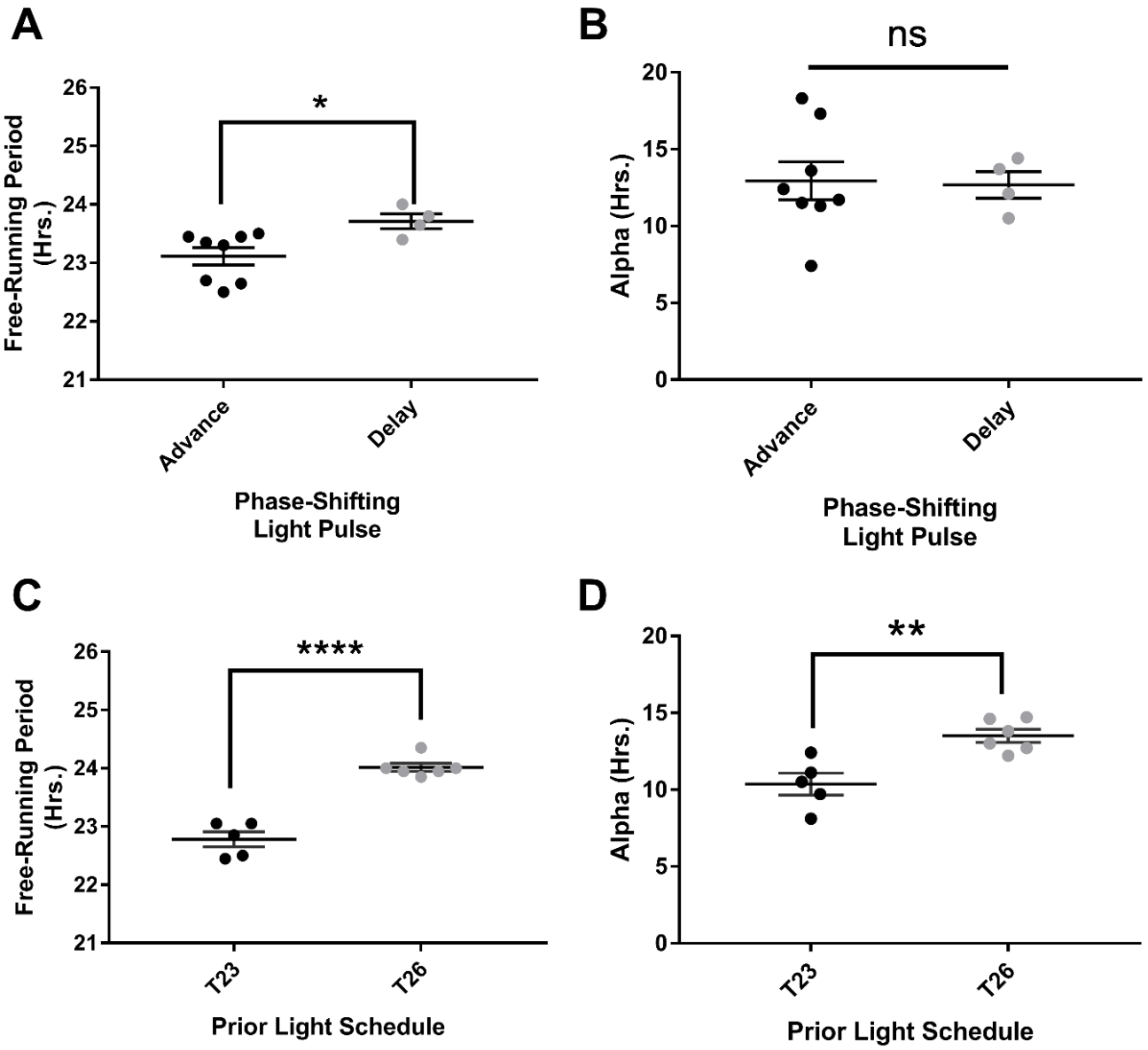

Figure 2-2. The effect of phase shifts on free-running period and alpha. **A**, a single phase shifting stimulus in the advance zone (mean shift +1.44 hrs., black circles, 23.11 ± 0.1481, n = 8) results in a significantly shorter free-running period compared to a single phase shifting pulse in the delay zone (mean shift -0.38 hrs., grey circles, 23.71±0.1264, n = 4; p = 0.0265, t-test). **B**, the phase shifting stimuli described in A have no significant effect on alpha (advance, black circles, 12.94±1.235; delay, grey circles, 12.68±0.8702; p = 0.8919, t-test). **C**, repeated phase advances result in a significantly shorter free-running period ("T23", black circles, 22.78±0.13, n = 5) than repeated phase delays ("T26", grey circles, 24.02±0.07032, n = 6; p < 0.0001, t-test). **D**, the light cycles described in C result in a significantly shorter alpha in T23 (black circles, 10.36±0.7167) compared to T26 (grey circles, 13.5±0.4211; p = 0.0034, t-test). All values mean ± SEM, in hours.

delay zone and assayed for changes in free-running period and activity duration in DD (Figure 2-2 A-B, Figure 2-S1A). We found that while phase advancing stimuli and phase delaying stimuli induced significantly different subsequent free-running periods (Figure 2-2A), there was no significant effect on the duration of locomotor activity on subsequent cycles (Figure 2-2B).

Repeated phase shifts produce changes in both free-running period and alpha

Because stable entrainment normally consists of repeated (daily) shifts, we then exposed animals to repeated phase shifts in the form of altered T cycles of 23 hours (T23, 11.5:11.5 L:D) and 26 hours (T26, 13:13 L:D, Figure 2-S1B). These cycles allow for the induction of a phase shift of a particular direction each day, without providing asymmetric photoperiodic input. Synchronization to these cycles resulted in repeated phase advances (T23) or delays (T26) from the near 24-hour free-running period of the mouse biological clock. We found that the repeated phase advances of T23 resulted in a significantly decreased free-running period when subsequently assayed in DD compared to the repeated phase delays of T26 (Figure 2-2C), suggesting a link between daily phase shift direction and the resulting period after-effect. Unlike single phase shifts, the repeated phase shifts also resulted in a significant change in activity duration, with animals previously entrained to T23 having a significantly shorter subsequent activity duration compared to animals entrained to T26 (Figure 2-2D). Given that a common factor between T23 and a long photoperiod is the presence of light in the late subjective night/early subjective day (typically a phase advancing stimulus), these results suggest a non-parametric effect of phase shifts on circadian after-effects.

Discussion

These results formally reaffirm that phase shifts have profound effects on after-effects in free-running period, and demonstrate that repeated phase shifts more strongly influence period after-effects than a single phase shift. Interestingly, these results also show that while a single phase shift has no measurable effect on locomotor behavior duration (alpha), there is a significant change in alpha after repeated phase shifts. Repeated advances produce a contracted alpha, and repeated delays an expanded alpha.

Given that long photoperiods produce a contraction in alpha, our results show a linkage between repeated phase advances and long photoperiods. This association is logical, as the long duration of light in a long photoperiod likely spans the phase response curve such that onset and offset cues occur both in the advance and the delay region, regardless of net phase shift. These results show that changes to alpha and period do not require changes to the light duty cycle, and demonstrate that phase shifts are capable of driving changes to these circadian properties.

2.2. Distinct Components of Photoperiodic Light are Differentially Encoded by the Mammalian Circadian Clock

Michael C. Tackenberg & Douglas G. McMahon

Modified from: Tackenberg, M.C., McMahon, D.G. Distinct components of photoperiodic light are differentially encoded by the mammalian circadian clock. *Journal of Biological Rhythms* (Under Review, 2019)

The duration of daylight, or photoperiod, represents a predictable and dynamic signal of seasonal change throughout the year across much of the planet. The predictability of this signal is harnessed by organisms to initiate or avoid a variety of biological functions at specific times of year, including reproductive behaviors[99], resource conservation[105,118], and migration[31]. In many organisms, including mammals, behavioral changes characteristic of a particular photoperiod can persist beyond exposure to that photoperiod[69], implying that information about photoperiod is stored internally. The master circadian pacemaker of the brain, the suprachiasmatic nucleus (SCN) of the hypothalamus, plays a major role in encoding these seasonal light signals (for review, see Tackenberg and McMahon, 2018[119]).

Recent work has shown that the SCN undergoes changes in organization after exposure to different photoperiods, including characteristic changes in the phase dispersal of its constituent neurons[89] and the waveforms of its firing rate and gene expression rhythms[69,71]. Much of this work has focused on how the patterns of SCN circadian neuronal activity are changed in response to these photoperiods, how it maintains those changes through differential chloride transporter activity[95] and neurotransmitter signaling[94], and how it reorganizes over time after transfer to constant conditions[92]. While much is known about the mechanisms of SCN

plasticity, less is known about which aspects of photoperiodic light cycles are encoded in the SCN.

There are considerable seasonal influences in human biology[35]. A variety of disorders and non-communicable diseases have seasonal correlations[38,40], with perhaps the most striking seasonal influence being on depression-anxiety behaviors[37,107]. In the seasonal regulation of mood, the shorter, winter-like photoperiods are generally associated with negative mood while the longer, summer-like photoperiods are generally more associated with improved mood[120]. Our lab has previously examined the developmental influence of seasonal light exposure, showing that the same long/short patterning in depression-anxiety behavior responses exists within nocturnal mice[107]. Despite the attention that seasonal light has received in recent years, and despite better characterization of what behaviors seasonal exposure drives, we still lack a firm understanding of exactly which aspects of seasonal light initiate these changes.

In order to extract the critical aspects of photoperiodic light signals, a better understanding of the mammalian response to different photoperiods is required. Here, we analyze the effects on the circadian clock of the constituent components of photoperiodic light cycles. We demonstrate that the persistent compression or expansion of locomotor activity duration (alpha), a circadian response to photoperiod, is induced by the duration of the interval between light/dark transitions regardless of concurrent repeated phase shifts in either direction, while plasticity in locomotor circadian period and phase is influenced by both net phase shift direction and light interval. We further demonstrate that an increase in phase dispersal of SCN neurons, like behavioral duration, is induced by light duration regardless of concurrent phase shifts. Plasticity in locomotor behavior duration in response to seasonal light therefore persistently encodes the interval between morning onsets and evening offsets of light, and we provide further evidence that seasonally-induced SCN neuron phase dispersal likely underlies changes in locomotor behavior duration.

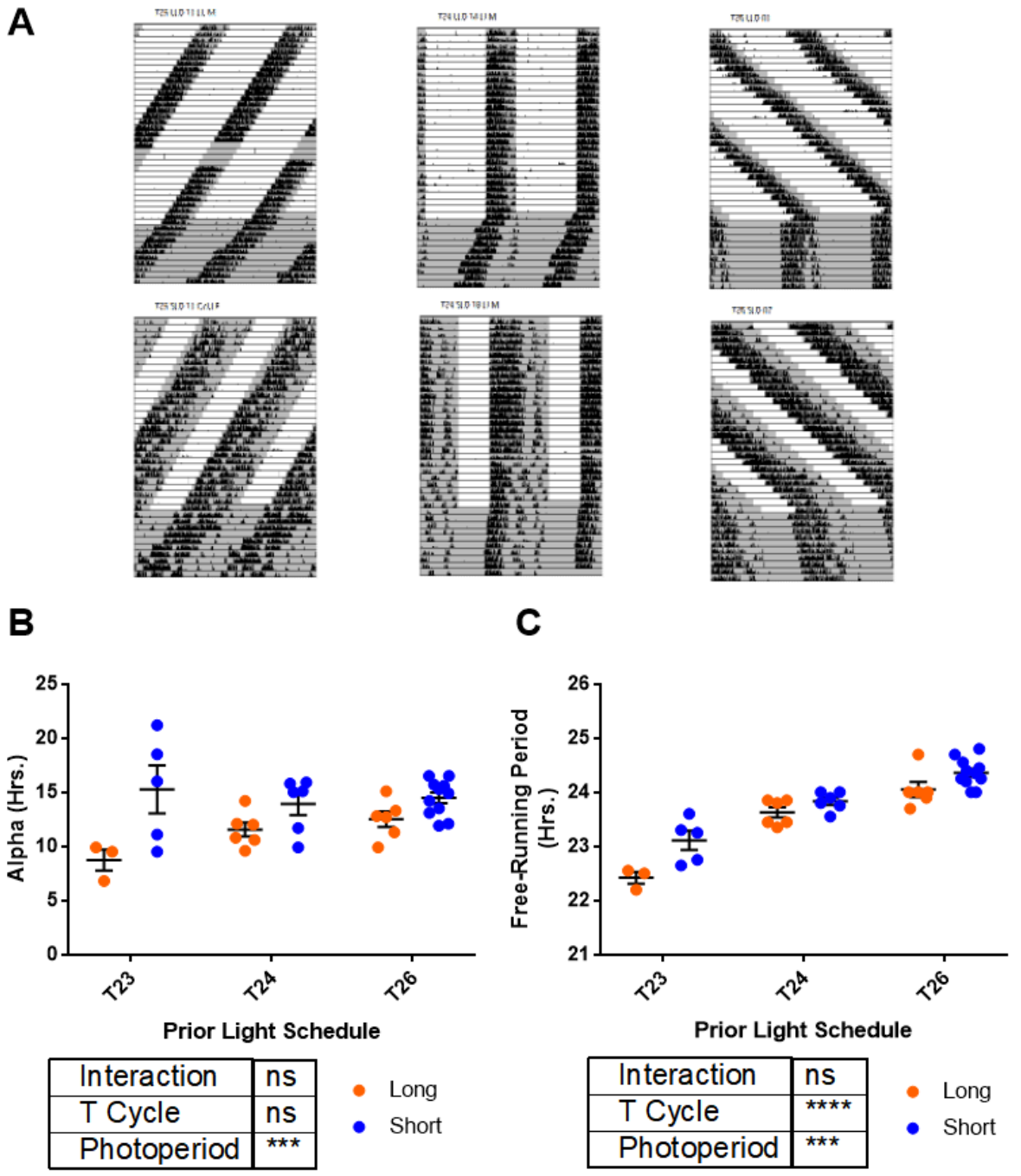

Figure 2-3. After-effects in alpha and period induced by prior entrainment to various T-cycle/photoperiod combinations. **A,** representative long (top row) and short (bottom row) actograms from T23 (left column), T24 (center column), and T26 (right column). **B**, alpha responds to photoperiod rather than T cycle. Alpha is shorter after long photoperiods compared to short photoperiods across all T cycles (source of variation: interaction, 9.25%, $p = 0.1120$; T cycle, 3.89%, $p = 0.3837$; Photoperiod, 33.69%, $p = 0.0002$; two-way ANOVA). **C**, period responds to T cycle and photoperiod. Period length increases with T cycle and decreases as photoperiod duty cycle increases (source of variation: interaction, 1.99%, $p = 0.1691$; T cycle, 72.59%, $p < 0.0001$; Photoperiod, 9.01%, $p = 0.0003$; two-way ANOVA). Note: the gap in activity during the LD epoch of T23 Long (A, top left) is the result of a data-acquisition error.

Results

Duration of the light phase drives after-effects in activity duration

Light affects the period and phase of the clock both through the induction of resetting phase shifts and as a function of light input duration. To differentiate between the phase-shifting effects of photoperiodic light cycles and the effect of light duration on clock plasticity, we combined the repeated phase shift component of non-24 T cycles with altered light/dark duty cycles. These T-cycle/photoperiod combinations (T23 Long, LD 15:8; T23 Short, LD 8:15; T24 Long, LD 16:8; T24 Short, LD 8:16; T26 Long, LD 17:9; T26 Short, LD 9:17, Figure 2-S1) allow for the separation of the main effects of net phase shifts and light duration on photoperiodic encoding. We hypothesized that after-effect measurements across the 6 groups would align in one of four possible patterns (Figure 2-S2). First, if strictly dependent on the duration of the light interval, then the groups may segregate into two levels, corresponding to long or short light phases, regardless of T cycle influence (Figure 2-S2A). Second, if plasticity is strictly dependent on the net daily phase shifts, then the measurements would segregate into three groups based on T cycle with little influence from the duration of the light interval (Figure 2-S2B). Third, a significant influence from both T cycle and photoperiod would result in after-effects with each of the 6 groups having a characteristic level (Figure 2-S2C). Last, if the presence of a significant daily phase advance component (a property shared between all T23 cycles and T24 Long) is critical on its own, then measurements may fall into two groups with T23 (both Long and Short) aligning with T24 Long, and T26 (both Long and Short) aligning with T24 Short (Figure 2-S2D).

We measured activity duration and period for 7 cycles in DD following entrainment to these 6 light schedules for at least 28 days (Figure 2-3A). The duration of the light phase was found to be the driving influence on alpha, with persistent decreases in activity duration upon release into DD observed in long photoperiod (15-17 hours of light/day) compared to short (8-9 hours of light/day) across all three T cycles (Figure 2-3B). This pattern most closely resembles

the example in Figure 2-S2A. In contrast, we found the locomotor period in DD following entrainment to these 6 groups was influenced by both net phase shift direction and light phase duration (Figure 2-3C). This pattern most closely resembles the example in Figure 2-S2C.

The interval between light transitions is critical for the activity duration after-effect

The long photoperiod light cycles used with T23, T24, and T26 (15:8, 16:8, 17:9) could produce shortening of activity duration that persisted in DD either through extending the duration of light exposure or through the differential timing of light/dark transitions. To discriminate between these two possibilities, we used skeleton long or short photoperiods consisting of two 1-hour pulses of light, separated by intervals of darkness, that mimic full photoperiods of 16:8 and 8:16 (Figure 2-S1D). Skeleton photoperiods have been used historically to assess the mechanism of entrainment through seasonal changes in phase angle[9], as well as to determine the proximal effect on locomotor behavior duration[90]. In order to determine whether skeleton photoperiods can induce plasticity in alpha, we assessed after-effects in locomotor behavior duration in DD following 28 days of exposure to skeleton long or short photoperiods. This experiment allows us to assess whether a complete long photoperiod is required to induce the compressed activity duration after-effect (Figure 2-4A). Our results show that, even with only 2 total hours of light per day, the 16-hour interval between onset and offset pulses in the skeleton long photoperiod was sufficient to induce the compression of activity duration after-effect (Figure 2-4B). We found that the skeleton photoperiods had no significant effect on period (Figure 2-4C), however previous investigators have reported modest period after-effects of skeleton photoperiods[90]. Our findings demonstrate that the interval between light onset and offset, rather than the extended duration of light, is critical for establishing the activity duration after-effect.

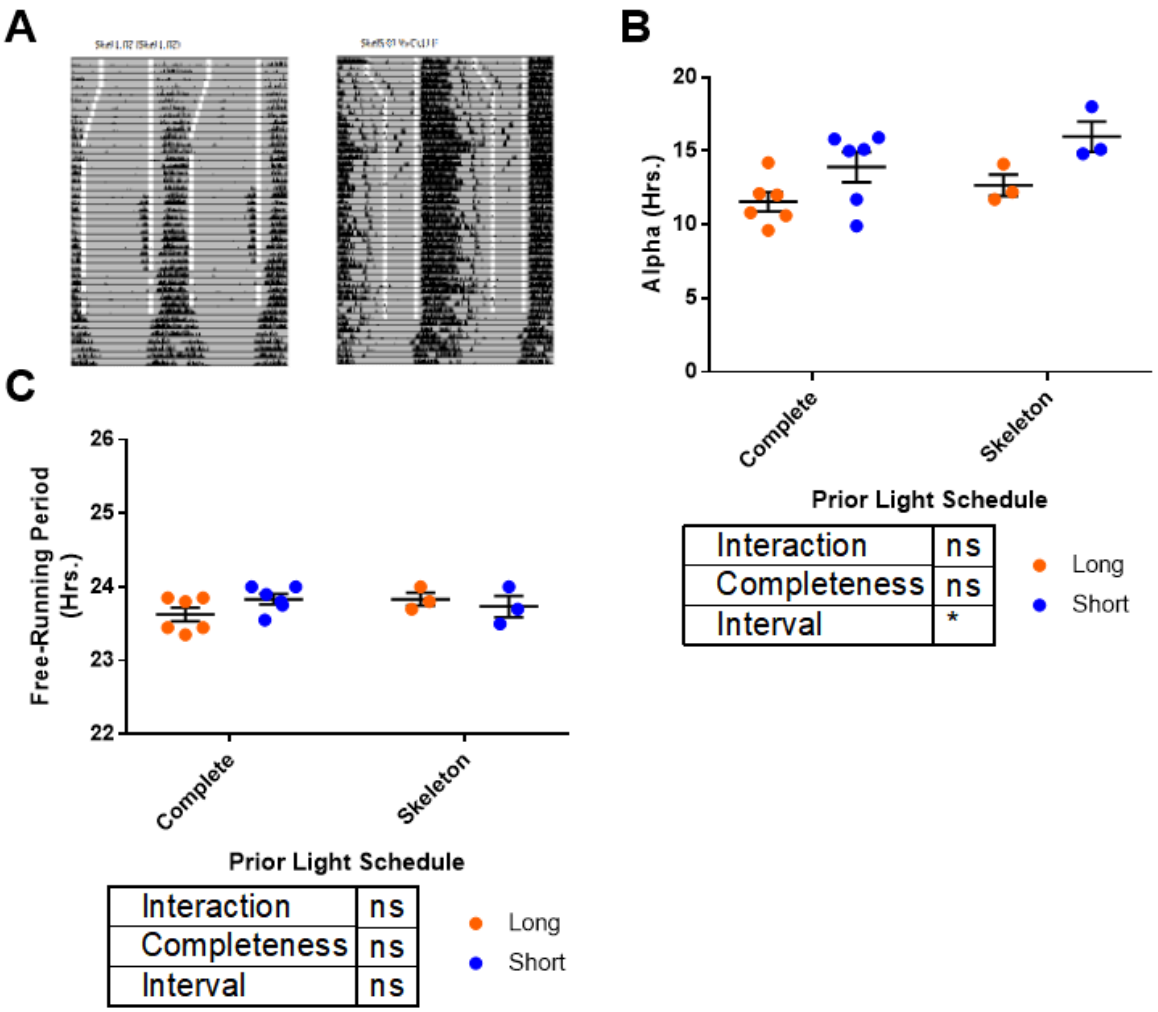

Figure 2-4. After-effects in alpha and period induced by prior entrainment to short and long skeleton photoperiods. **A**, representative actograms from skeleton long (left) and short (right). **B**, alpha is modified by photoperiod onset-offset interval rather than the duration of light per cycle. Alpha is shorter after both skeleton and complete long photoperiods compared with their short photoperiod counterparts (source of variation: interaction, 0.94%, p = 0.6340; "Completeness", 10.51%, p = 0.1252; Interval, 33.12%, p = 0.0118; two-way ANOVA). **C**, There is no differential effect of completeness or interval duration on period. Period effects remain flat between long and short complete photoperiods and between long and short skeleton photoperiods, as well as between the two overall groups (source of variation: interaction, 12.72%, p = 0.1555; "Completeness", 1.57%, p = 0.6061; Interval, 1.57, p = 0.6061; two-way ANOVA).

Changes in the phase distribution of SCN rhythms underlie changes to activity duration

We next investigated the effect of photoperiodic light exposure on plasticity of the SCN pacemaker, using *ex vivo* real-time gene expression imaging following entrainment to the range of light cycles described above. Previous studies have found that photoperiod has significant effects on the phase distribution of neuronal rhythms within the SCN[69,71,89], with long photoperiods driving a widening of SCN neuron phase distribution and short photoperiods driving a tightening of that distribution. Those results demonstrate that there is an influence of photoperiod on SCN neuron phase dispersal, but like photoperiod effects on alpha, further characterization is required to determine the aspects of light input required to drive this change. We hypothesized that SCN neuron phase distribution, which is thought to underlie behavioral activity duration, would also be driven by the light interval component of photoperiods. Thus we sought to determine the relative influences of light duration and repeated phase shifts on SCN phase dispersal.

To do so, we housed animals in identical conditions to our complete photoperiod *in vivo* experiments (Figure 2-S1C), including running wheels, and collected SCN slices from PERIOD2::LUCIFERASE (PER2::LUC) animals after at least 28 days of exposure to each of the light schedules discussed above. Slices were collected within 4 hours prior to lights off, maintained in organotypic culture, and PER2::LUC luminescence recorded *ex vivo* for 5-7 days (see Methods). We found that the duration of the light interval in the preceding entraining light cycle modulated the distribution in phase of SCN rhythms regardless of T cycle length of the previous light cycle (Figure 2-5A-B), resulting in broader phase distributions of SCN neurons in slices from animals entrained to long photoperiods compared to short. These results comport with activity duration after-effects *in vivo*, closely resembling the light interval-dependent example pattern (Figure 2-S2A).

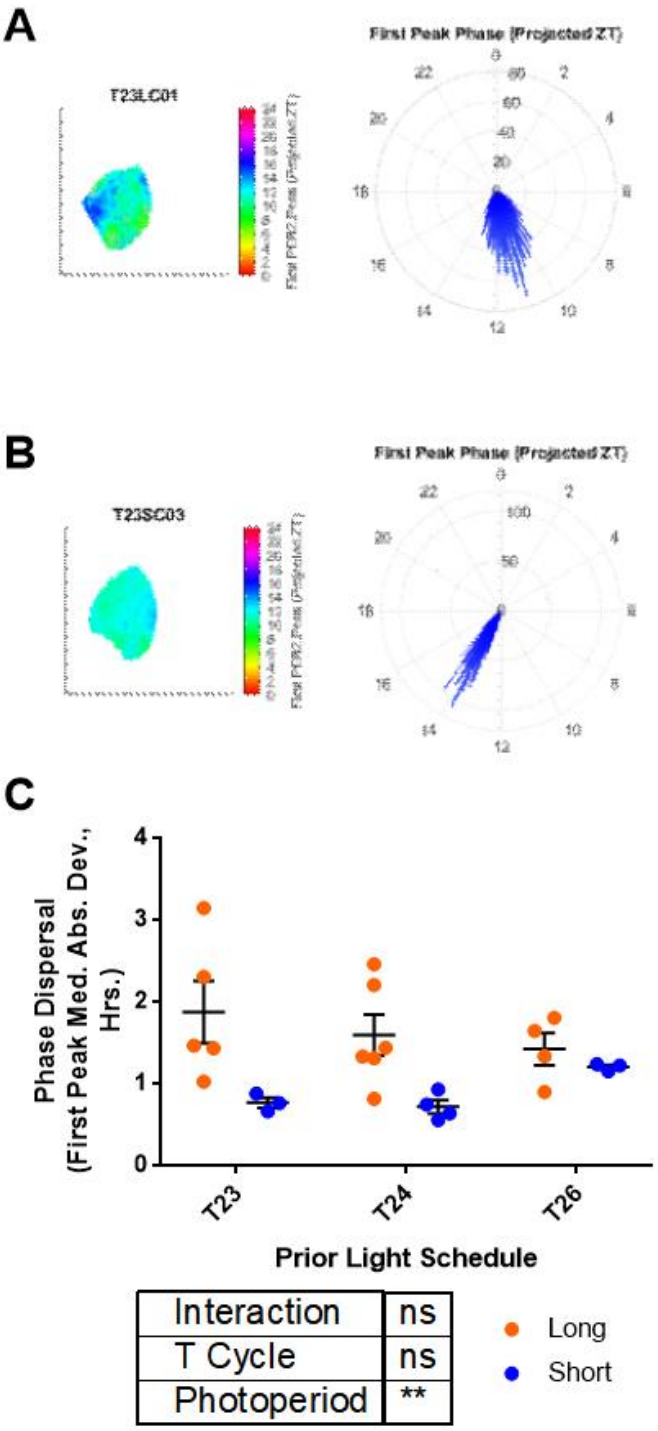

Figure 2-5. Phase dispersal in the SCN. Representative phase maps (left) and phase distribution plots (right) for T23 Long (**A**), and T23 Short (**B**). **C**, The effect of 6 photoperiod and T cycle combinations on phase distribution *ex vivo***. P**hase distribution across the SCN increases in long photoperiod slices regardless of T cycle (source of variation: Interaction, 7.788%, p = 0.2828; T cycle, 1.542%, p = 0.7681; Photoperiod, 32.32%, p = 0.0034; two-way ANOVA). All values measured as median absolute deviation.

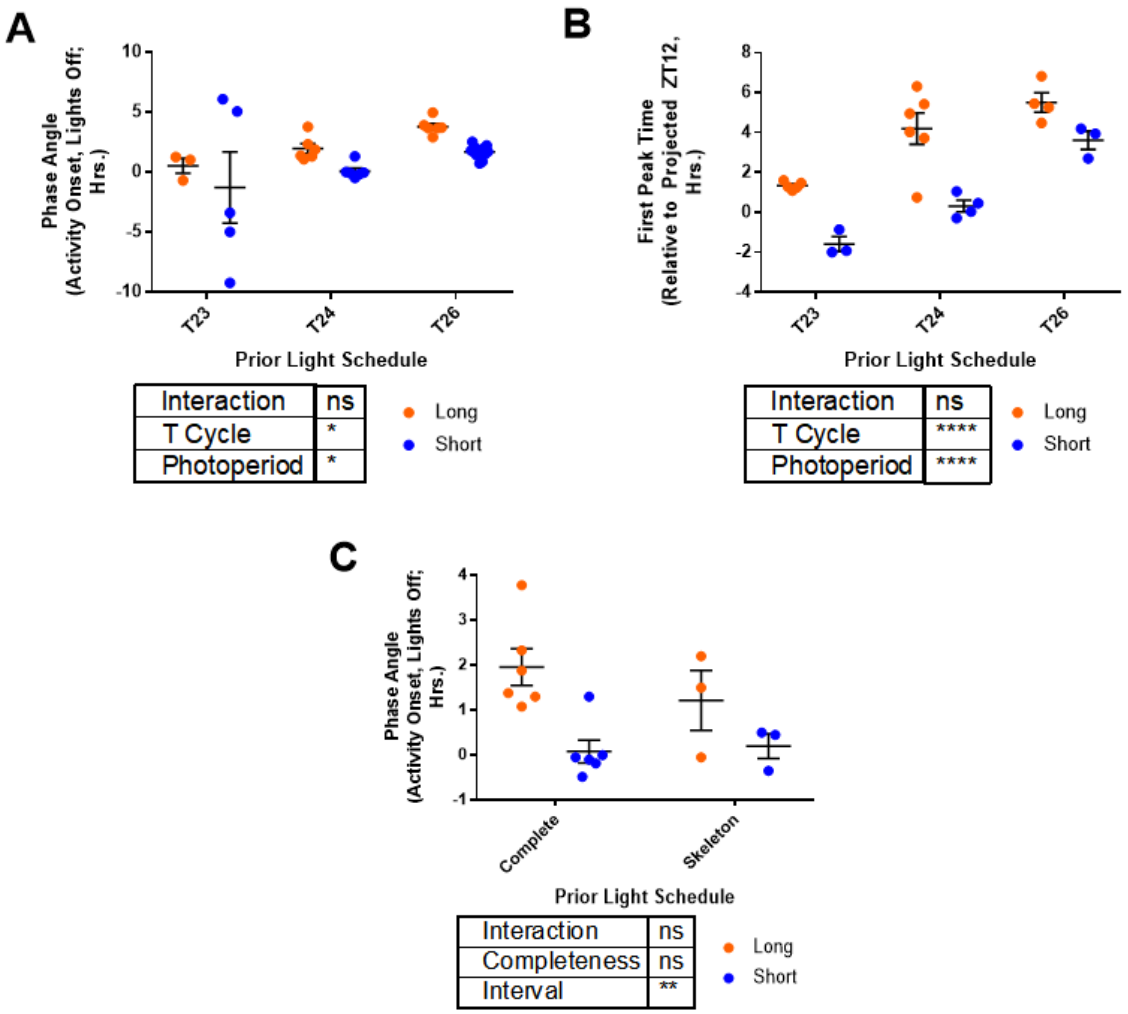

Figure 2-6. Phase angle measurements. A, *in vivo*, phase angle is more advanced in long photoperiods compared to short and in longer T cycles compared to shorter T cycles (source of variation: Interaction, 0.06%, $p = 0.9876$; T cycle, 19.21%, $p = 0.0221$; Photoperiod, 10.92%, $p = 0.0341$; two-way ANOVA). **B**, *ex vivo*, phase angle is more advanced in long photoperiods compared to short, and in longer T cycles compared to shorter T cycles (source of variation: Interaction, 2.52%, $p = 0.2426$; T cycle, 49.86%, $p < 0.0001$; Photoperiod, 31.22%, $p < 0.0001$; two-way ANOVA). **C**, entrainment to skeleton photoperiods *in vivo* show that onset/offset interval is critical for establishing photoperiod-dependent phase angle of entrainment (source of variation: Interaction, 3.281%, $p = 0.3269$; Completeness, 1.724%, $p = 0.4737$; Interval, 37.14%, $p = 0.0042$; two-way ANOVA).

The effects of seasonal light on phase angle of entrainment of overt behavioral rhythms are well documented[9]. To examine whether the light schedules described above have comparable effects *in vivo* and *ex vivo*, we measured the phase angle of the circadian rhythm in both behavior and in the *ex vivo* SCN (Figure 2-6). We found that both *in vivo* (Figure 2-6A)

and *ex vivo* (Figure 2-6B), the alignment of the rhythm (locomotor activity and PER2::LUC expression, respectively) was earlier relative to the projected time of lights offset of the light/dark cycle in long animals vs. in short animals. There was also a significant effect of T cycle, with phase angles becoming more advanced with increasing T cycle length both *in vivo* and *ex vivo*. This pattern followed the example given in Figure 2-S2C. In response to skeleton photoperiods, the interval between onset and offset light pulses was again sufficient to induce phase plasticity (Figure 2-6C). These results indicate that the SCN network and the overt behavioral rhythm respond similarly to exposure to these light schedules, with the presumption being that the plasticity observed in the duration, period, and phase of locomotor rhythms is an outcome of the network level photoperiodic plasticity induced in the SCN.

Discussion

We sought to examine the specific influences of different components (repeated phase shifts, light duration, onset-offset interval) of the daily light cycle in inducing photoperiodic plasticity in the SCN, represented as circadian after-effects of exposure to long and short photoperiods. We found that the interval between light onset and offset has a strong effect on activity duration after-effects (Figure 2-3A) independent of daily net phase shifts. In contrast, after-effects on locomotor period and encoding of phase were influenced by daily net phase shifts, as well as light interval duration (Figure 2-3B, Figure 2-6A). Focusing on the light-interval-mediated after-effect on activity duration, we showed that onset-offset interval, rather than the continuous duration of light, was critical for inducing plasticity in activity duration (Figure 2-5A).

The degree of synchrony between neurons in the SCN network sets the overall waveform of SCN rhythms and likely underlies the duration of daily locomotor activity. Building on previous results that investigated the degree of synchrony of SCN neurons encoded to

different photoperiods, we expand those findings by examining the response to different aspects of light cycles. We find that, like activity duration after-effects following photoperiodic entrainment, the degree of phase dispersal in the *ex vivo* SCN increases as a function of previous light duration, independent of repeated phase shifts (Figure 2-5). Interestingly, we found that both previous light duration and the direction of repeated phase shifts had a significant influence on the phase of both locomotor and gene expression rhythms (Figure 2-6A-B). Entrainment to skeleton photoperiods revealed that the onset-offset interval was the critical aspect of the light phase influence on locomotor rhythm phase (Figure 2-6C).

Measurements in constant conditions reveal properties of the SCN and downstream circadian outputs free of light input, and as such the study of after-effects is one means to understand the plasticity of the SCN in response to seasonal light conditions. Understanding after-effects is also useful *per se*, as the encoding of light information within the SCN allows seasonal circadian properties to remain stable across ephemeral changes in the environment. Organisms in the wild experience fluctuations in light exposure during the annual photoperiodic cycle because of weather, nesting, hibernation, and other factors. Stable but flexible encoding of seasonal light inputs within the circadian system would allow for consistency across these light exposure fluctuations.

Changes to SCN synchrony may also have additional ramifications in the form of altered responses to light input, potentially explaining previously observed larger phase shifts after exposure to short days and smaller phase shifts after exposure to long days[121]. The role of SCN neuron phase dispersal in mediating those altered responses and altered free-running period has been explored computationally[122] and through altered GABA signaling[94]. In their analysis of after-effects on free-running period, Pittendrigh and Daan (1976b) suggested that this change in circadian property may provide some functional significance in terms of priming future

responses to light, but it remains to be seen whether any of these after-effects constitutes an adaptive advantage or if they are simply a side effect of altered network synchrony.

Because current methods for *in vivo* imaging are limiting, the measure of activity duration after-effects may be a useful proxy for inferring the waveform of the SCN. The integrity of this SCN waveform/activity duration connection depends on how well we can characterize the correlation between the two. Our findings that alpha and SCN neuron phase dispersal associate across multiple lighting conditions regardless of net daily phase shift do not address causality, but strengthen the association between the two measurements. As the broadened electrical waveform of the SCN is associated with the compressed activity duration seen in long photoperiods (and the contracted waveform with extended activity duration in short photoperiods), the spread in phase of SCN neurons and the corresponding widening of overall firing that occurs as a result should account for the observed changes in activity duration[124].

The degree of SCN neuron phase dispersal is a characteristic attribute of photoperiodic encoding, as it represents a change in state of the SCN that is induced by the duration of the light interval of the light cycle and then is maintained after transfer to constant conditions[69,71,89]. The spread in the timing of neuronal rhythms allows for the overall high firing phase of the SCN to be broadened or contracted without required alteration to the waveforms of individual SCN neurons although this aspect is modulated by developmental inputs[71]. As such, the degree of phase distribution within the SCN is a potential target for artificial SCN manipulation – driving neurons to adopt the phase distribution characteristic of a photoperiod, such as by pharmacologically, optogenetically, or chemogenetically extending the high firing phase, would be expected to induce the behavioral activity duration characteristic of that particular photoperiod, and perhaps other photoperiod-dependent responses, such as reproductive state and affective behaviors. Last, we demonstrate that the SCN clock gene rhythms correlate with

the overt behavioral rhythm in our studies, providing evidence that our *ex vivo* work has relevant ties to our *in vivo* experiments (Figure 2-6).

Taken together, our results show that the impact of photoperiodic light exposure on the circadian system has separable input components, with light interval driving plasticity in activity duration and phase shifts and light interval driving plasticity in period and phase. These results open the door to selective manipulation of circadian plasticity in activity duration or period for experimentation or therapy. The results shown here also demonstrate the utility of deconvolving overlapping types of input when studying complex processes within the SCN. With new techniques currently being established in our field to measure firing rate, calcium signaling, and activity levels with high cellular specificity and extended timeframe, there will be an improved ability to characterize the specific effect of photoperiodic influences on these circadian components.

Materials and methods

Animals

Animal experiments were conducted in accordance with Vanderbilt University Institutional Animal Care and Use Committee regulations. All animals used were of *Per2::Luciferase*$^{+/-}$ genotype.

Activity monitoring, housing, and optogenetics

Animals were singly-housed in light-tight boxes with activity monitored by wheel revolutions detected by ClockLab acquisition software (Actimetrics, Inc.). Animals were transferred to the

specified light schedule after post-natal day 21 (weaning), and housed there for at least 28 days before transfer to DD or brain extraction for slicing.

Skeleton photoperiods were set up by housing animals in 12:12 LD complete photoperiods for approximately 5 days before transitioning to a 12:12 skeleton (1:10:1:12 L:D:L:D). After several cycles on this skeleton, the onset pulse was gradually advanced (0.5 hour – 1 hour per day) or delayed (1 hour per day) until a skeleton long (1:14:1:8 L:D:L:D) or skeleton short (1:6:1:16 L:D:L:D) photoperiod, respectively, was established. Once the final skeleton was established, animals were given 28 days until transfer to DD.

Actogram analysis

Locomotor behavior was analyzed using ClockLab Analysis software. Period was determined using chi square periodogram over the first 7 days of DD. Alpha was measured by tau-adjusted 7 day activity profile, with onsets and offsets automatically selected using a threshold hinged on the root mean square of the average noise of activity monitoring for an individual animals' lowest activity bins (see **Chapter 4.3**)

Slicing and slice cultures

Within 4 hours of lights off, animals were sacrificed by cervical dislocation and the brain removed. SCN slices of 200-μm were made, and the SCN further isolated by scalpel cut under a dissecting microscope. Slices were transferred to a 6-well plate with cell culture membrane insert (Millipore, PICMORG50) and 1.2-mL of slice culture media. Slice chambers were sealed with a coverslip and vacuum grease and placed into an incubated light-tight inverted microscope

(Zeiss Axioskop). Luminescence was detected using an intensified CCD (Stanford Photonics) controlled by µ-*Manager recorded for 2' every 10' for at least 1 week.*

Ex vivo analyses

Luminescence recordings were analyzed using Fiji and MATLAB. OME-TIFF files from µ-Manager were opened in Fiji and smoothed using a two-frame minimization (frame rate reduction from 6/hour to 3/hour, Figure 2-S3A, left). A 102x102 grid of 10x10-pixel ROIs was overlaid on the images (Figure 2-S3A, middle, right) and brightness measured for each of these 10,404 ROIs measured for every frame. These grid measurements were then exported to MATLAB for further analysis. The first 8 hours of recording were excluded from peak-finding to prevent slicing artifacts from interfering with measurements (see Figure 2-S3 and **Chapter 4.4**)

First, the ROIs comprising the SCN were separated from background through 2-cluster k-means clustering (Figure 2-S3B). Among these ROIs, the two SCN were then separated using hierarchical agglomerative clustering (Figure 2-S3C). Of the two SCN in each image, only the SCN with the most ROIs was used for analysis. The timing of each peak of luminescence was then detected for each ROI and used to calculate the initial phase, phase angle, and period (via average interpeak interval time across the recording). Distribution measurements were made by median absolute deviation across all SCN ROIs.

Acknowledgments

The authors would like to thank Maria Luísa Jabbur, Carl Johnson, Terry Page, and Chloe Snider for their helpful comments and discussions. This work was supported by NIH R01 GM117650 to D.G.M., NIH F31 NS096813 to M.C.T., and NSF GRFP 0909667 to M.C.T.

Author contributions

M.C.T. and D.G.M conceived the experiments. M.C.T. performed the experiments. M.C.T. and D.G.M. wrote the paper.

Supplemental figures

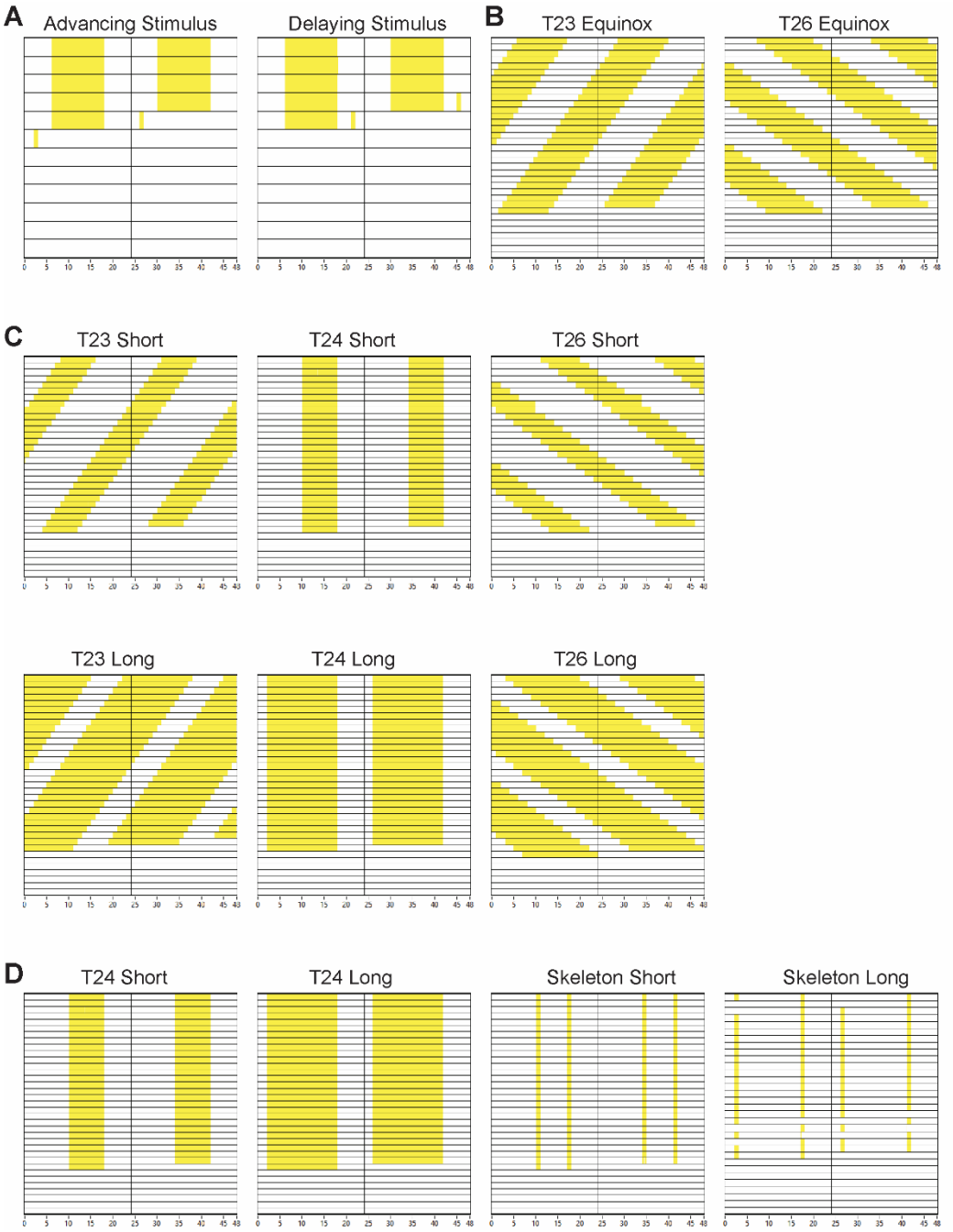

Figure 2-S1. Light schedules used in non-optogenetic experiments. **A**, T24 Equinox with an advancing stimulus (left) or a delaying stimulus (right) on the first day of DD. **B**, T23 Equinox (left) and T26 equinox (right). **C**, T23 (left column), T24 (center column), and T26 (right column) cycles as short (top row) or long (bottom row) photoperiods. **D**, Re-plotting of T24 Short and Long from C (left) in comparison with Skeleton Short (third column) and Skeleton Long (right-most column). Gaps in skeleton long were photodiode light sensor disruptions, rather than actual light disruptions.

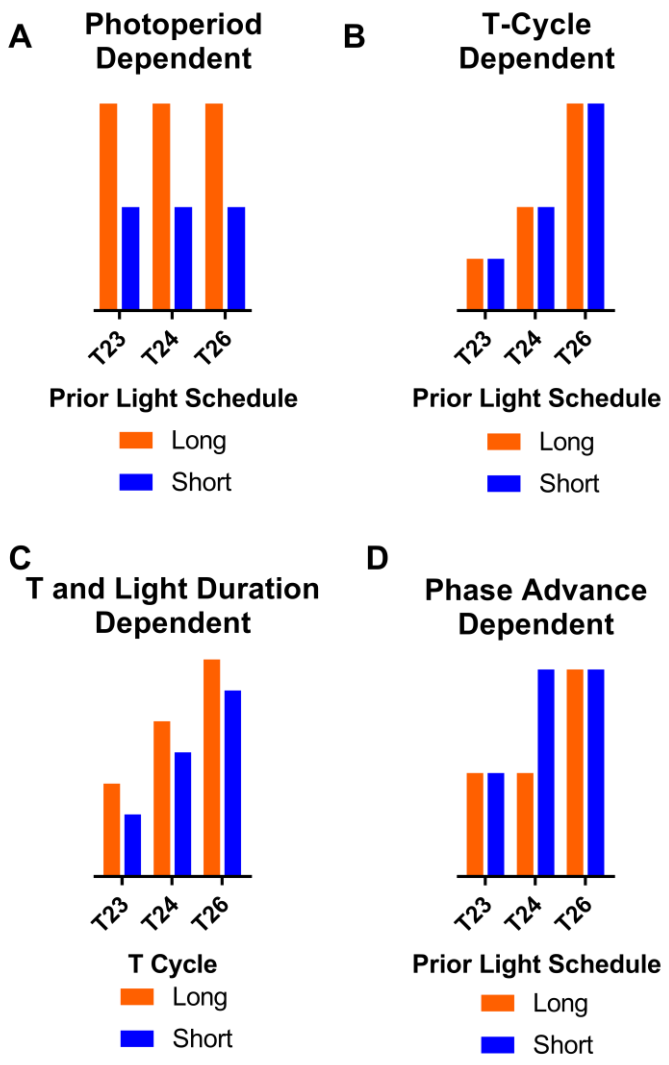

Figure 2-S2. Schematic of possible patterns of measurements across T23 L/S, T24 L/S, and T26 L/S. **A**, a T-cycle dependent response where the measurement is graded depending on the T cycle and photoperiod within the T-cycle has negligible effects. **B**, a photoperiod-dependent response where light duty cycle dictates the measurement regardless of T cycle. **C**, a combination of photoperiod and T cycle influences, with each of the 6 combinations having a characteristic measurement level. Note that in all examples, the polarity of the measurement change is arbitrary (e.g., T cycle response in A can increase or decrease with T cycle, photoperiod response in B can have either Long or Short measure higher). **D**, a phase-advance dependent response resembling a step-function in which T24 Long (advance component present) aligns with T23 (advance component present) and T24 Short (little/no advance component) alongs with T26 (little/no advance component).These patterns are illustrations of individual and combined main effects; possible interaction effects are not shown.

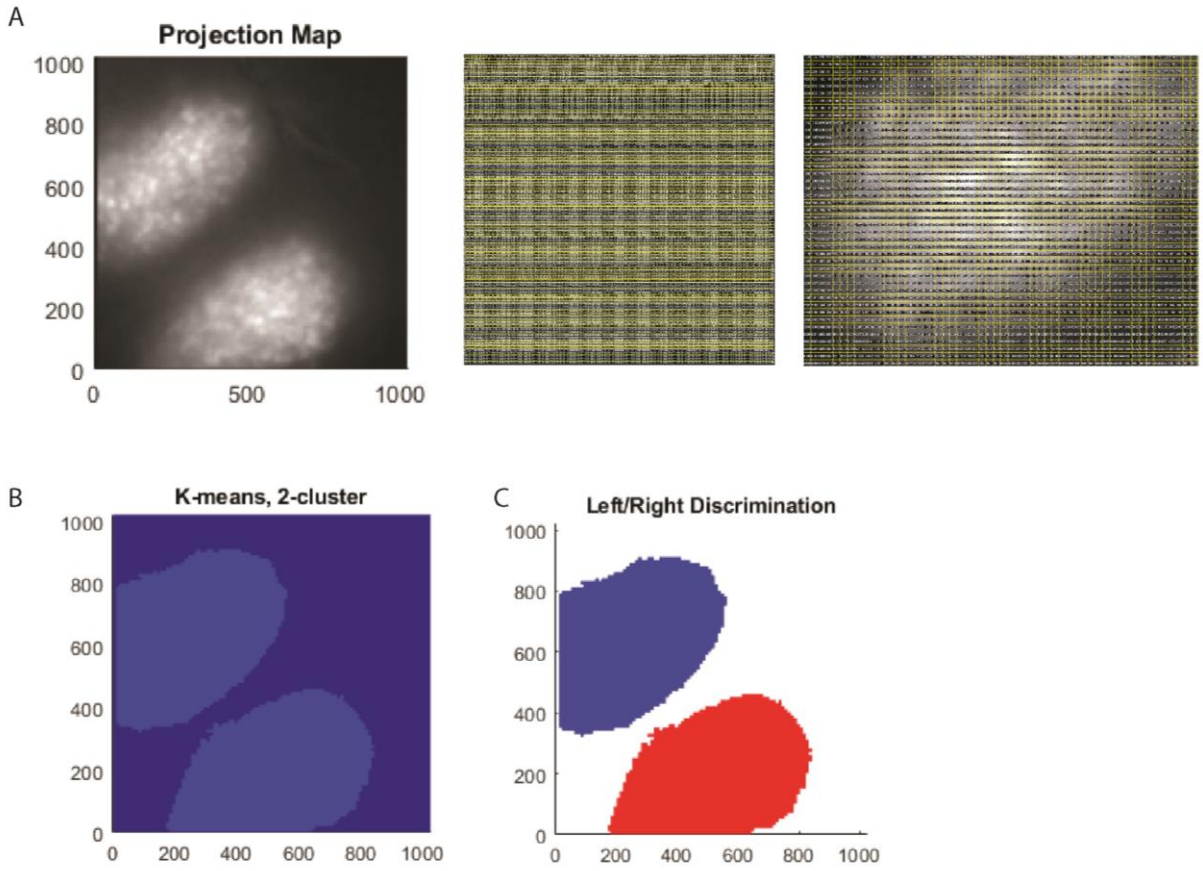

Figure 2-S3*. Ex vivo* workflow. A, SCN projection map (left) overlaid with 10 x 10 pixel ROIs (center), with zoomed in example (right). **B**, k-means determined separation of tissue from non-tissue. **C**, hierarchical agglomerative clustering separation of left and right SCN.

Chapter 3

The Role of VIPergic SCN Neuron Activation in Photoperiodic Response

3.1. The Cellular Basis of Photoperiodic Induction

The mechanism of communication within the SCN network is an important research focus in circadian biology. These questions surround the way in which an ensemble of 20,000 individual units, all of which are capable of self-sustaining oscillations, collectively drive an overall circadian rhythm that persists in constant conditions but also integrates light input. As a brain structure, the avenues with which the SCN communicates are predominantly neurotransmitter and neuropeptide mediated. The SCN is largely GABAergic, with the size and morphology of its neurons fitting the characteristics of inhibitory interneurons[19]. Despite this motif, the neurons of the SCN are functionally quite different from interneurons. As described in **Chapter 1.1**, tight circadian transcriptional and translational regulation of ion channel expression leads to daily windows of spontaneous firing. Another distinguishing factor is the prominent use of neuropeptides, signaling molecules that differ from traditional neurotransmitters by their larger size, dense-core vesicle packaging, cell-body synthesis, and lack of reuptake. In the context of the SCN, chief amongst these neuropeptides is vasoactive intestinal polypeptide, or VIP.

VIP is a deservedly well-studied component of the mammalian circadian system. It is expressed in approximately 15% of SCN neurons, largely within the ventrolateral or “core” SCN[19]. As such, it is expressed in the same region that features heavy retinal innervation. The receptor of VIP, $VPAC_2R$, is far less restricted in its expression[125], expressed in approximately 60% of SCN neurons with no subregion-specific distribution. Functionally, $VPAC_2R$ is a G-

protein coupled receptor associated with the $G_{\alpha S}$ subunit. VIP binding with $VPAC_2R$ therefore leads to a signaling cascade that converges upon the upregulation of CREB-mediated genes (such as the *Per* genes) and an increase in intracellular calcium. This $G_{\alpha s}$ signaling is particularly interesting, as other SCN neuropeptides (such as gastrin releasing peptide and arginine vasopressin) bind to receptors that initiate $G_{\alpha q}$ signaling (bombesin, V1A/V1B) or (like neuropeptide Y) $G_{\alpha i}$ signaling (NPYR).

The disruption of VIP synthesis and reception has been well studied. In mice lacking VIP expression, rhythmicity in DD is severely impaired if not eliminated, phase angle of entrainment is altered, and masking (non-entrained synchronization to LD cycles caused by clock-independent direct activity drive) is also decreased[126]. The lack of $VPAC_2R$ has similar effects, with decreased rhythmicity in DD and minimal synchronization in LD[127]. *Ex vivo*, dispersed cultures of SCN neurons showed decreased percentage of rhythmically firing neurons without VIP signaling[128]. The lack of VIP signaling has been shown by Ciarleglio *et al.* to interfere with overt rhythmicity likely through a decrease in synchronization[129].

Because VIP signaling disruption prevents coherent free-running behavioral rhythms, but does allow for some masking in LD, the role of VIP may be to perpetuate in constant conditions the type of excitatory input that is, in LD, provided by retinal-mediated light input. VIP signaling converges on a similar set of circadian genes, and the position of VIPergic SCN neurons in the retinorecipient region of the SCN reveal an association between those two forms of SCN communication.

Interestingly, VIP signaling is critical for maintaining seasonally induced after-effects in alpha. While wild type mice show a compression of alpha both during exposure to a long photoperiod and afterwards, VIP-KO mice in the same conditions revert back to an equinox-level alpha after transfer to DD[96]. Given that VIP signaling disruption is known to decrease synchrony between SCN neurons, and that SCN phase dispersal has been shown to be an

associated factor in alpha after-effects (see Buijink, *et al*. 2016[89] and **Chapter 2.2**), VIP likely plays a role in the seasonal encoding that the SCN undergoes when exposed to photoperiodic light. In the following section, I will address that possibility by examining the role of activation of VIPergic SCN neurons in seasonal encoding of locomotor behavior duration using targeted optogenetic stimulation *in vivo*.

3.2. Activation of VIPergic SCN Neurons is Sufficient to Induce Photoperiodic Changes to Behavior and SCN Phase Distribution

The responses to seasonal light, or photoperiod, include well known effects on reproductive and hibernation behaviors in some mammals, but also on complex human cognitive factors like depression and anxiety. Though we have improved our understanding of seasonal responses in recent years, particularly with regard to their relationship to the circadian clock, there remain several poorly understood underlying mechanisms. Previous work from our lab and others has demonstrated that seasonal light induces proximal and persistent changes in locomotor behavior duration and in the mammalian master clock, the suprachiasmatic nucleus (SCN), in the form of altered neuronal phase dispersal[69,71,89] (see **Chapter 2.2**). These results strongly suggest that seasonal light drives changes in SCN phase dispersal, which in turn alter the overall signaling waveform of the SCN and lead to downstream changes to locomotor behavior and other physiological properties.

It remains an open question, however, how the SCN network alters its phase distribution in response to seasonal light exposure. The first and most important step in unveiling this mechanism is to determine the network component within the SCN that propagates this seasonal signal to the rest of the network. One strong candidate for such a network component is the SCN neurons that express vasoactive intestinal polypeptide (VIP). The VIPergic SCN is largely retinorecipient and located within the ventrolateral portion of the nucleus. These neurons have recently been shown to be critical for normal phase shifting responses to light[130]. The VIP neuropeptide itself has also been shown to be critical for the maintenance of photoperiodic after-effects into constant darkness (DD)[96]. Further, the VIP signaling that these neurons facilitate has been shown to be associated with synchronization levels across the SCN.

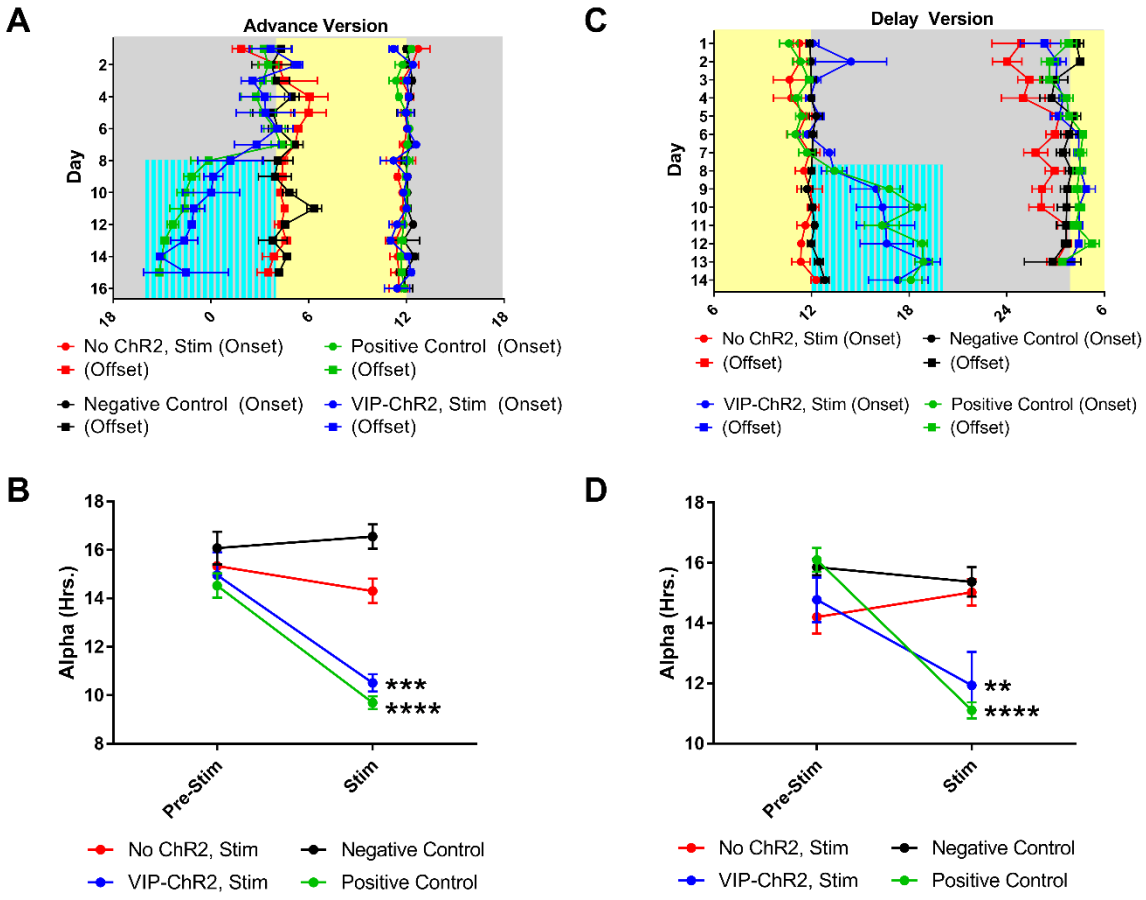

Figure 3-1. Optogenetic activation of VIPergic SCN neurons is sufficient to compress alpha. **A**, daily onset (circles) and offset (squares) times plotted against light and optogenetic stimulation intervals, with optogenetic stimulation occurring in the 8-hours before lights on (blue vertical stripes). Animals receiving fiber-optic-delivered blue light to the SCN shifted their activity offsets earlier if expressing VIP::Cre-driven ChR2 (VIP-ChR2, blue) than if no ChR2 is expressed (No ChR2, red). VIP-ChR2 animals match the responses of positive controls (green) that were actually switched from short to a long LD that matched the OS:L:D schedule. No ChR2 animals match negative controls that remained on short LD (black). In all groups, onset time remained static. **B**, alpha is compressed significantly in VIP-ChR2 and Positive control animals (Pre-Stim alpha - Stim alpha: No ChR2, 1.034 hrs., adj. p = 0.5077; VIP-ChR2, 4.451 hrs., adj. p = 0.0007; Negative Control, -0.4785 hrs., adj. p = 0.9357; Positive Control, 4.83 hrs., adj. p < 0.0001; two-way ANOVA with Sidak's multiple comparisons test). **C**, Groups and experimental set-up as in A, but with the optogenetic stimulation occurring in the 8 hours following lights off. Offsets for all groups remain static, but positive control and VIP-ChR2 onsets become later during photoperiod extension or optogenetic stimulation, respectively. Negative controls and No ChR2 mice have no change in onset time. **D**, alpha is compressed significantly by the delay version of the optogenetic stimulation (Pre-Stim alpha - Stim alpha: No ChR2, -0.8162 hrs., adj. p = 0.4751; VIP-ChR2, 2.834 hrs., adj. p = 0.0018; Negative Control, -0.4869 hrs., adj. p = 0.8523; Positive Control, 4.987 hrs., adj. p < 0.0001; two-way ANOVA with Sidak's multiple comparisons test).

The neuropeptide vasoactive intestinal polypeptide, VIP, has been shown to be necessary for the persistence of photoperiodic changes beyond direct exposure[96]. The neurons that express VIP within the SCN, having recently been shown to exhibit light-evoked and spontaneous activity in a manner that is required for typical light-mediated phase shifts[130], are strong candidates for mediating the response to photoperiodic signals both during their induction and in their persistence. As discussed in **Chapter 2.2,** the underlying direct mechanism of the induction of shortened activity duration after-effect is likely an expansion of the daily overall high firing phase through a change in phase distribution of SCN neurons[69]. We therefore sought to test the role of VIPergic SCN neurons in regulating activity duration (Figure 3-1). To do so, we employed VIP::Cre-driven channelrhodopsin-2 (VIP-ChR2). We have previously shown that the optogenetic channel ChR2, targeted to SCN neurons, is capable of increasing SCN neuron activity upon direct stimulation with high-intensity blue light[131].

Results

VIP-ChR2 animals were implanted with fiber optics targeting the SCN and entrained to T24 Short (8:16 LD). After 7 days of baseline activity monitoring, we initiated daily direct blue light stimulation (Optogenetic Stimulation, OS) of the SCN, beginning at the offset of environmental light each day and terminating 8 hours later (8:8:8 L:OS:D, delay version) or beginning 8 hours before lights on and ending at lights on (8:8:8 L:D:OS, advance version). In both versions, stimulated VIP-ChR2 animals (VIP-ChR2, Stim; blue) are compared to animals receiving the same fiber implant surgery and stimulation, but that do not express ChR2 (No ChR2, Stim; red), non-surgery animals that remained in 8:16 short LD (Negative Controls; black), and non-surgery animals that switched from 8:16 short LD to 16:8 long LD (Positive Controls; green). In the advance version, VIP-ChR2 offsets move earlier upon stimulation while onsets remain static (Figure 3-1A), compressing activity duration similar to Positive Controls

(Figure 3-1B). No ChR2 controls and Negative Controls have their onsets and offsets both static, maintaining a long activity duration throughout both epochs. In the delay version, VIP-ChR2 animals move their onsets later while maintaining static offsets (Figure 3-1C), mimicking Positive Controls and compressing activity duration (Figure 3-1D). As in the advance version, No ChR2 and Negative Control animals maintain their long activity duration throughout both epochs.

Discussion

These results indicate that VIPergic SCN neuron activation is sufficient to produce changes in alpha during optogenetic stimulation. As discussed in **Chapter 3.1**, the function of VIP signaling and the position of VIPergic SCN neurons within the SCN provide a clear link between the typical delivery of light information to the SCN and VIPergic neurons. Recent results demonstrating that these neurons are important for light-mediated phase shift responses, combined with the findings shown here, build a compelling argument that the VIPergic SCN neurons are a mediator of multiple types of retina-mediated light input to the SCN.

Chapter 4

Improving Methods for Measuring Circadian Properties

4.1. Introduction

The study of circadian rhythms involves a set of unique challenges. Because virtually all worthwhile experimental questions in circadian biology require the observation of more than a single daily oscillation, even the most basic experiments can require weeks to complete. As an added challenge, measurements, sample collections, and condition changes are required at particular and often peculiar times, sometimes conflicting greatly with the circadian cycles of the experimenters themselves. The general approach to circadian rhythm experimental design is of crucial importance to understanding the technical challenges inherent in the field.

Generally, experimental biology consists of implementing a set of test conditions (along with corresponding control conditions) for research subjects (e.g., mice, cells, patients) and taking a set of measurements. In the most simple experiments, the conditions are set and the measurements taken once at the termination of the trial. The product is a set of observations from the control and experimental group, comparable using established statistics. Often, these observations are strengthened by taking measurements before and after changes in conditions. More infrequently, the experiment consists of repeated measurements taken at particular intervals over the course of one or several condition changes.

As the number of measurements increases, so does the complexity of the experiment. Therein lies the challenge of circadian research, in which the oscillatory nature of the subject of study commands a high level of repeated sampling. In ideal conditions, samples are collected from the same individual at a large number of timepoints throughout the day (e.g., every ten

minutes). More realistically, these samples must be taken at much wider intervals depending on factors like sampling cost, experimenter availability, and subject livelihood. Often, samples cannot be taken from the same individual, such as in the case of animals or cells where the measurement process may be terminal, or in human samples where measurements are made on donated post-mortem tissue.

The factors described above lead to two separate challenges surrounding data analysis. The first is the need for analysis methods that produce the most statistical power from limited sampling, either in the form of limited temporal resolution, limited experimental duration, or limited subjects. The second is the need to evaluate metrics that are relevant to circadian biology, such as free-running period and phase shifts, while accommodating the nature of repeatedly sampled, time-series type data sets. The first challenge is continually being improved by talented researchers in the field, producing solutions such as JTK cycle[132] for the analysis of robustness of rhythmicity (as well as period) in single-cycle low-temporal resolution gene expression data. The subject of this chapter will be the second challenge, the development of tools to analyze circadian-specific parameters: free-running period (τ), phase (ϕ) and shifts therein ($\Delta\phi$), activity duration (α), and distribution of ϕ across the SCN.

Free-running period

The period of a circadian oscillation is its most fundamental property. Its accurate quantification has, accordingly, received careful attention from the field over the years. Given a truly reliable phase reference point, as activity onset is often hoped to be, the free-running period is approximated by the average time between recurrence of those reference points. In actigraphy, where locomotor behavior is plotted as activity counts (e.g., wheel running revolutions or infrared beam breaks) over the course of 24 – 48 hours with multiple days

stacked vertically, these inter-phase-reference point intervals can be traced as a diagonal line through several days of records. Unfortunately, these phase reference points can be ambiguous and their identification subjective. The quantification of period, then, depends on more sophisticated mathematical techniques.

Like many circadian properties and values, the measurement of free-running period is a strong overlap between the worlds of biological sciences and physics. Being the reciprocal of frequency, period is measurable using any technique used to assess signals in the frequency domain. The basis of most analyses of frequency is the contribution by Joseph Fourier that all signals can be represented by some combination of sine waves. The Fast Fourier Transform (FFT), in general use in one form or another since the late 1800s, has been applied to circadian studies on its own. In the 1950s-1970s, techniques built on the same principles as FFT, called "periodograms", were developed. Essentially, these techniques sought first to tailor the frequency-domain transformation of FFT into the realm of circadian rhythms, then to introduce the ability to statistically assess the periodicity of a rhythm.

While the Enright (evenly distributed sampling required) and the Lomb-Scargle (unevenly distributed sampling allowed) periodograms assessed rhythms statistically using the principles of analysis of variance, an improvement was made in the form of the Chi-Square Periodogram introduced by Sokolove and Bushnell[133]. In this version of the periodogram, statistical significance was determined using the Chi-Square distribution, and generally proved to be more robust than its predecessors against false-positive errors (for review, see Refinetti 2007[134]). The output of the Chi Square periodogram is a series of power values (Q_P) corresponding to each analyzed period length (P). The highest amplitude of these Q_P values is taken to be the free-running period, and that period is considered statistically significant if the amplitude is higher than the Chi-Square distribution's null threshold. The Q_P value is computed by iteratively summing the data that occurs P data points apart, shifting repeatedly to cover the

entire data set, subtracting from that value the mean overall activity, and then squaring. For instance, if a data set is composed of the values [1, 2, 3, 4, 5, 6, 7, 8, 9, 10] and Q_P is to be calculated for P = 3, the calculation will sum [1, 4, 7, 10], [2, 5, 8], [3, 6, 9], [4, 7], and so on. These sums will themselves be combined, and then the mean of the entire data set subtracted and that value squared. In this way, the Chi Square periodogram assesses the harmonic power of each possible period value and reports using the Chi Square distribution a statistical assessment of its power.

Another strategy employed for period detection, particularly in gene expression data sets, is cosinor analysis. Here, collected time series data are fitted to cosine curves with flexible parameters for phase, amplitude, and other variables. While useful in certain circumstances, the utility of cosinor analysis can be disrupted by missing data points or inconsistent period.

More recently, computationally intensive techniques for the analysis of period have emerged. These include autocorrelation, maximum entropy spectral analysis (MESA), and discrete wavelet transformation (DWT). In autocorrelation, the time series is overlapped upon itself, creating a correlation of 1. It is then shifted by one unit, compared again, and the resulting correlation computed. This shifting is repeated for a specified width of possible periods, and the correlations are plotted against the putative periods. Rhythmic data will produce higher correlation values at each harmonic of the free-running period, and so the underlying period can be gleaned by the maximum correlation from the shifted data. In MESA, shortcomings of discrete Fourier transforms are addressed using an autoregressive model that seeks to take into account the entropy of the system[135]. Wavelet transformations seek to locally model the data series using wavelets to identify the frequency components of the signal across time- especially useful for determining instantaneous period and changes thereto across an experiment[136].

Phase and phase shifts

Another fundamental property of circadian oscillations is phase. Unlike period, which generally stays stable over the course of time, phase is by nature constantly changing. Measuring the phase of a rhythm allows us to understand the state of the rhythm at the moment, the temporal relationship between it and other oscillations (i.e., its phase angle relative to another rhythm), as well as atypical jumps in phase (phase shifts). As described in **Chapter 1.1**, phase shifts are an important part of daily entrainment and an increasingly common factor in heavily lighted modern life. Though a critical part of circadian rhythms research like free-running period, the technical approaches to phase shift measurement have not received the same level of attention.

Phase shifts are typically measured using what is described in **Chapter 4.2** as the "actogram approach." This approach involves the comparison of a period-adjusted projection of the progression of the rhythm with the actual, potentially phase-shifted, observed rhythm. While solid in principle, this approach has suffered from poor standardization and certain oversimplifications. **Chapter 4.2** discusses an improvement to the actogram approach, τ-Independent Phase Analysis, that addresses these concerns.

Activity duration

Because the circadian pacemaker itself can be thought of as a theoretical construct, an emergent property of a particular set of rhythmic components, experimental circadian biology focuses on overt rhythms. The most commonly measured overt rhythm is locomotor activity, which can be considered one of the most basic and easily observed outputs of the underlying circadian rhythm. While the strategies for measuring the core properties of a rhythm – its period

and phase – using its overt rhythm are discussed above, there is also much to learn from the measurement of accessory properties of a rhythm, such as the shape of its waveform.

The simplest visualization of a circadian rhythm is a symmetrical sine wave, repeatedly progressing with constant angular velocity through 360 degrees of phase. In reality, the shape of this wave can be altered significantly while still maintaining a particular period. Changes to the duration that the wave remains at or near its maximum (or minimum) can lead to differences in threshold-gated downstream physiology. For instance, if locomotor activity is induced when the overall firing rate rhythm of the SCN is below 50% of its maximum amplitude, the amount of hours of activity will change with the alterations to the SCN's firing rate waveform. As a result, measurements of activity duration (alpha) can provide valuable insight into an accessory feature of the circadian pacemaker. Unlike phase shift measurements described above where standardization and accuracy were a primary issue, manual detection of alpha is largely adequate. The difficulty in alpha measurement is generally the speed and regularity with which these measurements can be made. **Chapter 4.3** details a computational strategy for calculating alpha for mouse activity records.

SCN analysis

Many circadian studies are carried out using dissected and cultured SCN tissue, and these experimental preparations come with their own technical challenges. Unlike behavioral records in which activity forms a simple two dimensional data set (activity over time), imaging of SCN tissue over time introduces space as a variable as well. One of the most common concerns in these experiments is regional changes (particularly between the dorsal and ventral portions of the SCN) as well as phase dispersal changes. One limitation to studying phase dispersal is that the dispersal is typically of phase between cells, and cell detection in images

with varying focus and image quality can be difficult. While automated cell detection algorithms exist, these are best employed in situations with high contrast, which may not be the case for long term SCN imaging. **Chapter 4.4** discusses a strategy for measuring phase dispersal using the median absolute deviation in phase of uniformly distributed sub-cellular ROIs.

The strategies contained in this chapter are intended to improve – either through accuracy, throughput, and/or standardization – the various components of circadian data analysis that are required for research topics discussed within this dissertation and elsewhere.

4.2. Tau-Independent Phase Analysis: A Novel Method for Accurately Determining Phase Shifts

Michael C. Tackenberg, Jeff R. Jones, Terry L. Page, Jacob J. Hughey

Modified from: Tackenberg, M.C., Jones, J.R., Page, T.L., Hughey, J.J. Tau-independent phase analysis: A novel method for accurately determining phase shifts. *Journal of Biological Rhythms*, **2018** 33(3):223-232.

Accurate quantification of period, τ, and phase, ϕ, is a critical component of many studies of circadian rhythms. While multiple methods exist to quantify period[137,138], ranging from relatively simple (linear regression of onset time, cosinor analysis), to more complex (chi-squared periodogram, autocorrelation, discrete wavelet transformation, maximum entropy spectral analysis[133,135,136,139]), there are fewer options for estimating changes in phase. Phase analysis suffers from two large issues. First, methods to quantify changes in phase are less standardized, and thus potentially less reproducible, than those used for period analysis. Second, because phase shifts often coincide with changes in period[140,141], measurements of phase change can be affected by the magnitude of the coincident period change. Here we seek to improve upon both of these deficits by proposing a computationally simple but rigorous strategy for measuring phase shifts in multiple types of circadian data.

The measurement of a change in phase of a circadian pacemaker typically involves comparing how a pacemaker *would* have progressed if unperturbed (a null model) to how it actually progressed (Figure 4-1). Within rhythmic data are overt phase reference points, such as onsets in actigraphy (Figure 4-1A) or peaks in bioluminescence imaging (Figure 4-1B). Phase reference points are a valuable property in the estimation of phase and period, as they

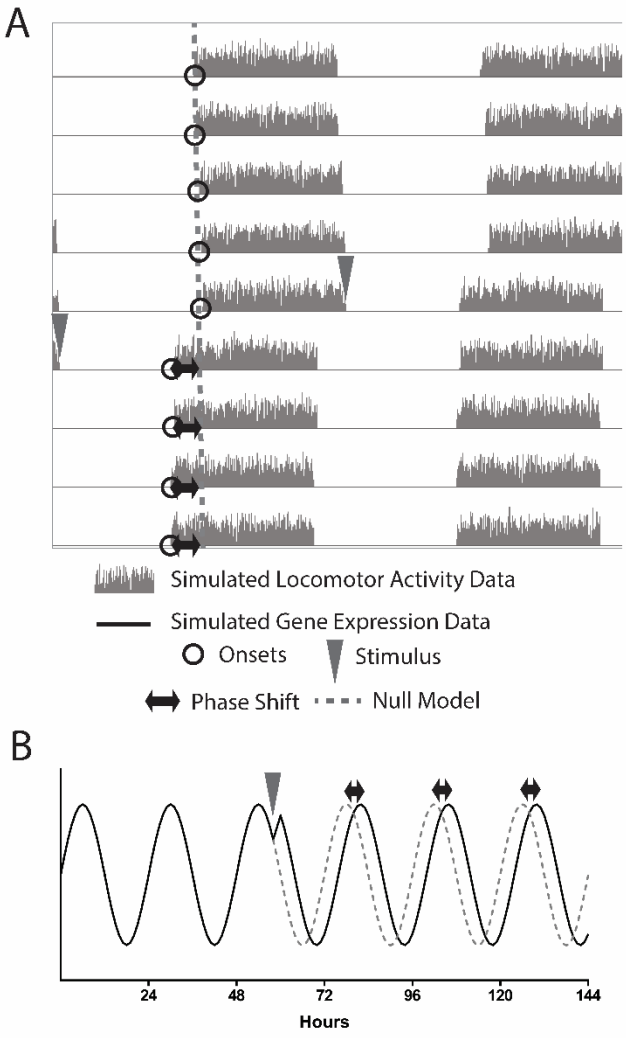

Figure 4-1. Schematic view of phase shift estimation. A, a simulated actogram depicting a phase shift. Onsets before the shift are projected (dashed line) and the difference between the post-stimulation onsets and the projection is taken to be the phase shift. B, a simulated circadian waveform. A stimulus induces a phase delay, and the original trajectory of the wave is projected (dashed line). In both cases, the phase shift (black arrows) is calculated as the difference between the projected and the actual data.

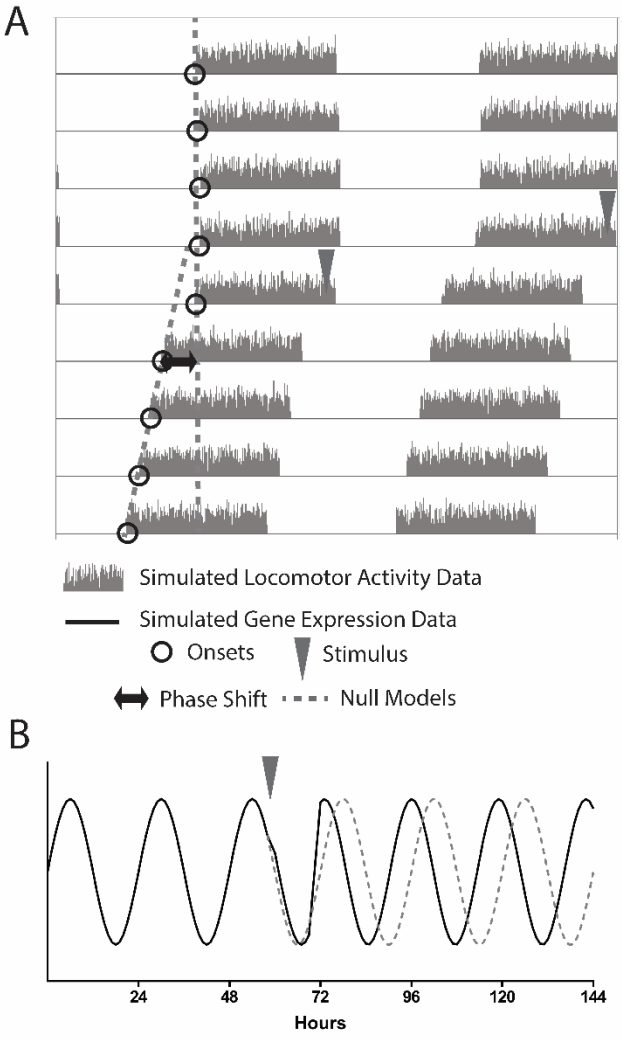

Figure 4-2. Period changes affect phase shift measurements. When a stimulus induces a period change along with a phase shift, the calculation must be adjusted. The phase relationship between the post-stimulus phase reference points and the projected null model is not consistent from cycle to cycle (see Figure 4-S1). To account for this, the phase shift is calculated as the difference between the projection of the pre-stimulus phase reference points and the linear fit of the post-stimulus phase reference points. In this way, the change in period is included in the analysis.

represent a way to assess the progression of the pacemaker over time. Two successive phase reference points are assumed to occur one circadian cycle apart, and at those phase reference

points the pacemaker is assumed to be at the same phase. Phase reference points are chosen for their recognizability and for the likelihood that their timing will remain consistent across changes to the overt, measured rhythm. For example, acrophase, the peak of a cosine fit to a circadian wave, is assumed to remain consistent even if the waveform broadens. In an experiment in which a pacemaker undergoes a potentially phase-shifting stimulus, a null model indicates the expected timing of these phase reference points after the stimulus, assuming no period or phase change (Figure 4-1A-B, dashed lines). The difference between the expected and observed timing of the post-stimulus phase reference points can then be used to estimate the phase shift (Figure 4-1A-B, black arrows). If the stimulus also changes the period, however, the phase relationship between the observed post-stimulus phase reference points and those of the null model is not consistent, and as such the difference between the real progression of the pacemaker and the null model varies across each cycle, producing different measurements of $\Delta\phi$ (Figure 4-S1). One strategy for calculating phase shifts in the presence of period changes, most frequently used in actigraphy, involves altering the null model to include the change in period (Figure 4-2). The original progression of the pacemaker, as well as the null model with the changed period, are depicted on the actogram as lines. The phase shift, $\Delta\phi$, is then calculated as the distance between the two lines on the cycle after the stimulus occurs. This difference is represented in either circadian hours (relative to the period of the pacemaker after the stimulus) or in degrees. Using these units ensures that changes in phase can be compared across experiments.

Measuring the difference between the null model and the real data on the first cycle after the stimulus can be visualized as an altered version of the null model (Figure 4-S2). In this view, the null model is projected one cycle, and then beyond that first cycle the slope of the model is altered to take into account the post-stimulus period. Because this post-stimulus null has the same period as the real post-stimulus pacemaker, it maintains a stable phase relationship with

the post-stimulus phase reference points but is anchored to the pre-stimulus null model. The difference between the null model and the data on the first post-stimulus cycle, which represents the phase shift (Figure 4-2), is now recapitulated on every cycle (Figure 4-S2). These representations are two depictions of the same phase shift estimation.

Because the pre-stimulus and post-stimulus data are used to create linear regressions, their respective periods are represented in the slope of those lines. This estimation therefore attempts to account for changes in period. In theory, if there were no change in phase, these pre- and post-stimulus linear fits would intersect at the point of comparison (or, in the case of the altered visualization, the lines would overlap), and the estimated phase shift would be 0. In practice, however, changes in period between the pre- and post-stimulus cause systematic error in the measurement of the phase change (Figure 4-3). When using this strategy, which we term the "actogram approach," the estimated phase shift becomes more negative (i.e., towards a delay) as the period decreases and more positive (advance) as the period increases, regardless of whether the actual phase shift is a delay (Figure 4-3, left) or advance (Figure 4-3, right), or

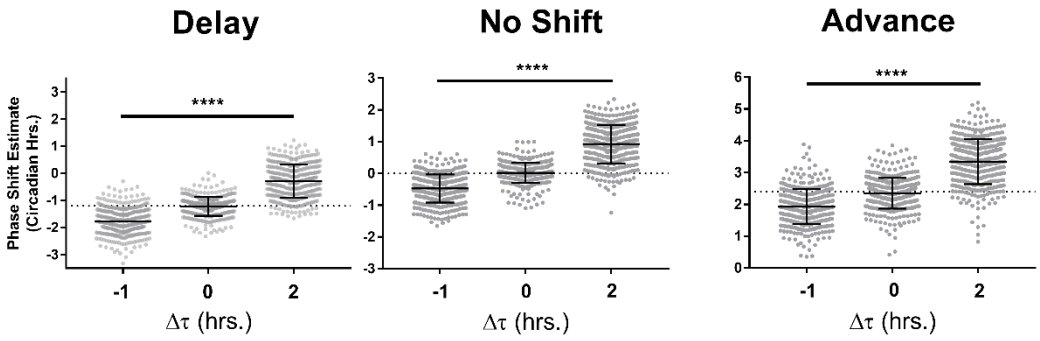

Figure 4-3. Period change affects phase shift estimates using the actogram approach. The phase shift estimate in circadian hours using the "actogram approach" is plotted against the magnitude of the period change in simulations with a phase delay (left, $\Delta\phi$ = -1.2), no phase change (middle, $\Delta\phi$ = 0), or a phase advance (right, $\Delta\phi$ = +2.4). Each point represents one simulation of a circadian time-course. The dotted line represents the actual shift for that group of simulations. In all cases, period shortening produces a more delayed phase shift estimate and period lengthening produces a more advanced phase shift estimate. One-way ANOVA, (****) corresponds to $p < 0.0001$. $\Delta\phi$ values are represented in circadian hours. Error bars represent the standard deviation.

whether there is no shift at all (Figure 4-3, middle). The average magnitude of the error in the phase shift estimate is about half the magnitude of the change in period (e.g., a typical error of -0.5 hours for a period change of -1 hour).

These inaccuracies are caused by an improper assumption about the relative time that the pacemaker undergoes a change in period, phase, or both. When measuring the difference between the two regression lines on the stimulus cycle, the actogram approach assumes that if the pacemaker's phase and/or period were altered, that change occurred one full circadian cycle after the last pre-stimulus phase reference point. This assumption is made whether the stimulus occurs at the last pre-stimulus phase reference point, hours later, or nearly at the time of the next cycle's phase reference point (Figure 4-S2). The slope of the line for the null model begins operating under the post-stimulus period parameter only at the first projected post-stimulus phase reference point.

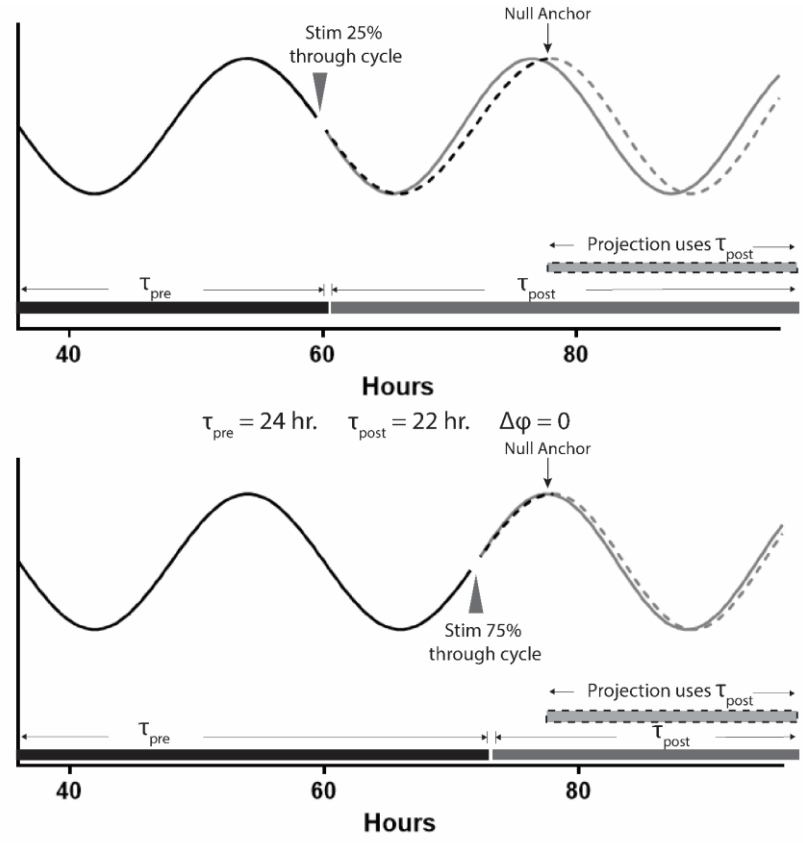

Figure 4-4. Schematic view of null model anchoring. When the post-stimulus projection is anchored to the first projected post-stimulus phase reference point (the "Null Anchor"), the projection begins operating under the τ_{post} parameter one full cycle after the last pre-stim phase reference point. This is the case whether the stimulus occurs early (top) or late (bottom) in the circadian cycle. In both examples, the stimulus does not cause a phase shift, but the period is shortened from 24 to 22 hours. Using the difference between the projected peak and the actual first post-stimulus peak, the phase shift estimate is different between the two conditions. In A, the estimated phase shift would equal -1.5 hours (0.75 * $\Delta\tau$) and in B, -0.5 hours (0.25 * $\Delta\tau$), despite no phase shift having occurred.

This assumption explains why, if the stimulus changes the pacemaker's period, the actogram approach's phase shift estimates are biased. The actogram approach does not account for the speed with which the pacemaker resets after a phase-shifting stimulus. This speed is a fundamental property of circadian pacemakers that has been measured experimentally. Classic experiments by Chandrashekaran[10] and later by Pittendrigh[142] established that the phase of the pacemaker resets within, at most, 1 hour. Since that time, the field has made substantial progress in establishing the molecular underpinnings of the clock in multiple organisms, including the molecular basis for the phase shift response[80]. While much remains unknown about the mechanism of the phase shift response, the work by Chandrashekaran and Pittendrigh demonstrates the timeframe within which the molecular resetting must occur. Because the expected phase response change in the clock is achieved within at most 1 hour, the molecular changes within the pacemaker that are required for that response are then known to occur within this window. The rapid induction of *Per1* has been established as a portion of the molecular mechanism for pacemaker resetting within this timeframe[80]. This fast resetting is critical to accurately measuring phase shifts. If we assume that any changes in period and phase occur within an hour of the time of the stimulus (for stimulus lengths < 1 hour; for longer stimuli, see below), we can see a source of error in the actogram approach. The estimated phase shift includes not only the actual phase shift but also the change in period, weighted by the percentage of the cycle that occurs prior to the next phase reference point. Figure 4-4 illustrates this schematically, with two circadian waveforms with pre-stimulus periods (τ_{pre}) of 24 hours undergoing an instantaneous period change (a period shortening of 2 hours, post-stimulus period τ_{post} of 22 hours) but no phase change. The projection begins operating the τ_{post} period parameter at the first projected post-stimulus peak regardless of the stimulus time, which creates gaps between the projection and the post-stimulus data that would be interpreted as phase shifts (dashed and solid lines, respectively; Figure 4-4).

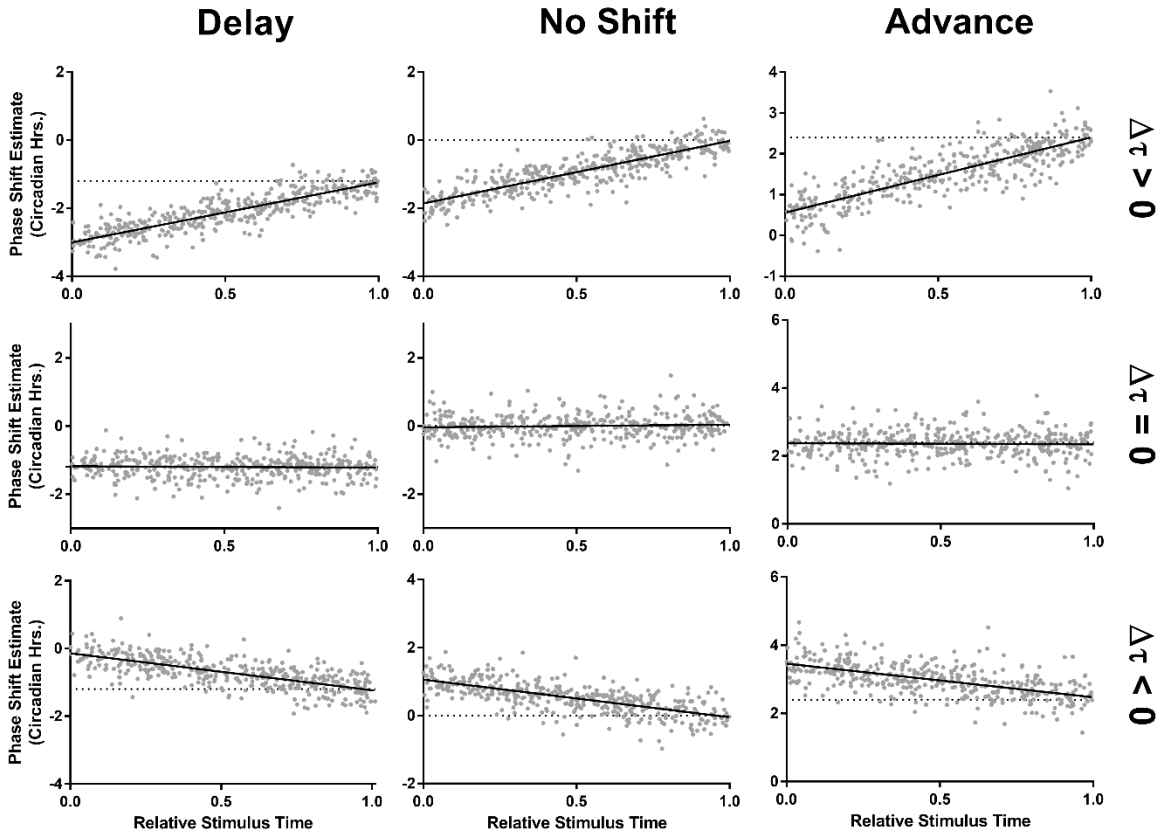

Figure 4-5. Relative stimulus time has systematic effects on the phase shift estimate using the actogram approach. Using the actogram approach, the relative time of the stimulus compared to the last pre-stimulus phase reference point has a predictable effect on the phase shift estimate, depending on the size and direction of the period change. When there is a period change (top and bottom rows), the estimate is least accurate when the stimulus occurs at or near the time of the last pre-stimulus phase reference point. This occurs whether there is a phase delay (left column, $\Delta\phi$ = -1.2), no phase shift (center column, $\Delta\phi$ = 0), or a phase advance (right column, $\Delta\phi$ = +2.4). The direction of the error is dependent on the period change, with lengthening (top row, $\Delta\tau$ = +2) producing more negative (delayed) estimates and shortening (bottom row, $\Delta\tau$ = -1) producing more positive (advanced) estimates. When there is no period change, the actogram approach is generally accurate (middle row, $\Delta\tau$ = 0). Each point represents one simulation, and each black line shows a linear fit of estimated phase shift vs. relative stimulus time. $\Delta\phi$ values are represented in circadian hours, $\Delta\tau$ values are represented in hours.

To more accurately quantify the error in the actogram approach and to adjust for it, we assessed the relationship between the phase shift estimate and the time of stimulus relative to the last pre-stimulus phase reference point in a series of simulated phase shifts. In each

simulation, the stimulus time is represented as the fraction of the circadian cycle that has elapsed when the stimulus occurred. We examined the error in the actogram approach's phase shift estimate as a function of the stimulus time across nine different conditions covering phase advances, delays, and no phase shift, as well as period lengthening, shortening, and no change in period (Figure 4-5). We observed a clear relationship between the estimation of the phase shift and the stimulus time that was dependent on the change in period. When the period remained constant between the pre- and post-stimulus conditions, using the actogram approach produced an accurate estimation of the phase shift (Figure 4-5, middle row). When the period changed, the actogram approach was least accurate when the stimulus time was near the last pre-stimulus phase reference point, and most accurate when the stimulus time approached one full circadian cycle later.

τ-Independent Phase Analysis (TIPA)

An ideal method for calculating phase shifts should be accurate regardless of the stimulus time and period change. We therefore sought to develop a method that would address the deficiencies of the actogram approach. The basis of τ-Independent Phase Analysis (TIPA) is the creation of a null model of the pacemaker's progression (represented by the time of occurrence of a chosen phase reference point) anchored appropriately to the actual time of phase and/or period change using the stimulus time described above (Figure 4-6). This null model is based on the assumption that the pacemaker has undergone a change in period but no change in phase, and that the change occurred exactly at the stimulus time. The differences between the observed times and the expected times according to the null model are then used to calculate the phase shift (Figure 4-6, black arrows).

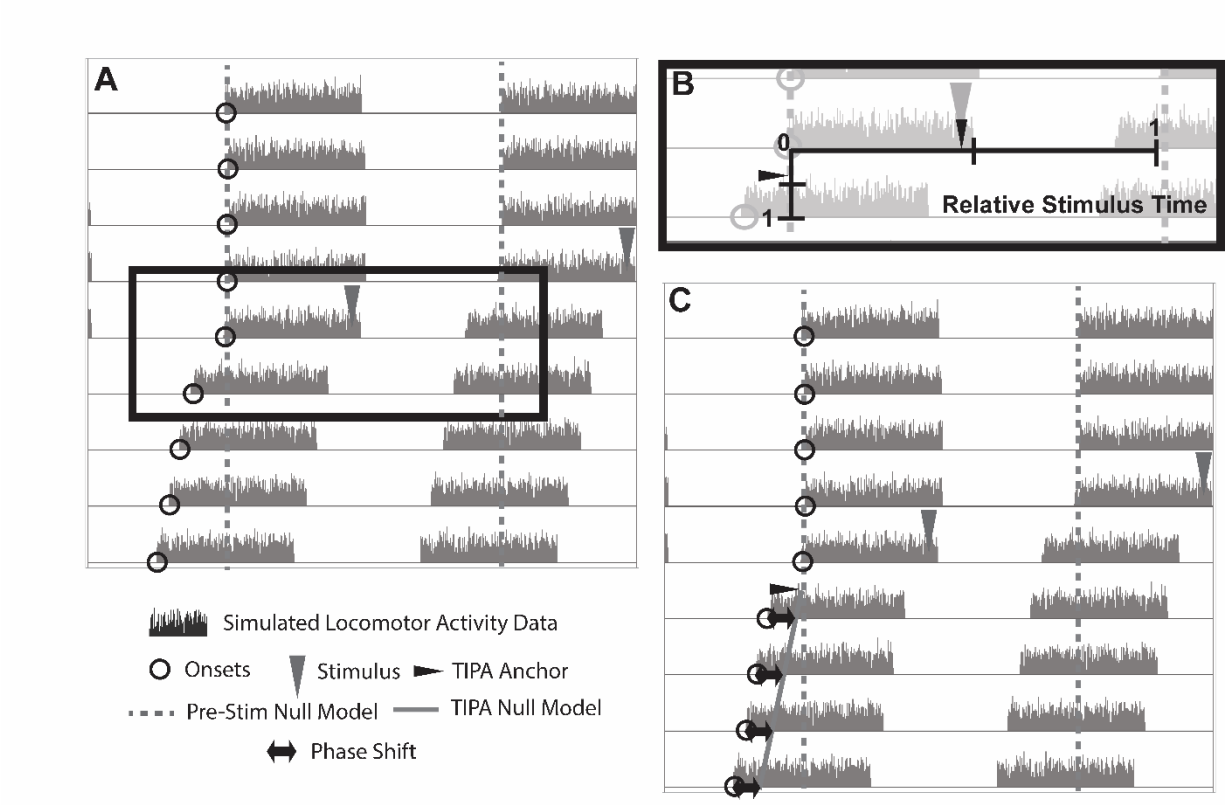

Figure 4-6. Schematic of tau-Independent Phase Analysis. A, a simulated actogram displaying a phase advance and a period shortening. B-C, Using TIPA, the post-stimulus null model (solid grey line) operates under the assumption that there is a period change but no phase change, and that the period change occurred instantaneously at the time of the stimulus (grey triangle). The horizontal position of the stimulus is transposed vertically to show the TIPA anchor (black arrowhead in panel B). The sloped line representing the post-stimulus null model is therefore anchored to a position along the pre-stimulus null model (grey dashed line) corresponding to the time of the stimulus. In panel C, the phase shift estimate (black arrows) for each cycle is shown as the difference in hours between the phase reference point (open circles) and the position of the TIPA null model (solid grey line) for that cycle.

The set-up to this calculation is similar to the altered version of the actogram approach described above (Figure 4-S2). Whereas the actogram approach anchors the post-stimulus linear regression to the final pre-stimulus phase reference point, TIPA anchors its post-stimulus null model to the stimulus time (Figure 4-6, black arrowhead). The vertical position of the TIPA anchor can be determined by establishing the fraction of the circadian cycle that has elapsed by the time the stimulus occurs. In an actogram, time is represented both horizontally and vertically. Figure 4-6B shows the fraction of the circadian cycle horizontally from 0 to 1, with the stimulus occurring just before half the cycle is complete. The same 0 to 1 scale is then shown

vertically as the height of a single actogram day. Again, the stimulus is represented, occurring just before half the cycle is complete. This is where the TIPA anchor is located, at the vertical position of the stimulus. The position of the anchor is intended to coincide with the instant of the period and phase change. For stimuli shorter than one hour, it is placed at the end of the stimulus. While maximum phase resetting occurs within 1 hour of the onset of a stimulus[80], period changes have been shown to align with the mid-point of the stimulus[140]. For stimuli longer than one hour, the TIPA anchor is therefore placed at the midpoint of the stimulus. Using this anchor, TIPA null estimates are then produced for each post-stimulus cycle based on this origin at the time of stimulation, the fraction of the stimulus cycle that is operating under the post-stimulus period parameter, and the post-stimulus period (see Methods). For each cycle, the difference between the actual post-stimulus phase reference point and the TIPA null for that cycle is determined. The circular mean of these differences is the estimate of the phase shift (see Methods).

Results

To verify the accuracy and precision of the TIPA method, we analyzed the phase shift of 3,600 simulations with known phase shift parameters (Table 4-S1). Two specific weaknesses of the actogram approach described above are the influence of a change in period (Figure 4-3) and the relative time of stimulus (Figure 4-5). Compared to the actogram approach, TIPA was robust against changes in period (Figure 4-7A) and remained consistently accurate regardless of the time of stimulus (Figure 4-7B). We also assessed the precision of the two methods in the case of no period change, where the relative stimulus time has no significant effect on the phase shift estimate of the actogram approach (Figure 4-8). We found that TIPA was significantly more precise across phase delays (Figure 4-8A), advances (Figure 4-8C), and cases in which there was no shift in phase (Figure 4-8B). We further tested the precision of the

two methods in cases where there was no change in period using simulations with varying levels of noise and numbers of cycles (Figure 4-S3). While both TIPA and the actogram approach showed lower precision in high noise simulations, the variance of TIPA's estimates was significantly lower (Figure 4-S3A). Neither the actogram approach nor TIPA showed reduced accuracy in simulations of four vs. five post-stimulus cycles, though TIPA had lower variance in each condition (Figure 4-S3B).

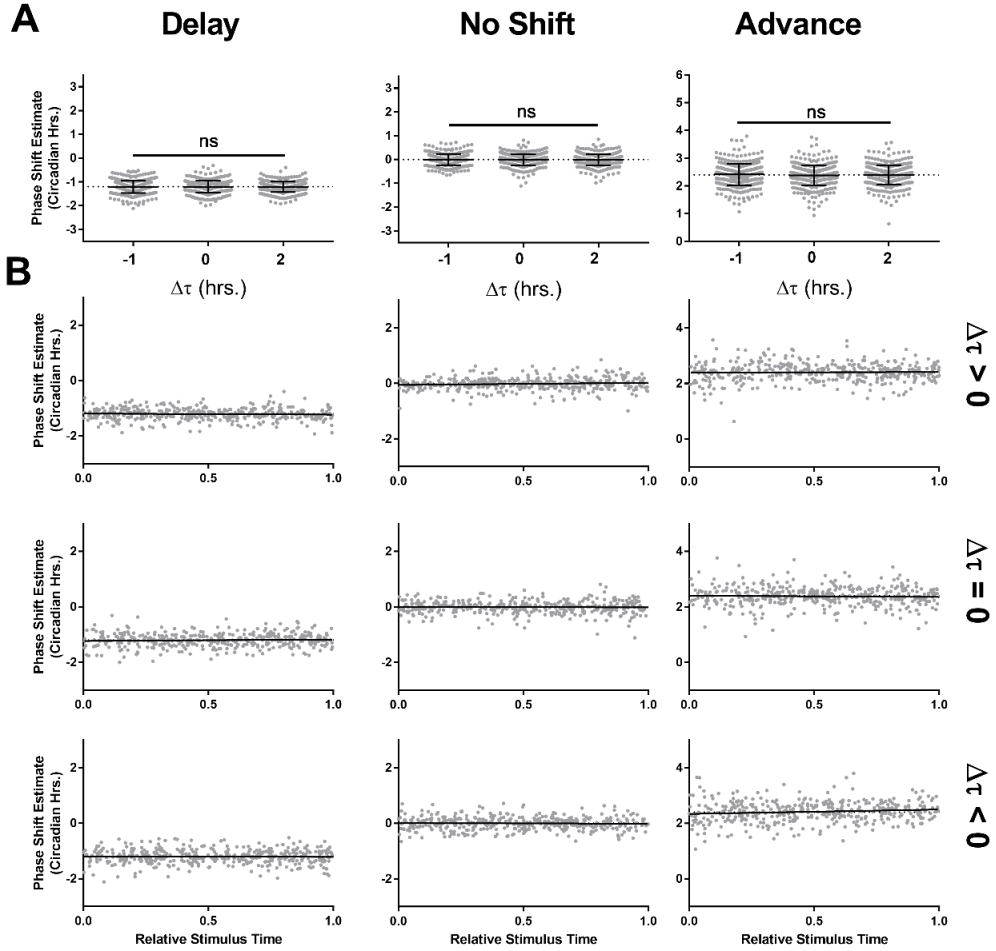

Figure 4-7. TIPA eliminates the effect of period changes and stimulus time on the phase shift estimate. A, the estimate of the phase shift using TIPA is plotted against the period change for phase delays (left, $\Delta\phi$ = -1.2), no phase shift (middle, $\Delta\phi$ = 0), and phase advances (right, $\Delta\phi$ = +2.4). One-way ANOVA, **ns** corresponds to $p > 0.05$. B, The TIPA estimate of phase shift is independent of the relative stimulus time, across phase delays (left column, $\Delta\phi$ = -1.2), phase advances (right column, $\Delta\phi$ = +2.4), and no phase change (middle column, $\Delta\phi$ = 0), as well as across period lengthening (top row, $\Delta\tau$ = +2), shortening (bottom row, $\Delta\tau$ = -1), and no period change (middle row, $\Delta\tau$ = 0). Each point represents one simulation, and each black line shows a linear fit of estimated phase shift vs. relative stimulus time. $\Delta\phi$ values are represented in circadian hours.

The actogram approach is sometimes modified for late-cycle stimulus times by anchoring the post-stimulus null model to the last pre-stimulus phase reference point (Figure 4-S4). We found that this version of the actogram approach produces a trend with a similar pattern to that of the previously described approach, but with the estimate being most accurate as the relative stimulus time approaches 0 (Figure 4-S4, green) rather than 1 (Figure 4-S4, magenta). Using a hybrid of the two approaches, in which the phase reference point before the stimulus is used as an anchor for relative stimulus times of < 0.5 and the predicted point τ_{pre} hours afterwards is used as an anchor for relative stimulus times > 0.5, results in estimates that surround the true phase shift parameter of the simulations (Figure 4-S5, blue). The hybrid approach is most accurate when the stimulus time is close to either the last pre-stimulus phase reference point or one full cycle later, but is less accurate when the stimulus time is between these two points in the cycle. Although the hybrid version improves the accuracy of the actogram approach, this accuracy is due to counter-acting errors in opposite directions (Figure 4-S5, green, magenta) that only cancel each other out if relative stimulus times are evenly distributed below and above 0.5. Even with this increase in accuracy, we found that the precision of TIPA significantly exceeded that of the hybrid actogram approach (Figure 4-S5).

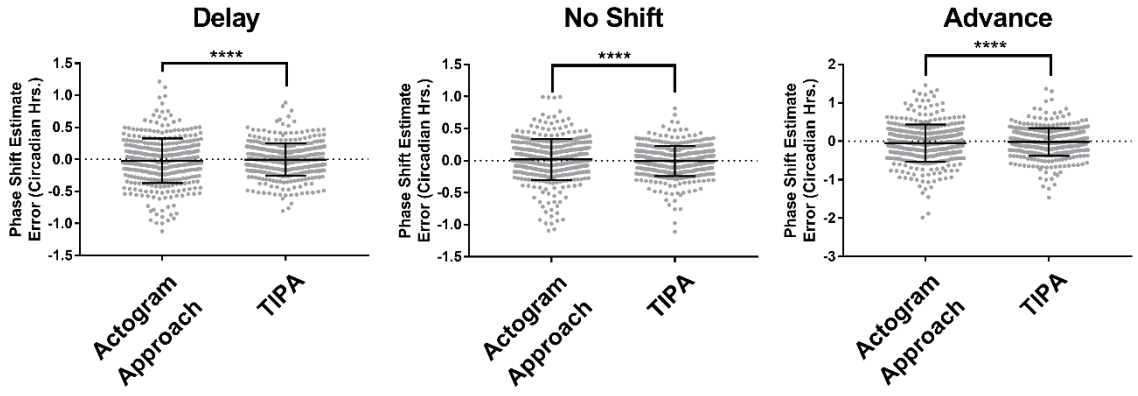

Figure 4-8. TIPA is more precise even when there is no change in period. In delay (left, $\Delta\phi$ = -1.2), advance (right, $\Delta\phi$ = +2.4), and no phase shift (middle $\Delta\phi$ = 0) simulation groups, TIPA's estimates of phase shift had lower variance than the actogram approach. Brown-Forsythe test for unequal variances, (****) corresponds to $p < 0.0001$. Error bars represent standard deviation.

Discussion

Accurately quantifying changes in phase in circadian data sets is a critical aspect of many circadian analyses, but has received less attention than quantification of period. The typical actogram approach described here is not the only strategy used to measure phase shifts, but in using linear fits of pre- and post-shifted data, it is one of the only approaches that takes period changes into account (see description of cross-correlation in Dowse, 2009[137]). Though we have used actograms as examples, the underlying strategy for measuring phase shifts using the progression of phase reference points is the same across virtually all data types and fits. As described above, the estimation of phase shifts must involve the comparison of how the pacemaker *would* have progressed, and how it actually progressed. Making that comparison, whether by distilling full locomotor activity or gene expression rhythms down to identifiable phase reference points or by analyzing the entire wave through cosinor analysis, requires assumptions about how the pacemaker will progress after the stimulus. Previous applications of these methods are subject to bias based on assumptions regarding the change in period of the pacemaker after the stimulus. We show here that τ-Independent Phase Analysis is an accurate and versatile approach to determining phase shifts in circadian data by remaining consistent across changes in period and relative time of stimulus. TIPA can be applied to any type of circadian data with multiple cycles and identifiable phase reference points, while maintaining precision throughout differing noise levels and cycle numbers.

In our study, TIPA and the actogram approach were used to estimate the phase shift in simulations, which enabled us to compare the values estimated by each method against the known phase shift parameter for that simulation group. This differs from experimental biology where the true phase shift values are unknown. TIPA, like any method designed to summarize a biological phenomenon into a single number, will have a range of error. Based upon our results, this range of error likely surrounds the true phase shift value regardless of period changes or

the relative time of stimulus, in contrast to the actogram approach where the typical range of error is compounded by baseline changes dependent on those two factors. Comparing TIPA to the hybrid version of the actogram approach where the range of error surrounds the true phase shift value, TIPA's range of error is significantly narrower.

Like all phase shift estimation methods based on phase reference points, TIPA assumes that the identified phase reference points represent the same phase of the pacemaker from cycle to cycle, even if the period of the pacemaker changes. Although this assumption is likely valid if the period changes are relatively small, it may break down as period changes become large. TIPA also assumes that the post-stimulus period is stable. In many circadian experiments in which a period and/or phase change occurs, there are transient cycles post-stimulus in which the rhythmic output being measured lags behind the underlying pacemaker, and therefore does not reflect the pacemaker's true phase. If applying TIPA to a dataset with transients, we recommend limiting the window of comparison to post-stimulus cycles that have a stable period.

Finally, TIPA assumes that any potential phase and period changes occur nearly instantaneously. While there is experimental evidence to support the instantaneous resetting of the pacemaker's phase[80], the assumption that period changes occur instantaneously has not been successfully tested experimentally. The concept of an instantaneously changed period serves as an improvement over other methods, however, which ignore the specific timing of the period change by bluntly anchoring period changes to phase reference points. This anchoring leads to inconsistent post-stimulus modeling (see Figure 4-4).

TIPA has the potential to greatly improve the quality of phase shift estimates in most types of circadian data, provided that they have some form of phase reference point and at least 3 cycles with a stable period. As mentioned above, all phase shift estimations rely on the comparison of pre-stimulus and post-stimulus models. While many aspects of data collection vary (e.g., amount of cycles, sampling resolution, signal and noise levels), the comparison

strategy remains the same. There is therefore a need for consistency in making these measurements for proper comparison from experiment to experiment and from experimenter to experimenter. TIPA, and the underlying strategy for period change compensation on which it is based, offers an opportunity for cleaner and more accurate measurements of phase changes in multiple types of circadian data. In this way, the method is a versatile tool for chronobiologists, allowing for accurate phase estimation to join accurate period estimation in having standardized and rigorous approaches.

Methods

We simulated time-courses of circadian oscillations before and after a stimulus. Rather than simulating the full waveform, we directly simulated the times of phase reference points (e.g., activity onset times or peaks in bioluminescence). We varied multiple parameters of the simulated time-courses: the period of the oscillator before the stimulus, the number of cycles observed before and after the stimulus, the standard deviation of inter-reference point times, and the phase shift induced by the stimulus (Table 4-S1). For each combination of parameter values, we generated 100 simulations. The period of the oscillator prior to the stimulus was fixed at 24 hours. In each simulation, phase-reference point intervals (produced separately for pre- and post-stimulus epochs) were drawn from a Gaussian distribution with mean corresponding to the period of the oscillator and the given standard deviation. The fraction of the cycle elapsed at the time of the stimulus was drawn from a uniform distribution between 0 and 1. Any changes in period or phase induced by the stimulus were modeled as occurring instantly.

The simulations were imported into MATLAB where they were parsed into pre- and post-stimulus subsets, with each subset being fit with a linear regression. The parameters from these regressions were used to make a set of predicted phase reference points for each simulation.

For the actogram approach phase shift estimate, the pre-stimulus and post-stimulus predictions were compared on the cycle after, or the cycle of, the stimulus, as indicated.

TIPA

The phase-shift estimate of TIPA is calculated by measuring the difference, in circadian hours or degrees, between the observed post-stimulus phase reference points and a set of post-stimulus null estimates that we term $TIPA_{null}$. The times of the phase reference points and the $TIPA_{null}$ points are represented in the elapsed time of the experiment, such that phase reference points that occur at Projected ZT 12 each day would be represented as 12, 36, 60, 84…. $TIPA_{null}$ for each post-stimulus cycle *i* is calculated as follows:

$$TIPA_{null}(i) = t_s + \tau_{post}(i + f_s) \mid i = 0, 1, 2 \ldots$$

where t_s is the time of the stimulus and f_s is the fraction of the cycle that remains at the time of the stimulus. The difference ($\Delta\phi$) between the observed post-stimulus phase reference points ($\phi_{R,\,post}$) and $TIPA_{null}$ for each post-stimulus cycle *i* is calculated as:

$$\Delta\phi(i) = TIPA_{null}(i) - \phi_{R,post}(i)$$

The phase-shift estimate of TIPA is calculated as the circular mean of $\Delta\phi(i)$ for all values of *i*.

For values reported in this study, circular means were calculated using the CircStat MATLAB toolbox[143]. Period parameters were estimated using linear fits of the phase reference points for the actogram approach and mean phase reference point intervals for TIPA. Because of the limitations of linear regression, it may be more suitable to estimate the period of the pre- and post-stimulus data subsets using an external method, such as Chi Squared periodogram or autocorrelation, and then fixing the τ_{pre} and τ_{post} parameters with those values. In cases where

there are limited numbers of cycles available in the data, the authors recommend using the average interval between phase reference points as an estimate of period.

Actograms were simulated using sets of simulated phase reference points selected from the generated set of simulations. The actograms values were created in MATLAB by creating a 10-day, 14,400-bin array with 12-hour runs of randomly generated numbers 1-100 starting on each cycle with that cycle's simulated onset time. Actograms were then formatted as TriKinetics monitor files and visualized using the ImageJ plugin ActogramJ (Schmid et al., 2011). Schematics of gene expression data were made using the curve generation function within Prism (GraphPad). Markings were then added in Adobe Illustrator. A spreadsheet for calculating the TIPA phase shift for all 3,600 simulations generated for this analysis, the R code used to generate the simulations, and an R package for calculating phase shifts using TIPA are available online at https://figshare.com/s/b521a5f23aa0802e252b.

Acknowledgements

The authors would like to thank Maria Luísa Jabbur, David Simon, Allison Leich Hillbun, Carl H. Johnson, and Doug McMahon for their insightful comments. This work was supported by NIH NINDS F31 NS096813 to M.C.T. and NIH NIGMS R35 GM124685 to J.J.H.

Author Contributions

M.C.T. conceptualized the method. M.C.T., J.R.J., T.L.P, and J.J.H. refined the method. J.J.H. generated the simulations. M.C.T. analyzed the simulations using the method. M.C.T., J.R.J., T.L.P., and J.J.H. wrote the paper.

4.3. Automated Alpha Measurement

The measure of activity duration in circadian data sets is typically done either manually or by computer with manual adjustments. While techniques have been developed to computationally determine the onset and offset of activity data sets of varying quality, the primary concern of alpha measurement is typically the speed and regularity with which the measurements can be made. In order to increase the throughput and consistency of alpha calculations, a programmatic approach is required. Here, we demonstrate an algorithm for the rapid detection of alpha in mouse activity records.

Alpha measurements are made by subtracting the time of activity offset from the time of activity onset. The accurate detection of these transition times is often visually obvious but difficult to define concretely. Generally, an activity onset is the beginning of a substantial bout of activity that follows a substantial bout of rest. Flat calculations that look for long stretches of inactivity followed by long stretches of activity to define onset can be quickly derailed with small blips of activity or inactivity at unexpected times. Given that activity records are rarely perfectly clean, these untimely blips of activity are very common. The solution to this issue is an iterative approach that takes each continuous bout of activity or inactivity within the context of its occurrence.

Strategy for measurement

The input for this method will be an activity record of one or more days, with a previously measured period. From this record, a period-adjusted activity profile will be created, representing activity at each circadian phase as an average across all provided days. This average is smoothed using the Savitzky-Golay method. Next, a threshold for activity or inactivity

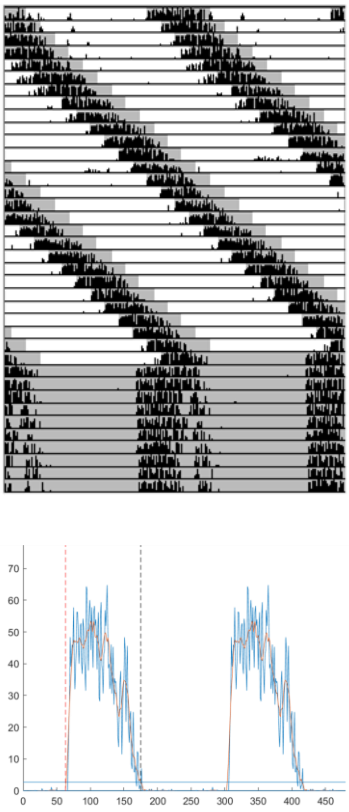

Figure 4-9. Example activity duration detection. The DD portion of an activity record (top) is averaged in a tau-dependent manner to produce an activity profile (blue lines, bottom). The onset (red dashed line) and offset (black dashed line) are detected using the rules described in the text.

is defined in two steps. First, a preliminary threshold is set at 10% of the maximum smoothed profile activity. Second, the root mean square (RMS) of the data below this preliminary threshold is calculated, and a final threshold is set at four times the amplitude of the low-activity RMS. At this point, the record is broken into segments starting and ending at each crossing point of the smoothed activity profile and the final RMS threshold. Each segment is preliminarily classified as “active” or “inactive” based on its position above or below the threshold.

From here, active and inactive segments are subjected to a series of quantitative tests to determine if the segment should be considered truly active or inactive. The workflow proceeds in two phases, and is performed on the activity waveform in a double-plotted format to avoid issues with onsets and offsets being split. The first phase of the workflow determines whether the preliminarily-sorted active and inactive segments need to be switched based on their segment length and the length of the surrounding segments. Given that the segments are created from transitions from activity to inactivity, for any given segment, neighboring segments will have the opposite classification. For example, every “active” segment at this stage is preceded and succeeded by an “inactive” segment. If the segment in question is less than 1 hour long, and both neighboring segments are greater than 1 hour, the segment is switched- if active, it is designated inactive, and vice versa.

After this first phase, the segments are re-drawn to account for switches. The second phase assesses active and inactive segments separately. For active bins, the segment is maintained as active if longer than 3 hours. If shorter than 3 hours, the designation is switched to inactive if a) the segment is either the first or last segment in the double plot, or b), there is no activity 3 hours before the start of the segment or 3 hours after the end of the segment. For inactive bins, the designation of inactive is maintained if a) the segment is 6 hours or longer, b) if the segment is the longest inactive segment in the data set, c) the segment is the first or last segment in the double plot, or d) there is no activity 3 hours before the beginning of the segment or 3 hours after the end of the segment. If any of these conditions are met, the segment is kept as “inactive,” otherwise it is switched to “active.” After this workflow is complete, the longest active stretch is identified, which is considered the activity duration. From this, the onset and offset times are also found as the beginning and end of this segment.

The result of this workflow is the identification of activity profile onset and offset times that compare to the times that the experimenter would identify manually. The identifications are performed faster than if done manually, and ideally closer to the quality of manual selection than previous automated attempts.

4.4. Measurement of SCN Neuron Phase Distribution without Cell Detection

The detection of the level of phase distribution of SCN neurons has become an important topic in circadian rhythms research, particularly in studies focusing on the interaction between photoperiodic light and the circadian clock. Strategies for studying this factor include simply analyzing the dorsal and ventral SCN separately, setting unbiased subregions of varying number across the SCN, using unsupervised community detection algorithms to identify cell-like ROIs, and manually or automatically detecting cellular ROIs. Approaches with large subregional analyses provide valuable information about phase angle differences between regions, but suffer from the grouping of nearby cells together solely because of anatomical position. Cell detection strategies – supervised, unsupervised, or manual – provide more independent information but sample only cells that are imaged with high enough focus quality to be included

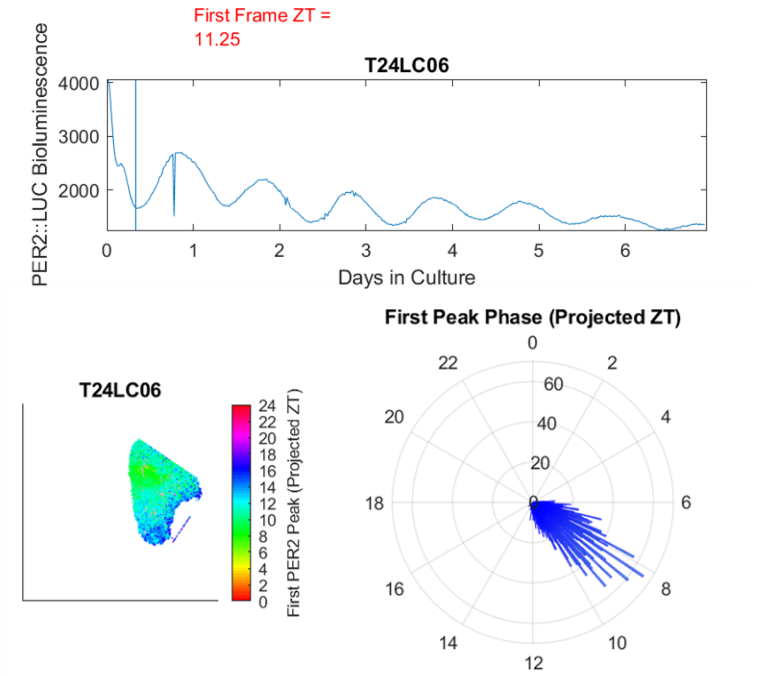

Figure 4-10. Processing and output of SCN ROI analysis. A, the overall SCN waveform showing the 8-hour exclusion cutoff (vertical line). **B**, phase map showing the circadian phase of each of several thousand SCN ROIs. **C**, polar histogram showing the spread of SCN ROI phases.

in that detection strategy. I have therefore employed a strategy that combines the unbiased sampling of the subregional ROI detection with the goals of assaying cells individually.

Recording parameters and pre-processing

In this technique, SCN slices expressing *Period2::Luciferase* (*Per2::Luc*) are cultured for 5-10 days with luminescence recorded at 20x magnification throughout (2 minute image acquisitions every 10 minutes). After a 2-frame minimization, each frame represents 20 minutes of time from the last, for a rate of 3 frames per hour. Based on the image resolution of the camera used (Stanford Photonics Inc. XR/Mega 10Z, 10.35 μm/pixel) at 20x magnification, each pixel within the image corresponds to 0.5175 microns. A grid of 10 pixel by 10 pixel (5.175 x 5.175 μm) regions of interest (ROIs) were overlaid in a 102 by 102 square pattern for a total of 10,404 ROIs. Because of their small size, no single ROI is likely able to encompass an entire cell. The brightness within each of these ROIs for every frame recorded is measured and exported to MATLAB.

In MATLAB, the remainder of the pre-processing involves detecting which ROIs correspond to the SCN, and which SCN ROIs are located in the left and right imaged SCN. To perform the first classification, the average brightness for each ROI across the entire recording is subjected to k-means clustering, separating the ROIs into groups of SCN and background. From here, those identified ROIs are referred to as SCN ROIs. These SCN ROIs are sorted into left and right SCN using hierarchical agglomerative clustering taking into account X/Y position and brightness. The SCN comprised of a greater number of ROIs is used for the rest of the analysis, and named SCN 1.

Calculations

For each SCN 1 ROI, the phase is calculated by identifying preliminary peaks with the peakfinder MATLAB algorithm. The first 8 hours of the data is excluded to prevent slice-window artifacts from affecting measurements (**Figure 4-10A**). The data is then segmented to form windows surrounding these tentative peaks. Within each window is one rise and fall of the PER2::LUC rhythm. The maximum value is taken within this window, and a quadratic approximation is used to estimate the peak time beyond the restriction of the 3 frames-per-hour resolution. The first peak time for each ROI is used to compute the distribution using the median absolute deviation, a more robust measure of data spread than standard deviation.

Output

The ROI analysis strategy allows for the display of a heat map showing the phase of each ROI (**Figure 4-10B**), as well as polar histogram views of the spread of the ROIs (**Figure 4-10C**). The quantitative output includes the phase of each ROI, the mean phase, as well as the median absolute deviation of phase. The mean phase can be used with the timing of lights of and the first frame imaged to determine phase angle. Other analyses, such as cosinor analysis or interpeak measurements for period or peak duration measurements for waveform, can also be performed on each ROI to produce mean and distribution measurements and map outputs.

Supplemental figures and tables

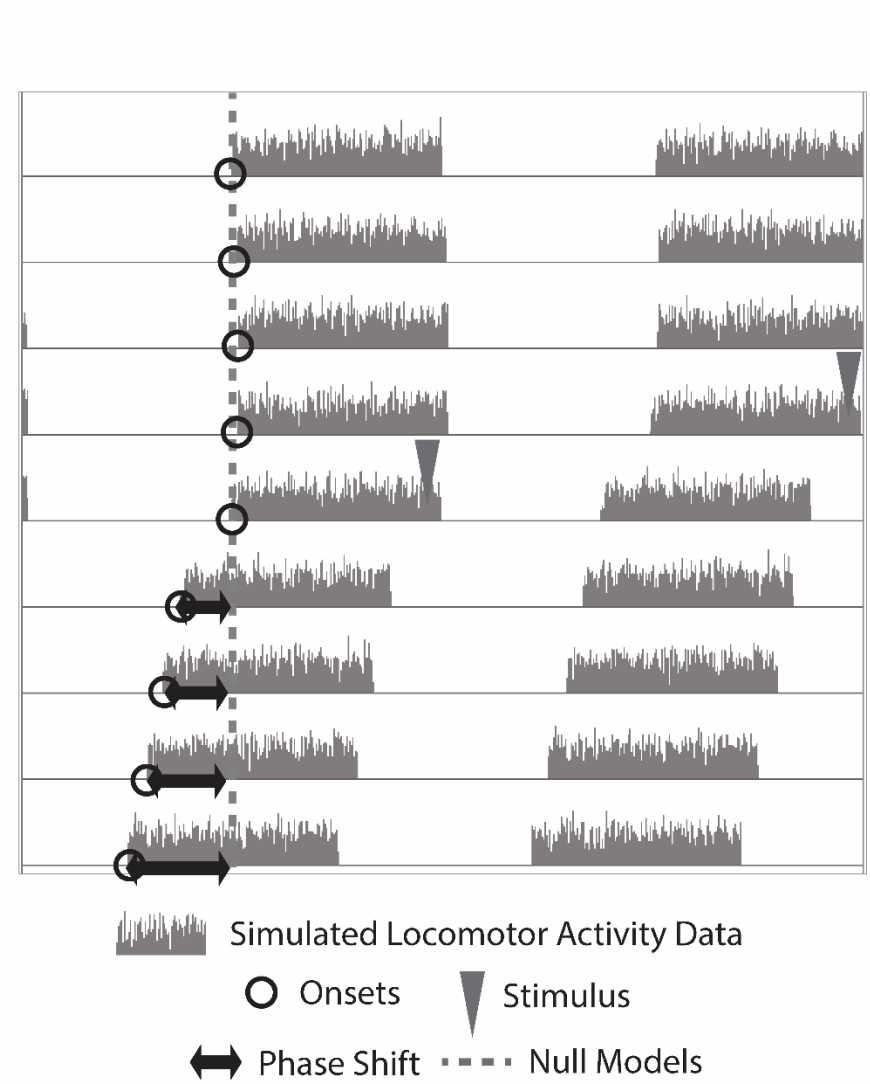

Figure 4-S1. Period changes have effects on phase shift estimation. When the period changes between pre- and post-stimulus epochs, the comparison of the phase reference points (open circles) to the pre-stimulus null model (dashed grey line) can produce widening or narrowing estimates of phase shift (black arrows).

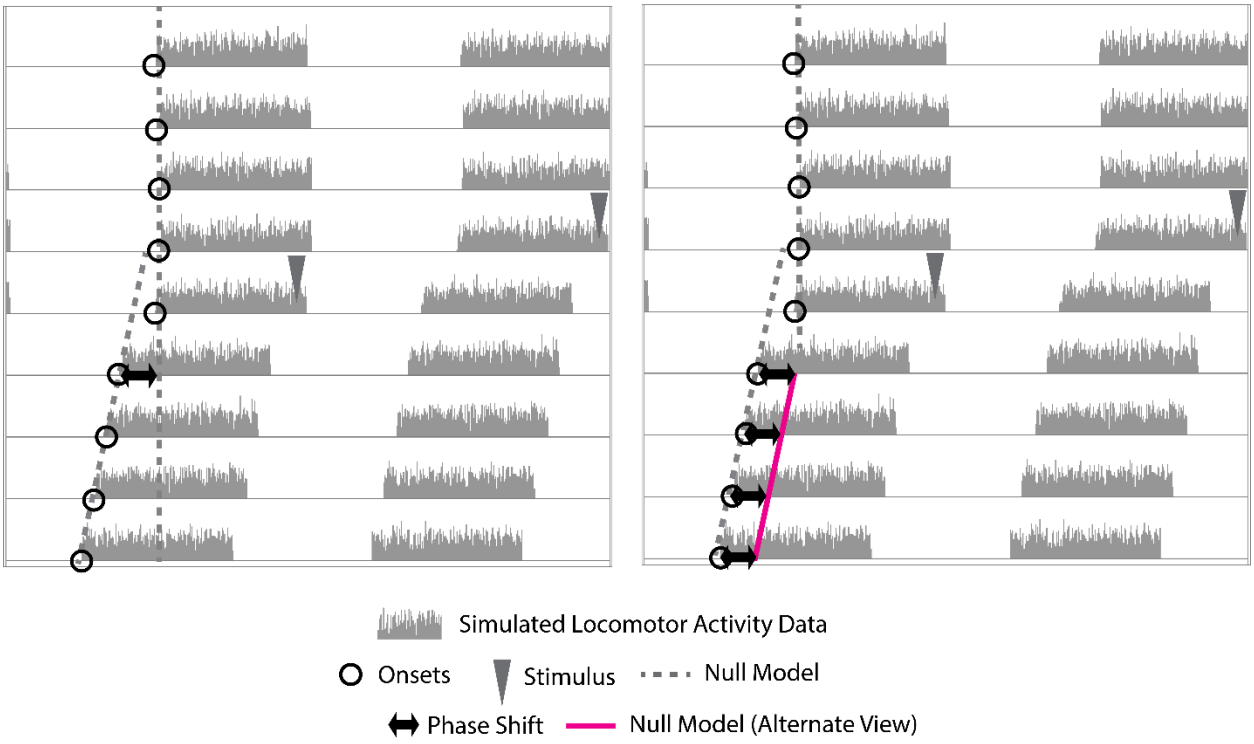

Figure 4-S2. The basis of the actogram approach is the anchoring of a null model to the pre-stimulus model. The actogram approach can be replotted by anchoring the post-stimulus null model to the projection of the pre-stimulus null model on the first post-stimulus cycle. This produces an equivalent estimation of phase shift, because the underlying null hypothesis remains the same: that the stimulus is inducing a known period change, but no phase shift. Because this replotted null model (magenta line) has the same slope as the post-stimulus null model passing through the post-stimulus phase reference points (grey dashed line), the phase relationship between the two lines is stable and the comparison between them can be made on each cycle.

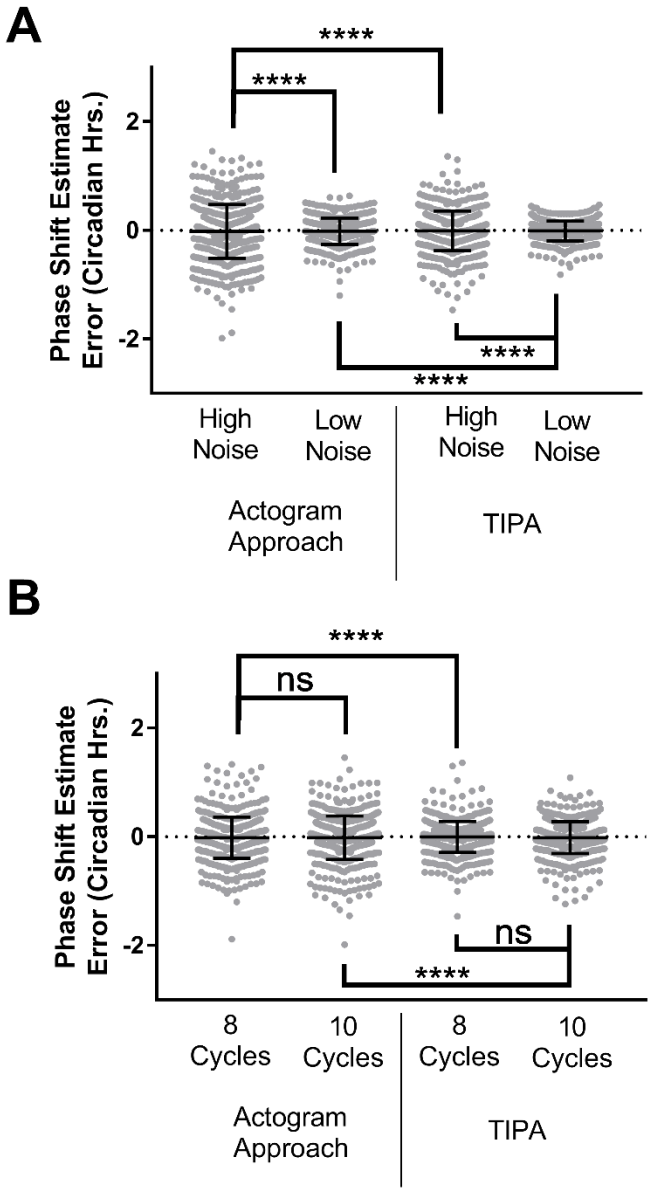

Figure 4-S3. TIPA remains more precise despite noise level and cycle number. A, comparison of TIPA and the actogram approach in simulation groups that had high and low noise levels. For both methods, precision is higher (variance is lower) in the low-noise simulations. For both high and low noise simulations, TIPA has a higher precision (lower variance) than the corresponding actogram approach. B, comparison of TIPA and the actogram approach in simulation groups that had 8 (4 cycles pre- and post-stimulus) or 10 (5 cycles pre- and post-stimulus). Both methods had equivalent precision across each cycle number. TIPA had a higher precision than the actogram approach for both cycle numbers. Brown-Forsythe test for unequal variances, (****) corresponds to $p < 0.0001$, **ns** corresponds to $p > 0.05$.

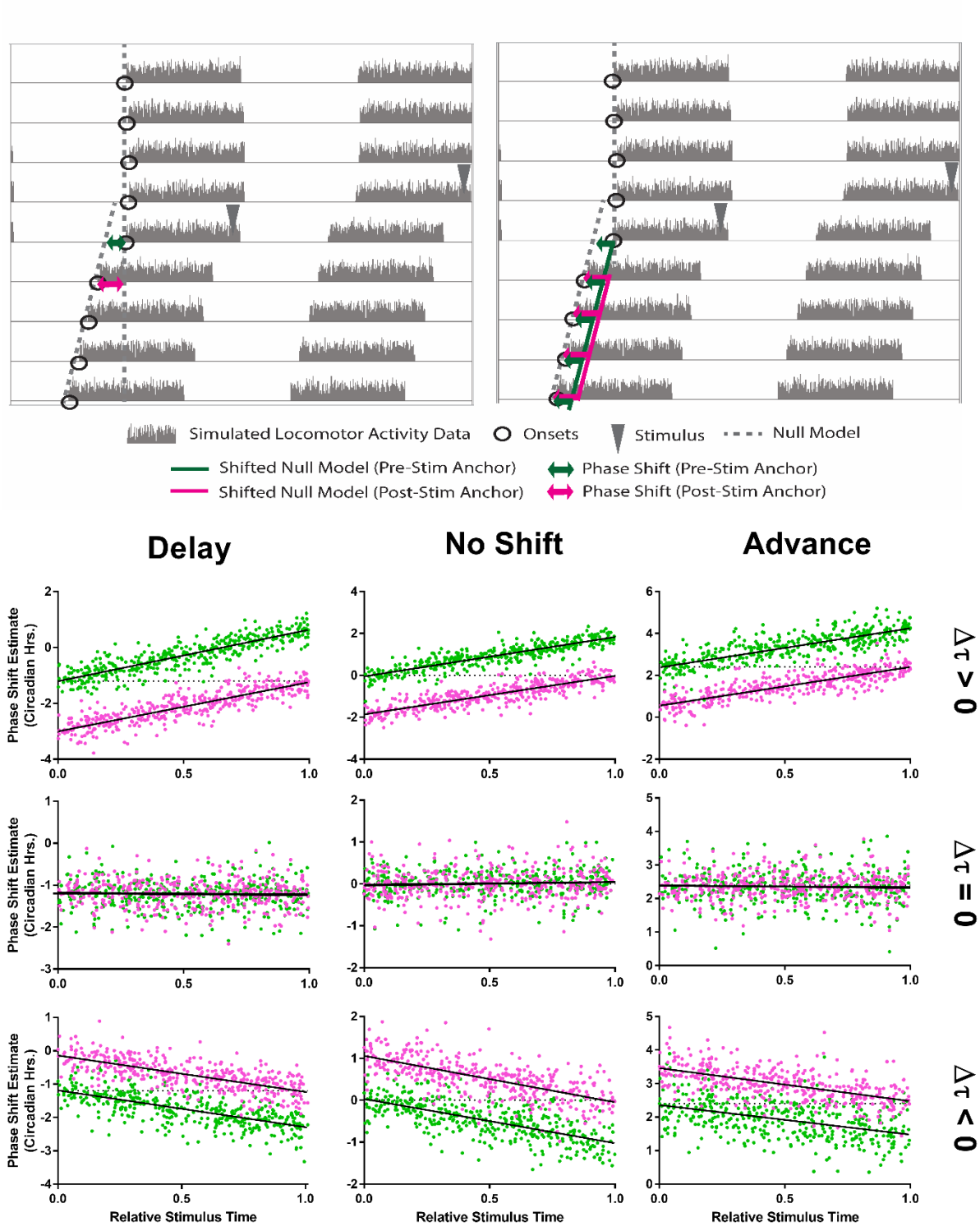

Figure 4-S4. Anchoring the actogram approach to the last pre-stimulus phase reference point produces a complementary error in the phase shift estimate. Phase shifts can be calculated by anchoring the null model to the last pre-stimulus phase reference point (green) or the first phase reference point projected by the null (magenta, see Figure 2). This can be visualized using the traditional

actogram approach (top, left) or the alternate anchor-based plotting (top, right). The phase shift estimate using each anchor is dependent on the relative stimulus time (bottom array of 9 panels, see Figures 5 and 7). The pre-stimulus anchor (green) is most accurate when the stimulus occurs near the last pre-stimulus phase reference point, and the post-stimulus anchor (magenta) is most accurate when the stimulus occurs near the first post-stimulus phase reference point as projected by the pre-stimulus null model.

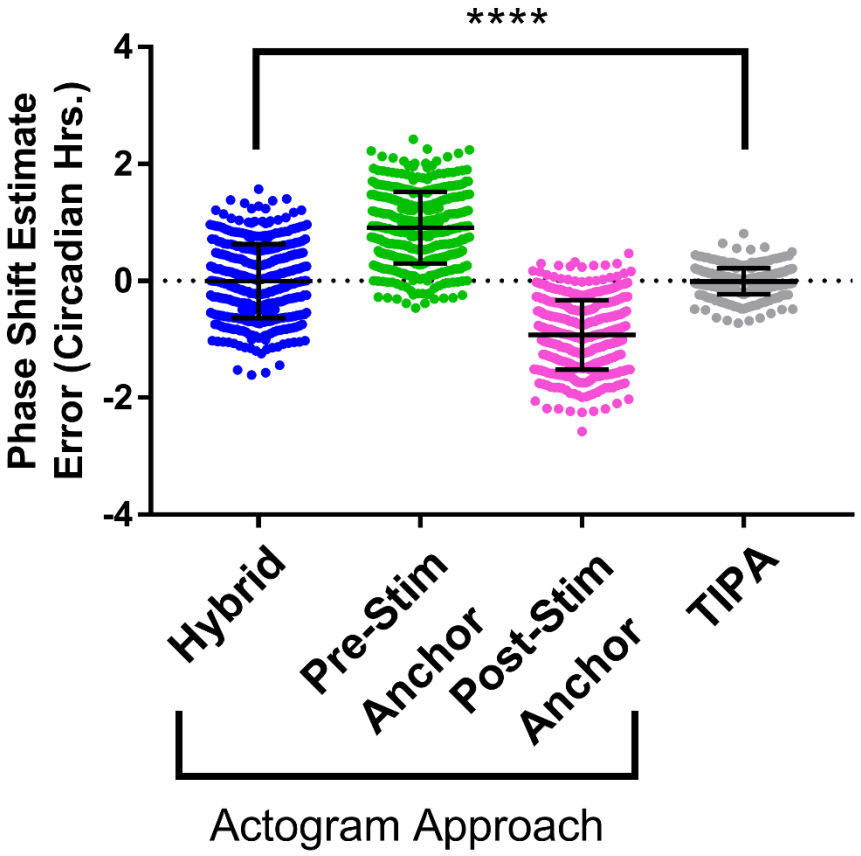

Figure 4-S5. An example of the two actogram approach anchor points, and their hybrid, estimating the phase shift of a phase delay, lengthened period simulation group. Though the hybrid actogram approach (blue) has an error that surrounds 0, its variance is higher than that of TIPA (grey). This is because the hybrid approach is averaging the over-estimation error of the post-stimulus anchor (magenta) and the pre-stimulus anchor (green) versions. Brown-Forsythe test for unequal variances compared between TIPA and Actogram Approach Hybrid, (****) corresponds to $p < 0.0001$.

Group	*Δϕ*	*Δτ*	*Noise*	*Total Cycles*
1	Delayed	Shortened	High	8
2				10
3			Low	8
4				10
5		Not Changed	High	8
6				10
7			Low	8
8				10
9		Lengthened	High	8
10				10
11			Low	8
12				10
13	Not Shifted	Shortened	High	8
14				10
15			Low	8
16				10
17		Not Changed	High	8

18				10
19				8
20			Low	10
21				8
22			High	10
23		Lengthened		8
24			Low	10
25				8
26			High	10
27		Shortened		8
28			Low	10
29				8
30			High	10
31	Advanced	Not Changed		8
32			Low	10
33				8
34			High	10
35		Lengthened		8
36			Low	10

Table 4-S1. Description of parameters for each simulation group. 3,600 simulations were generated, divided into 36 groups of 100. Each group consisted of each combination of phase advance, delay, and no phase change; period lengthening, shortening, and no period change; high or low noise; and 8 or 10 total cycles generated. High and low noise correspond to 0.5 and 0.25 standard deviations of the Gaussian distribution used for the phase reference point interval generation.

Chapter 5

Summary and Discussion

5.1. Summary

In this dissertation, I have examined the input mechanisms of photoperiodic changes to circadian properties. Light is the primary source of environmental input to the circadian system and its effects on that system are complex. Aside from influencing the phase of a circadian rhythm, light is able to induce changes to behavior that are characteristic of particular seasons. Considering that current circadian light treatments attempt to manipulate a simplified version of daily light exposure, I set out to determine what specific cues light provided to induce those behavioral changes.

To do so, I focused on measuring two circadian behavioral properties well-known to be changed in response to different seasonal light exposure, free-running period and locomotor behavior duration. Taking inspiration from historical experiments examining the parametricity of entrainment, I sought to differentiate between the instantaneous phase-shifting influence of light and the parametric influence of continued light exposure. Measuring period and alpha in mice exposed to a single phase shifting stimulus revealed differences in period between advanced and delayed mice while alpha was the same across both shifts (Figure 2-2). This period after-effect corresponds with those previously observed in multiple species of rodent, including mice[141]. To determine if phase shift strength was a factor, I exposed mice to repeated phase shifts using non-24 hour T cycles of 23 and 26 hours. The period differences between a single advance and delay observed in the previous experiment were enhanced with repeated shifts, with a change in alpha also emerging.

These results prompted further investigation into the distinct components of photoperiodic induction. I implemented a set of photoperiod/T cycle combinations to induce repeated phase shifts while also providing particular light duty cycles. These groups consisted of three T cycles (23, 24, 26 hours) with short and long versions of each. I found that after exposure to these light schedules, the after-effects in alpha followed the duration of light exposure while the period was responsive to both the duration of light exposure and the direction of the repeated shift (Figure 2-3). Importantly, these results indicated that light was capable of manipulating these two factors independently.

Like in the study of the mechanism of entrainment, these results raised a question surrounding the parametricity of the changes in alpha and period. To examine this property, I entrained mice to skeleton photoperiods which feature two hour-long light pulses occurring at the would-be time of onset and offset each day, rather than a full, continuous photoperiod. I found that period remained largely unchanged between photoperiod lengths and between complete and skeleton photoperiods. Interestingly, alpha changes observed between T24 Long and Short complete photoperiods were also observed between T24 Skeleton Long and Skeleton Short photoperiods (Figure 2-4). These results indicate that alpha, found previously to be more responsive to the duration of light than to the direction of overall phase shift, is in fact most responsive to onset-offset interval length rather than continuous light duration. These results corresponded with the work of Pittendrigh and Daan[141], who observed decreases in activity duration length from short to long skeleton photoperiods. In that study, decreases of ~0.2 hours in period length from short to long skeleton photoperiods were also found, which we did not observe. In that study, mice were exposed to both photoperiods in succession, and so the difference in results in period after-effects may be related to the direct previous photoperiodic history of the animal.

Beyond the study of behavioral responses to photoperiod, changes to the master pacemaker, the SCN, are of particular interest. Understanding the cellular response to the photoperiodic input can inform a better understanding of the SCN network as a whole. Previous studies from our lab and others have shown that photoperiodic exposure leads to a change in SCN neuron phase dispersal[68,69,89]. Exposure to long photoperiods is associated with a wider distribution of clock gene expression peak timing, while short photoperiods lead to a contraction of peak timing. I sought to determine if SCN phase dispersal followed the behavioral responses of alpha or period by making organotypic SCN slices from mice exposed to each of the six T-cycle/photoperiod combinations described above. I found that, like alpha, SCN phase dispersal was strongly influenced by photoperiod (Figure 2-5). This correlation demonstrates the close link between activity duration and SCN phase distribution.

Another commonly seen effect of seasonal light exposure on circadian entrainment is a change in phase angle. Exposure to short photoperiods is associated with a more delayed alignment of the circadian rhythm with the light cycle, while exposure to long photoperiod is associated with an earlier alignment relative to the light cycle. Across the six groups discussed above, phase angle was influenced by overall phase shift direction and by photoperiod duration. This phase angle change was true for both *in vivo* activity rhythms and for clock gene expression, and was similar across complete and skeleton photoperiods (Figure 2-6).

Another interesting question surrounding the molecular mechanism of photoperiodic induction involves which cells in the SCN are responsible for encoding the light information provided from the retina, and what firing pattern encodes that message. As a largely retinorecipient population, the VIPergic neurons are a likely candidate for conveying that photoperiodic information. Using the optogenetic stimulation experimental set-up that our lab previously developed[131], I targeted channelrhodopsin-2 to VIPergic neurons. I then stimulated these neurons using blue light delivered from a surgically implanted fiber optic at a frequency of

10 Hz. For the experiment, I entrained animals to a short photoperiod, and then activated VIPergic SCN neurons using optogenetic stimulation for 8 hours following lights off or 8 hours preceding lights on. Animals exposed to optogenetic stimulation in addition to the short photoperiod experienced compression of alpha similar to animals moved from a short photoperiod to long photoperiod. Animals with fiber optic implants and blue light stimulation, but without channelrhodopsin expression, maintained the short photoperiod alpha throughout the experiment. These experiments show that activation of VIPergic SCN neurons is sufficient to alter downstream locomotor behavior associated with a particular photoperiod.

The above experiments, and other related experiments, require specialized techniques. In fact, the study of circadian rhythms in general requires a suite of measurements and calculations apart from those typically employed for the study of cell biology and neuroscience. In this dissertation, I presented technical approaches for the quantification of phase shifts, activity duration, and SCN phase dispersal. While phase shift measurements have been made for many years, the tau-independent phase analysis approach described here shows a marked improvement in accuracy and precision over past approaches as demonstrated by testing on simulated phase shift data. A strategy for quantifying alpha in a streamlined way to decrease ambiguity and increase throughput is also presented. Last, a method for quantifying the phase distribution across the SCN without identification of specific cells is described. These techniques allow for the proper analysis of the data presented within the dissertation, and provide useful tools for other chronobiologists moving forward.

5.2. Significance

The physiological response to light exposure has tended to appear more complex as more is revealed about its mechanisms. In additional to changing circadian phase, light has a role in inducing seasonal variations in physiology including other circadian properties like activity duration and free-running period. Generally the seasonal effect of long light exposure has been associated with a shortened free-running period and a compressed alpha and short light exposure with lengthened free-running period and expanded alpha. The results within this dissertation have demonstrated that properties of light other than the number of hours of exposure, namely phase shifts, are capable of inducing changes to alpha and reaffirmed and more carefully defined their effects on free-running period (**Chapter 2.1**). These experiments showed a photoperiod with 13 hours of light per cycle (T26) producing an after-effect of longer period and longer alpha than a photoperiod with 11.5 hours of light per cycle (T23), contrary to expectations based on long and short T24 photoperiods. Because the net phase shift direction was the primary differentiation between the two groups, the repeated phase shift component of light input is therefore more important than absolute light duration in driving these circadian properties.

This result is important because it demonstrates that physiological responses to light are not as simple as they may appear. Though photoperiods are distinguished by definition based on their light duty cycle, the interpretation of that light signal by the circadian system involves additional cues in the form of phase shifts. These additional cues can be used to manipulate the circadian system without full photoperiodic changes. The next experiments described in this dissertation examine these distinct components of light more closely. Photoperiods consisting of different combinations of repeated phase shift direction and light durations are used to drive alpha and period in different ways (**Chapter 2.2**). Most striking is the fact that alpha and period

changes can be dissociated depending on the type of input. Repeated phase advances are capable of inducing shortened free-running periods, but inducing those phase advances with long photoperiods produces lengthened alpha. While the experiments detailed in **Chapter 2.1** showed that alpha and period could be driven by factors other than light duration, the two properties still segregated together (lengthened or shortened). The experiments in **Chapter 2.2** show that alpha and period can be driven separately. Alpha is primarily driven by light duration and period is driven by both light duration and repeated phase shifts. These results demonstrate the importance of determining the exact component of light input that drives any physiological change of interest – if attempting to replicate a photoperiodic influence, it may be most effective to isolate the desired relevant input.

With changes to alpha being found to be dependent on photoperiod duration, it was important to further classify the input mechanism by testing whether continuous light exposure or onset-offset interval was more critical for setting alpha. While previous experiments have detailed the proximal effect of complete and skeleton photoperiods on alpha, the after-effects were not well-defined. My experiments with skeleton long and short photoperiods demonstrated that onset-offset interval, rather than light duration, was critical in setting alpha after-effects but not period. This result means that light therapies may take advantage of short, well-timed pulses rather than full photoperiod replication for certain outputs.

Previous studies have associated photoperiodic encoding with a change in the phase dispersal of SCN neurons. Given that the exposure to different combinations of repeated phase shifts and light durations drove changes in period and alpha in a different manner, it was an interesting question to see how SCN neuron phase dispersal responded to those same light schedules. My results show that phase dispersal within the SCN follows the pattern of alpha, responding to changes in light duration but not repeated phase shift direction. Because phase

dispersal did not respond to both factors like period, it provides an even stronger correlation between phase dispersal and activity duration.

The advent of optogenetics in the neuroscience community brought an enhanced ability to manipulate neural activity. With increases in temporal and spatial precision over previous techniques like pharmacological manipulations, optogenetics was well-suited for particular circadian experiments. My colleague, Jeff Jones, and I published the first usage of SCN-targeted optogenetics in 2015, detailing the use of channelrhodopsin-2 in manipulating circadian behavior[131]. I used this technique, refined slightly by targeting only the VIPergic SCN neurons, to demonstrate that activity within this subpopulation of the SCN was sufficient to drive a photoperiodic output (**Chapter 3.2**). This result was important because it demonstrated that firing rate manipulation could tune the SCN in such a way as to produce a behavioral phenotype associated with a particular season. While it was a stride forward to induce entrainment and phase shifts using upregulation of activity, the subtlety of inducing a photoperiodic-like behavioral change demonstrated the power of optogenetics in the SCN and revealed much about the role of VIPergic neurons and their sufficiency in propagating light-mediated information.

The technical advances described in **Chapter 4** of this dissertation are meant to address specific concerns in circadian data analysis. When measuring phase shifts, there previously existed an issue of accuracy and precision, which TIPA aims to remedy (**Chapter 4.2**). While the human measurement of alpha was acceptable, there is an issue with consistency and throughput. The alpha measurement strategy used in **Chapter 2** and described in **Chapter 4.3** is meant to create a more objective measurement and one that can be done faster than manual scoring. When measuring phase dispersal, the identification of clear cells can be tricky, and can also lead to selection bias. The strategy detailed in **Chapter 4.4** is an spatially unbiased attempt

at measuring phase dispersal throughout the SCN without the need for cell identification. All of these techniques are intended as usable improvements to existing strategies.

5.3. Future Directions

The results presented this dissertation have answered several key questions in circadian photoperiodic biology, including what light cues influence alpha and period and how alpha and SCN phase dispersal associate across different conditions. These new insights raise a number of interesting questions. The novel finding that alpha and period can be changed independently suggests that the light components driving those changes do so through differing mechanisms. Repeated phase shifts, a strong influence on period changes, may induce some form of alteration to DNA methylation states in order to change period[144]. Onset-offset interval, the stronger influence on activity duration changes, is highly related to changes in SCN phase dispersal and therefore may drive the spread in phase of SCN neurons through alternating phase shifts in opposite directions. This possibility corresponds well with the proposed theory of morning and evening oscillators within the SCN (and other non-mammalian pacemaking systems), with the phase difference between the two driving various daily and seasonal outputs.

Examining the relationship between activity duration and SCN phase dispersal is another exciting avenue of research raised by this dissertation. While very strong correlations have been shown here, with SCN phase dispersal being inversely related to activity duration across multiple light schedules, it is likely that phase spread within the SCN underlies changes to the activity duration output. Causation has not been shown, however, and to do so would require specific manipulation of phase dispersal within the SCN with simultaneous measurement of changes in activity duration. Such an approach is, at present, not technically possible. While certain pharmacological applications (such as the $GABA_A$ antagonist bicuculline) are reported to have effects on SCN neuronal coupling, they generally do so through alterations to excitatory and inhibitory GABA transmission and therefore are not solely changing phase dispersal. This area of research is very active, however, and more information about SCN cell-

to-cell communication and the nature of a possible morning-evening oscillator system may eventually allow for the specific manipulation of phase dispersal.

One of the major findings of this dissertation is the dependence of after-effects in activity duration on onset-offset interval, rather than complete light interval length. Given the link between phase dispersal and activity duration described above, an obvious next step is to determine the level of SCN phase dispersal that occurs after exposure to skeleton photoperiods compared to complete photoperiods. Results from that experiment would potentially provide another link association between alpha and phase dispersal, or demonstrate if there is a difference in how phase dispersal and alpha are encoded.

My work using the optogenetic activation of VIPergic SCN neurons also raises a number of interesting future experiments. The results within this dissertation have demonstrated that the activation of VIPergic SCN neurons for a portion of the day is sufficient to induce a proximal change in activity duration. Given sufficient cycles of optogenetic stimulation, it would be of interest to determine if after-effects are altered in the same way as proximal activity duration. Considering the similarities between optogenetic VIPergic SCN neuron activation and the endogenous activation pathway of light exposure transmitted to the retina, it is likely that the repeated optogenetic stimulation of these neurons would result in a similar encoding of alpha after-effects.

Another important optogenetic follow-up experiment surrounds the demonstration of necessity of VIPergic neurons. While the work shown here has demonstrated sufficiency, recent work from Jeff Jones *et al*. has shown that inhibition of VIPergic neurons is required for light-induced phase shifts[130]. Determining if inhibition of these neurons during a portion of a long photoperiod results in a short-photoperiod-like behavioral phenotype would provide new information about the role of these cells in setting the behavioral response to light duration. Lastly, it will be interesting to determine the effect of optogenetic stimulation *in vivo* on SCN

phase dispersal *ex vivo*. A resulting change in phase dispersal in optogenetically stimulated animals would indicate that the change in VIPergic neuron activation is sufficient to induce changes in phase dispersal, providing key information about the mechanism of phase dispersal change induction.

One factor that is a necessary component of all photoperiodic experiments but is largely understudied is the time of induction. Most protocols surrounding long or short photoperiods use at least two weeks, most often three or four, of exposure to the given photoperiod before transfer to DD or collection of samples. SCN changes are expected to take some time to fully take effect, but all of the ramifications of photoperiodic exposure (period changes, alpha changes, etc.) may not take the same amount of time to occur. A thorough analysis of the effects of different lengths of photoperiodic exposure would greatly enhance the field's understanding of the windows during which these changes can take place, as well as providing valuable information about any dependencies that may exist between different factors.

Photoperiodic studies, including those contained herein, often cite the effect of season on human mood as a relevant extension of the mechanistic questions they pose. While these links are entirely valid, there is much that must be learned about the exact way in which photoperiod affects humans. Unlike the strain of laboratory mice used in these experiments, humans are diurnal. As a result, the response of humans to the parametric and non-parametric influences of light may be different. Conversely, the similarity in circadian organization (i.e., a centralized circadian system) between humans and mice may indicate that these effects will be similar across most mammals. Human and animal studies comparing the effects of developmental exposure to different photoperiods provide great value in comparing the salient effects of a proximal photoperiod with the previously established effects of a historical light exposure. Recent work from the Hattar lab has shown that certain light-induced mood perturbations can occur in a manner independent of the SCN[145], but other SCN-dependent light-

to-mood effects may exist as well. Beyond mood, there are seasonal variations in a number of non-communicable diseases, indicating that human responses to photoperiod may be more varied than originally thought, and of course, that variation may indicate multiple parallel induction mechanisms (i.e., a seasonal change in susceptibility to breast cancer may be induced in an entirely different fashion that alterations to mood).

While conceptualizing the experiments described here and analyzing and interpreting the data those experiments produced, I have sought to take inspiration from circadian pioneers who posed incredibly intricate and well thought-out questions of a then-mysterious biological property. I have found their ingenuity and cleverness to be a source of amazement, and have found that their approach to biological problems is still very much relevant even with today's technical advances. In my experiments, I used light schedules (T cycles, photoperiods, skeletons) that have been implemented in some form or another for almost sixty years. I have done so, however, in conjunction with a set of techniques (optogenetics, high-sensitivity luminescence imaging) that are far newer. Even when using age-old measurements like those of free-running period and activity duration, the questions I asked with those measurements were built upon recent advances from cellular and electrophysiological studies, and the analysis approach I took were greatly improved with the aid of programming and processing power. It is my hope that the information contained within this dissertation will provide evidence not only for the resolution of several pertinent biological questions but also for the value of integrating historically validated thinking with modern approaches.

Appendix A

A.1. Revealing oft-cited but unpublished papers of Colin Pittendrigh and coworkers

Michael C. Tackenberg, Carl H. Johnson, Terry L. Page, Serge Daan

Modified from: Tackenberg, M.C., Johnson, C.H., Page, T.L., Daan, S. Revealing oft-cited but unpublished papers of Colin Pittendrigh and coworkers. *Journal of Biological Rhythms* **32**(4):291-294 (2017).

A motivating force in Pittendrigh's interest in entrainment was the notion first suggested by Erwin Bünning in 1936 that a circadian clock is involved in photoperiodic time measurement[28]. In 1960, Bünning expanded upon this notion, delineating his vision of the clock's involvement in the photoperiodic response[29]. His model postulated that two segments of the circadian cycle, one "light-requiring" and the other "dark-requiring", initiated "photoperiodic induction" under specific circumstances: long-day induction would occur when the "dark-requiring" process overlapped with the light, and short-day induction would occur when the "light-requiring" process overlapped with the dark. Pittendrigh accepted the general basis of Bünning's hypothesis: "In our view, there is no doubt that his general proposition (that circadian rhythmicity does effect the photoperiodic time-measurement) is correct"[9]. However, he found the model incomplete with regard to the phasing of the central pacemaker orchestrating the "light-requiring" and "dark-requiring" processes. In his view, the model did not address the dual role of the photoperiodic light cycle: setting the phase of the pacemaker as well as inducing long- or short-day seasonal responses. As Pittendrigh noted in 1964, "[i]t is a remarkable fact that so much effort has been put into testing the Bünning hypothesis without any fundamental inquiry being made into the mechanism of how light entrains (and hence phase controls) the rhythm"[9].

The two unpublished manuscripts included in the supplement encapsulate the efforts of Pittendrigh and his co-authors to develop more fully the “non-parametric” model of entrainment first proposed by Pittendrigh and Minis (1964). The first of the two manuscripts reports the experimental validation of the assumptions underlying the non-parametric (discrete) model of entrainment and offers a variety of experimental results that ultimately must be explained by any complete hypothesis of the mechanism of entrainment.

Despite the extensive experimental evidence that was consistent with the non-parametric model of entrainment presented in the first manuscript, there were deviations between some of the model's apparent predictions and the empirical results. Importantly, the model, simply applied, failed to properly estimate the limits of *Drosophila pseudoobscura* entrainment. Based only on the maximum magnitude of the phase shifts, the mathematical model predicted that flies should entrain to T cycles ranging from 12 to 36 hours – but computer simulations (with added noise) and experimentation revealed that the limits were narrower – closer to 18 to 30 hours. The model also failed to predict which of the steady-states would prevail in certain skeleton photoperiods (especially 11:13, 12:12, and 13:11) – this “bistability” was “assumed” to be the result of factors - such as initial phase and the order of the dark intervals – that the model did not take into account. Explaining these deviations from the model’s prediction is the focus of the second manuscript that explores analytically the criteria that must be met for stable entrainment in the face of biological instability in the pacemaking oscillation.

Phase response curves and the start of the entrainment debate (1958-1964)

Two years before Bünning published his 1960 paper linking the circadian clock to photoperiodism, Hastings and Sweeney (1958) reported the first phase response curve (PRC),

followed soon after by DeCoursey (1960). PRCs allowed the quantitative prediction of the response of the phase of the underlying master circadian pacemaker to light pulses. The PRC could therefore be used to determine certain properties of stable entrainment. When a pacemaker with a freerunning period of τ hours is stably entrained to an environmental cycle with a period of T hours, that pacemaker undergoes a phase shift of (τ – T) hours each cycle. If the environmental cycle consists of a single repeating pulse, that one pulse must elicit the (τ – T) hour phase shift. Using the PRC, the phase of the pacemaker at which a light pulse produces the necessary (τ – T) hour phase shift is easily identified. When the pacemaker is stably entrained to the light cycle, the phase of the pacemaker at which the light pulse occurs in each cycle is identical. When the pacemaker is not yet entrained to the environmental cycle, however, each successive pulse will strike the pacemaker at a different phase until steady-state entrainment is achieved. The magnitude of each phase shift can be determined using the PRC by shifting the curve horizontally commensurate with the phase shift of the pacemaker. As the pacemaker approaches and eventually reaches steady-state entrainment, the successive phase shifts will approach, over the course of several cycles, the requisite τ – T hour shift.

As measurements and analysis of entrainment grew more sophisticated, two prevailing theories of the underlying mechanism emerged. The first, championed by Jürgen Aschoff, was *parametric entrainment* (or continuous entrainment) involving the continuous modulation of the pacemaker's angular velocity to modify phase. The second, proposed by Pittendrigh, was *non-parametric entrainment* (or discrete entrainment) involving phasic and rapid modifications to the pacemaker's phase by light. This latter view of entrainment prompted the experiments detailed in Pittendrigh and Minis' 1964 paper that analyzed entrainment by "skeleton photoperiods."

By 1964, it was known that circadian pacemakers could entrain to a Zeitgeber cycle consisting of one pulse per cycle[9]. Pittendrigh took this approach one pulse further, reducing the entire photoperiod to its on/off transitions (a "skeleton photoperiod"). Under the skeleton

photoperiod paradigm, for example, the light phase of a skeleton photoperiod simulating LD 8:16 would be represented by two fifteen-minute pulses of light separated by 7.5 hours of darkness in one interval and 16 hours of darkness in the other interval. Using the *Drosophila* eclosion rhythm frequently employed by Pittendrigh, the phase of the rhythm was plotted for complete and skeleton photoperiods ranging from 1:23 to constant light. As expected, the eclosion peaks of flies in complete photoperiods maintained a steady phase relationship near the onset of light regardless of the time of the photoperiod's offset. Flies in 24-hour skeleton photoperiods did the same for relatively short skeleton photoperiods (e.g., PPs 1:23, 6:18, 9:15, etc.) Beyond a 10.5-hour spacing between the 15-min light pulses (simulating an 11-hour day), however, the average phase became ambiguous and at 13.5-hour intervals between the light pulses (simulating a 14-hour day), the phase of eclosion changed entirely. Because a skeleton photoperiod of 10:14 is very nearly the same as one of 14:10 (in L:D:L:D, 10:14 would be represented by a skeleton of 0.25:9.5:0.25:14 and 14:10 would be represented by a skeleton of 0.25:13.5:0.25:10), flies "ψ jumped" so that the subjective day now spanned the shorter interval and the eclosion peak occurred near the second pulse rather than the first. The fact that flies were able to set a stable phase relationship strictly using the discrete on/off transitions between light and dark and were able to reset their subjective day to span the shorter light-pulse interval demonstrated that major features of entrainment could be accounted for by non-parametric mechanisms. Pittendrigh acknowledged, however, that the differences observed between complete and skeleton photoperiods beyond 14:10 suggested that some aspect of the entrainment of the pacemaker might be parametric.

An experimentally validated model (1964-1976)

Since the 1970s, the debate between non-parametric and parametric entrainment has been set aside as effort has been directed towards a more thorough understanding of the

physiological and molecular complexities of the entrainment mechanism. Though Pittendrigh's "instantaneous" resetting model may better be exploited to generate (and test) quantitative predictions than the "level and threshold" theory of his close friend Jürgen Aschoff[148,149], there are aspects of each model that have been found to be accurate. Just as Pittendrigh acknowledged that the ψ-jumping seen in skeleton photoperiods suggested a parametric aspect of entrainment in continuous light cycles (Paper I), so too did Aschoff plainly state that some combination of the two mechanisms is most likely to be the case[150].

Pittendrigh was not satisfied with this loose combination of models, however. He maintained throughout the 1960s that despite the parametric model having some relevancy to the true mechanism of entrainment, the non-parametric model was more useful because it was more quantitative and predictive. Without a better way to continuously measure the velocity of the pacemaker itself in real time, it would be difficult to quantitatively investigate the parametric model. As such, he sought in 1964 to create a non-parametric model that would provide real predictive value using experimentally derivable period and PRC information. After testing its validity by subsequent studies that relied on its predictions, Pittendrigh intended to create a comprehensive and direct experimental test of his model. These tests are the focus of Paper I. After confirming its predictions, he set out to address two critical non-intuitive points of his model in Paper II: the existence of bistability and limits of stable entrainment.

Of the two manuscripts that are the focus of this introduction, the first was drafted soon after the publication of Pittendrigh and Minis' 1964 report on skeleton photoperiods. The second paper was drafted in 1974 at the time when one of the authors (SD) was a postdoc in Pittendrigh's lab at Stanford. The theory and experiments detailed in the unpublished manuscripts reflect the state of the art in the early 1970's. The manuscripts were repeatedly revised and updated until 1978. They were intended for publication in The American Naturalist, but – although widely spread among friends as "the Ottesen papers" – were never submitted for

publication. It is likely that a strong factor in that omission was Pittendrigh's ongoing uncertainty about the mechanisms of entrainment, as described by one of the authors[148] of this paper:

> Most of you, I am sure, consider the problem of entrainment basically as solved. Most have sat in courses in which the principle of phase resetting was explained. There is somehow an endogenous oscillation, which runs at a frequency slightly deviating from once per 24 h, and that deviation is corrected each day by an instantaneous, abrupt phase shift in response to light: every evening at dusk and/or every morning at dawn, as dictated by the laws of the phase response curve (PRC). Most of you have made your own exercises, either graphically or on the computer, and you have experienced that, indeed, entrainment **can** work this way. But few have been stubborn enough to ask, "**Does** it work this way in nature?" Colin Pittendrigh, who was the inspired genius behind this whole theory, remained uncertain, and questioning, until his death on March 16, 1996.
>
> -Serge Daan, during his delivery of the first Colin S. Pittendrigh Lecture at the 6th Meeting of the Society for Research on Biological Rhythms in 1998

Though many of the concepts and results introduced in the two manuscripts eventually made their way into the circadian literature in the years after the manuscripts were written, the full documents allow us to examine more fully the thought processes behind the work.

Since 1965, the concepts established here have been indirectly tested and examined by many researchers who set out to assess circadian properties in a variety of organisms. The fact that these core principles have held up well for so many years speaks to the value of Pittendrigh's contributions to the field. And despite the fact that these papers were not published

during Pittendrigh's lifetime, the essential results of these analyses were widely known by many chronobiologists and therefore influenced mainstream chronobiological research. The concepts of photoperiod and phase angle of entrainment become even more relevant as we examine contemporary phenomena like Seasonal Affective Disorder, Familial Advanced Sleep Phase Syndrome, and Delayed Sleep Phase Syndrome. Many of the components that Pittendrigh and his colleagues probed indirectly through the measurement of eclosion timing are now more readily accessible. For instance, two-pulse experiments described in these manuscripts and elsewhere[151] determine that phase shifts are realized within 1 hour – with current knowledge of the molecular pacemaker, there would be great value in determining the exact molecular mechanisms that dictate the pacemaker's reorganization during this first hour post-shift. Therefore, there is certainly a benefit to recalling the underlying work[1] that established these concepts with the possibility of guiding future experimental design.

Acknowledgments

The authors would like to thank Maria Luísa Jabbur for input on the text and proofreading of the transcripts, as well as Sandy Pittendrigh and Eric Ottesen for giving us the opportunity to publish these manuscripts.

[1]In the supplement, Papers I and II are provided with their original Figures, as well as a Guide written by the authors of this introduction to assist the reader of these important contributions of Pittendrigh and his co-authors.

A.2. A Guide to the Unpublished Papers of Pittendrigh and Co-Workers

Michael C. Tackenberg, Carl H. Johnson, Terry L. Page, Serge Daan

Paper I: The Empirical Basis of a Model

Pittendrigh and Minis laid out in their 1964 publication a general model of non-parametric entrainment based on the results of his skeleton photoperiod experiments[9]. The value of this work was confirmed in the following years as Pittendrigh observed “unanticipated” phenomena predicted solely by the model[30]. He wanted to go further, however, and set out to validate the model directly. In his view, the model required (1) the careful measurement of phase shifting effects of brief light pulses over the circadian cycle, and (2) a measurement of the underlying pacemaker’s oscillation (as opposed to the overt rhythms that it drives) during steady-state entrainment and after a phase shift.

Central to understanding the logical flow of this manuscript is recognizing the impetus for exploring the criteria for stable entrainment by skeleton photoperiods. Pittendrigh’s interest in the mechanism of entrainment was driven, at least in part, by Bünning’s hypothesis that photoperiodic time measurement depended on light coinciding with a restricted set of light-sensitive phases (the scotophil) in the circadian cycle. Pittendrigh recognized that under this scheme light would have two roles – first, setting the phase of the scotophil relative to the external light dark cycle, and second, in the case of a long-day, inducing a response when the scotophil (or a portion of it) is illuminated[9]. To further investigate the relationship between photoperiod and entrained phase, Pittendrigh employed skeleton photoperiods in which the light phase of the daily entraining cycle was simulated by two brief light pulses- one at the beginning of the light phase and another at the end. In this situation, entrainment would occur when the

sum of phase shifts caused by the two pulses was equal to the difference between the Zeitgeber period and the free-running period of the circadian system ($\tau - T = \Delta\phi 1 + \Delta\phi 2$).

The concept of the photoperiod inducing (1) a photoperiodic response and (2) setting the phase of the pacemaker is demonstrated in Figures 1-4 of Paper I. In Figure 1 of Paper I, the rhythm of emergence activity for *Drosophila* in complete photoperiods ranging from 1:23 to constant light are shown. The general phase of the rhythm is preserved across all photoperiods (not including constant light), preceding "dawn," though there is a steady trend towards a later phase as the photoperiod length increases. Figure 3 of Paper I represents the same paradigm, with skeleton photoperiods in place of complete photoperiods. As described previously, the eclosion rhythm for *Drosophila* in skeleton photoperiods of 1:23 to 11:13 match closely with their complete photoperiod counterparts. At 12:12 and beyond, the peak of the eclosion rhythm becomes bimodal, and at 14:10 undergoes a ψ-jump to lock onto the shorter interval. Figure 2 of Paper I shows this phenomenon with the complete and skeleton photoperiods side by side.

One of the major assumptions of the non-parametric model is that the effect of light on the pacemaker is "instantaneous" (to Pittendrigh, this meant that the phase shift had been accomplished within one hour after the end of the pulse). As Pittendrigh frequently mentions (often using Bünning's 1960 metaphor of a clock and its hands; Bunning, 1960), direct measurement of the pacemaker's phase is not possible, and therefore the best we can hope to accomplish is accurate estimations of its phase through measurement of secondary, overt rhythms, of which the *Drosophila* eclosion rhythm is an example. This separation is critical for understanding Pittendrigh's treatment of transients, which are examined in Figures 4-6 of Paper I. In Figure 4A, a single pulse of light is introduced into *Drosophila* pupae that are housed in constant darkness and at least three days from emergence. In Figure 4B, the same set of pulses is given to pupae that have already begun to emerge. The resulting phase of the eclosion peak is shown for the subsequent 7 days. Figure 5 replots the peaks of Figure 4A as

points in an attempt to illustrate the phase advances and delays that occur. Importantly, because each pupa has only one eclosion event, the emergences can be plotted relative to the number of days that have elapsed since the light pulse. These pupal eclosion events are plotted in Figure 6, with individual phase response curves plotted for flies that eclose 2-7 days post-stimulation. These curves clearly demonstrate the difference in the rhythm's response time between phase delays and phase advances. While delays are fully realized by 2 days post-stimulation, advances are nearly undetectable before day 4 and are complete only by day 5.

Pittendrigh proposes three criteria for differentiating between advances and delays. First, he suggests an arbitrary cutoff of 180° or 12 hours, indicating that an 18-hour delay would be considered a 6-hour advance. Second, that signal intensity (i.e., the duration of the light pulse) may increase the magnitude of phase shift, as shown by the difference in PRC for 15-minute pulses and millisecond pulses in Figure 7 of Paper I. Third, Pittendrigh proposes that all phase shifts may initiate one or more transient cycles of some duration. In the case of delays, this transient is greater in length than τ and therefore is nearly always complete in one cycle, but in advances, the transients take several cycles to complete. This is backed up by empirical evidence that for delaying phase shifts an instant delay in eclosion peak occurs, while in advances the eclosion peaks progress cycle by cycle either by the "advance route" or "delay route" to reach its final phase. Figure 8 of Paper I demonstrates this principle with raw data, perhaps best illustrated in the top right panel in which the response to pulses at CT18 and CT19 are plotted. As the PRC in Figure 7 of Paper I shows, the shift that occurs for pulses at CT18 is a 10-hour delay, and for CT19 is a 10-hour advance. These final phases are, in cyclical terms, only 4 hours apart, yet the pulse at CT18 produces a nearly instantaneous resetting while the pulse at CT19 takes 4-5 cycles to be fully effected. Pittendrigh notes that as the time of the pulse progresses deeper into the subjective night (CT12-24), the percentage of flies that take the quicker "delay route" decreases. This is plotted as an overlay on the PRC of Figure 7 in

Paper I, and reflects that for pulses at CT18, 70% of flies will take the “delay route” to reach their final phase of -10 hours, while for pulses at CT19, only 20% of flies will take this route to achieve their final phase of +10 hours (equivalent to -14 hours). This can be seen in the same panel of Figure 8 of Paper I, where a bimodal split for the CT19 pulse reveals a second peak that nearly instantly resets to the new phase.

The non-parametric model of entrainment is based on three major assumptions:

1. The change to the pacemaker is instantaneous[2]
2. After the phase shift, the pacemaker immediately resumes its steady-state motion
3. Transients are reflective of a lag in the coupling between a secondary oscillator that directly regulates eclosion and the master pacemaker that responds to the light

Pittendrigh proposed that the phase of the pacemaker (as opposed to the rhythm) was best reflected in the phase dependence of the response to light pulses. Thus the paradigm used to test these assumptions involves shifting the pacemaker using a single pulse, and subsequently probing the pacemaker phase with a second pulse to induce a second phase shift. Replicate cultures are tested with second pulses that span the entire 24-h cycle after the first pulse. Using the phase response curve, the resulting phase shift of the first pulse can be easily determined. If the pacemaker is reset to its new phase rapidly, the phase of the newly-shifted pacemaker at the time of the second pulse is predictable and the response to the second pulse is determined by an immediately shifted phase response curve. If the final phase of the pacemaker matches this prediction of the additive responses to the two pulses, the assumption is supported that the pacemaker was instantaneously reset. If this prediction is not met, the result was interpreted to mean that the pacemaker has not fully reset to its steady-state phase by the time that the second pulse arrives. This paradigm is outlined in Figure 9 of Paper I, and

[2] Though Pittendrigh here writes that the model assumes the change to the pacemaker is instantaneous, the model only requires that the change is completed before the next pulse. Based on his own work and that of Chandrashekaran (1967), that can be as quickly as 1-2 hours.

the data from that scheme is shown in Figure 10 of Paper I. As an example, we can look to Figure 10-9. The first pulse is given at CT 16.9. Each dot plotted in the Figure represents the time of a second pulse and the resulting phase shift magnitude and direction. For instance, when the second pulse occurs at ZT 40, the resulting shift is a 12-hour advance. If the pacemaker had been resetting slowly instead of instantaneously, the second pulse would have fallen in the dead zone (clearly visible in the dashed line representing the unperturbed or slowly-adjusting PRC) and no shift from the second pulse would have occurred. Though there were some trials in which the magnitude of the phase shift produced by the second pulse was as expected (Figure 10-3 to 10-9), there were others in which the magnitude of the second shift was stunted (10-1 and 10-2, 10-10). In all trials of this experiment, however, the pacemaker was shifted by the expected amount after the first pulse, indicating that the full phase shift was realized within the first hour.

As Pittendrigh notes, this type of experiment was first carried out in 1967 by M.K. Chandrashekaran (1967), and is also explored here with an extended time-course. This extension is shown in Figure 11 of Paper I. In an environmental cycle with a period of 21 hours, for instance, an organism (like *D. pseudoobscura*) with a free-running period of ~24 hours will require a daily advance of 3 hours. Figure 11 demonstrates how, after an initial pulse causes a 3-hour advance, the instantaneous resetting of the pacemaker *must* occur in order for the second pulse to appropriately strike the PRC and produce the same shift. Both Pittendrigh and Chandrashekaran observed that the prediction of rapid resetting was met. Given these results, the third assumption is also validated–if the pacemaker is shifted instantaneously and the overt rhythm is not, transients are a lag between pacemaker and overt rhythm rather than a reflection of the pacemaker's progression.

A few irregularities exist in the data collected in these experiments. The first is summarized in Figure 12 of Paper I, which shows phase response curves for flies that were

released into DD after being housed in photoperiods of 9, 12, and 18 hours (left) and those housed in photoperiods of 3 and 6 hours (right). It is apparent that flies that were in short photoperiods underwent phase shifts that were different from those predicted by the typical PRC. Similarly, Pittendrigh points out that in the first two panels of Figure 10 (10-1 and 10-2) in which the first pulse takes place within 4 hours of the pupae being transferred into DD, the pattern of phase shifts observed is as expected but their magnitudes are stunted. At the time, the prevailing thought was that constant light or any photoperiod with a length of greater than 10 or so hours would "stop" the clock at a phase of CT 12. Once a transition was encountered (e.g., being transferred into DD), the clock would begin again from that CT 12 phase. This conclusion was reinterpreted in 1974 in a study by Arthur Winfree, who found that in constant light the clock continued to tick but at the LL to DD transition it resets to CT 12. Through this lens Pittendrigh analyzes his irregular results and posits that during the first four hours of being placed into DD, the pacemaker has not yet reached steady state (i.e., the pacemaker has yet to reach the DD limit cycle) and as such phase shifts induced during this segment of the cycle produce irregularly low amplitudes. This same approach is used to explain the result seen in 10-10, where a pulse given at CT 17.7 results in the same decreased amplitude. Here, Pittendrigh suggests that this stimulation drove the rhythm off the limit cycle, to which it returns after a full cycle of passing through each isochron.

The establishment of the model's two main assumptions – that shifts to the pacemaker are instantaneous and that the pacemaker instantly resumes steady-state oscillation – was critical for solidifying its predictive value despite numerous prior successful implementations. Next, Pittendrigh, with Serge Daan and Eric Ottesen, seeks to enhance the model by improving its ability to properly estimate true biological limits of entrainment as well as predicting the rhythm's phase in ambiguous skeleton photoperiods.

Paper II: A Formal and Experimental Analysis

Despite the experimental evidence for the non-parametric model of entrainment presented in the first manuscript, there were inconsistencies between some of the model's apparent predictions and the empirical results. Importantly, the model failed to properly estimate the limits of *Drosophila pseudoobscura* entrainment. Based only on the maximum magnitude of the phase shifts, simple application of the mathematical model predicted that flies should entrain to T cycles ranging from 12 to 36 hours- but computer simulations (with added noise) and experimentation revealed that the limits were narrower –closer to 18 to 30 hours. The model also failed to explain certain aspects of bistability – the phenomenon that occurs when a two-pulse entrainment paradigm results in two different possible stable entrainment states. While the model accurately predicted when bistability is likely to occur (such as in PP_s of 11:13, 12:12, and 13:11), it failed to account for why certain predicted steady-states would produce stable entrainment while others did not. Explaining these deviations from the model's prediction is the focus of the second manuscript.

The failure of the non-parametric model to properly predict the limits of entrainment can be traced back to a limitation in using PRCs to identify candidate phases for stable entrainment. A system stably entrained to a single repeating pulse (one pulse/cycle) will have that pulse hit the pacemaker at the same phase (ϕ_e, i.e. entrainment phase) of the PRC every cycle. For stable entrainment to occur, that single pulse must cause a phase shift that corrects the difference between the free-running period τ of the pacemaker with the period T of the Zeitgeber cycle, thereby producing a recurring phase shift of $\tau - T = \Delta\phi_{ss}$ in steady state. Any point along the PRC that matches that $\Delta\phi_{ss}$ value is a candidate phase for stable entrainment to a particular Zeitgeber. For instance, if a pacemaker with a free-running period of $\tau = 21$ hours is entrained to a Zeitgeber cycle with a period of T = 24 hours, a daily phase shift of $\Delta\phi_{ss} = \tau - T = 21 - 24 = -3$ hours must take place. If on the PRC, pulses at CT 14 produce this shift, then that circadian

time would be a candidate phase for stable entrainment. Determining which candidate phases will actually produce stable entrainment requires a more thorough investigation of the pacemaker's phase response characteristics.

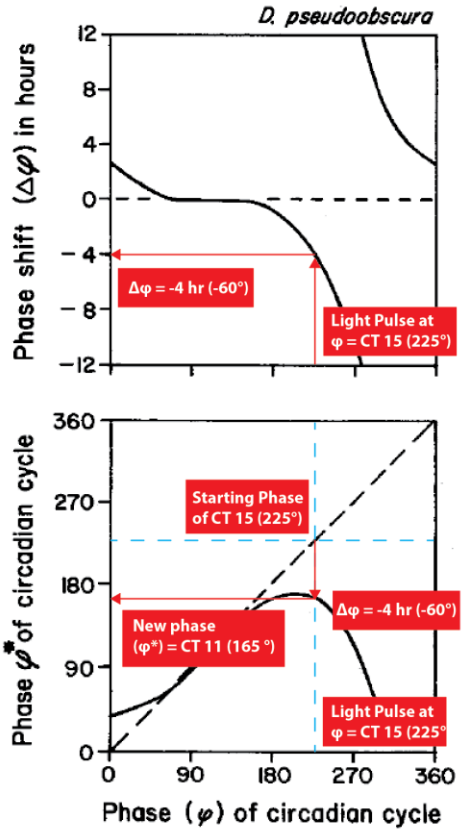

Figure A-1. Phase Transition Curves (PTCs) show the resulting phase after a phase shift. The Phase Transition Curve (PTC, bottom) is made using the phase response curve (PRC, top) by plotting the resulting phase that the pacemaker assumes immediately after the phase shift occurs. For example, if a light pulse is given at CT 15 (225°), the experimentally-derived PRC for *Drosophila pseudoobscura* tells us that the pacemaker will undergo a 4-hour delay (Δϕ = -4). In the PTC the new phase is plotted as a function of the original phase. The original phase, 225°, is found along the x-axis. If no phase shift were to have occurred, the resulting phase would remain 225°. So, the intersection between x = 225° and y = 225° is the starting point. From there, we subtract 4 hours, or 60°, from the y value to give us the resulting phase, 165°. Transforming the entire PRC into this format yields the full PTC.

The focus of Paper II's analysis is the phase transition curve (PTC). While the phase response curve (PRC) plots the response of a pacemaker to a perturbation (the direction and magnitude of the phase shift Δϕ that occurs as a function of the phase ϕ at the time of the perturbation, or Δϕ(ϕ)), the PTC plots the new phase as a function of the previous phase (the phase ϕ* to which the pacemaker resets as a function of the phase ϕ at the time of perturbation, or ϕ*(ϕ)). Thus, the PTC is constructed from the same information presented in the PRC: if a light pulse at ϕ = CT 12 produces a phase delay of 3 circadian hours, the new phase of the rhythm will be ϕ* = CT 9. As the x-axis plots the original phase ϕ and the y-axis plots the resulting phase ϕ*, this PTC would have a point at (12,9). A graphical description of the derivation of the PTC from the PRC is shown in Figure A-1, which is modified from Figure 2 of the second manuscript.

If we consider a Zeitgeber cycle that consists of a single pulse per cycle, we can show the phase of the pacemaker at the time of the second cycle's pulse as a

"secondary" PTC. Because we know the new phase of the pacemaker after a given pulse n, ϕ^*_n, and the length of the Zeitgeber cycle, T, we can determine at what phase the pacemaker will be hit with the next light pulse n+1. The phase of the pacemaker at the $n+1^{th}$ light pulse, ϕ_{n+1}, will be equal to the phase after the n^{th} pulse, ϕ^*_n plus the length of the T cycle in circadian hours (that is, if $\tau = 21$ and $T = 24$, each real hour is equal to 1.14 circadian hours, and so 24 real hours and 27.43 circadian hours will elapse between pulses). By taking the original PTC, which is referred to here and in the manuscript as the “primary” PTC, and shifting it up on the graph by 24 real hours’ worth of circadian time (27.43 circadian hours), the secondary PTC is realized. This process is depicted in Figure S2. In the manuscript, Pittendrigh shows a “family” of secondary PTCs, that is, a group of PTCs all representing different ϕ_{n+1} values for different Zeitgeber cycle lengths. In the case of *D. pseudoobscura*, τ is negligibly different from 24 hours, thus to find the phase of the pacemaker in a $T = 25$ light cycle the PTC is shifted upward along the new phase (y) axis by one hour (15°). The phase of the pacemaker at the time of the succeeding pulse (25 hours after achieving the new phase from the preceding pulse) can then be read directly from the secondary PTC. For a 23 hour T cycle, the light pulse occurs one hour prior to the completion of the 24-hour circadian cycle, so the secondary PTC would be shifted downward on the y-axis by one hour.

This representation of the changing phase of the pacemaker seems complicated and non-intuitive, but it optimally shows candidate phases for stable entrainment. A necessary attribute of steady-state entrainment is that the phase of the pacemaker at the time of the $n+1^{th}$ pulse must be the same as the phase of the pacemaker at the time of the n^{th} pulse, or $\phi_{n+1} = \phi_n$. As the cycles continue the pacemaker will be hit with pulses at different circadian times progressively closer to the phase of stable entrainment until steady-state is achieved. As the x-axis for the secondary PTC plots ϕ_n and the y-axis plots ϕ_{n+1}, the diagonal line $y = x$ plots all

values at which ϕ_{n+1} is equal to ϕ_n (Paper II, Figure 3). Any point along the secondary PTC that intersects with this diagonal line is a candidate phase for stable entrainment.

At this point, we have seen how both PRCs and PTCs can be used to predict *candidate phases* for stable entrainment, but have not determined how those candidates can be assessed for stability. As mentioned previously, this information is not intuitively obtainable from the PRC,

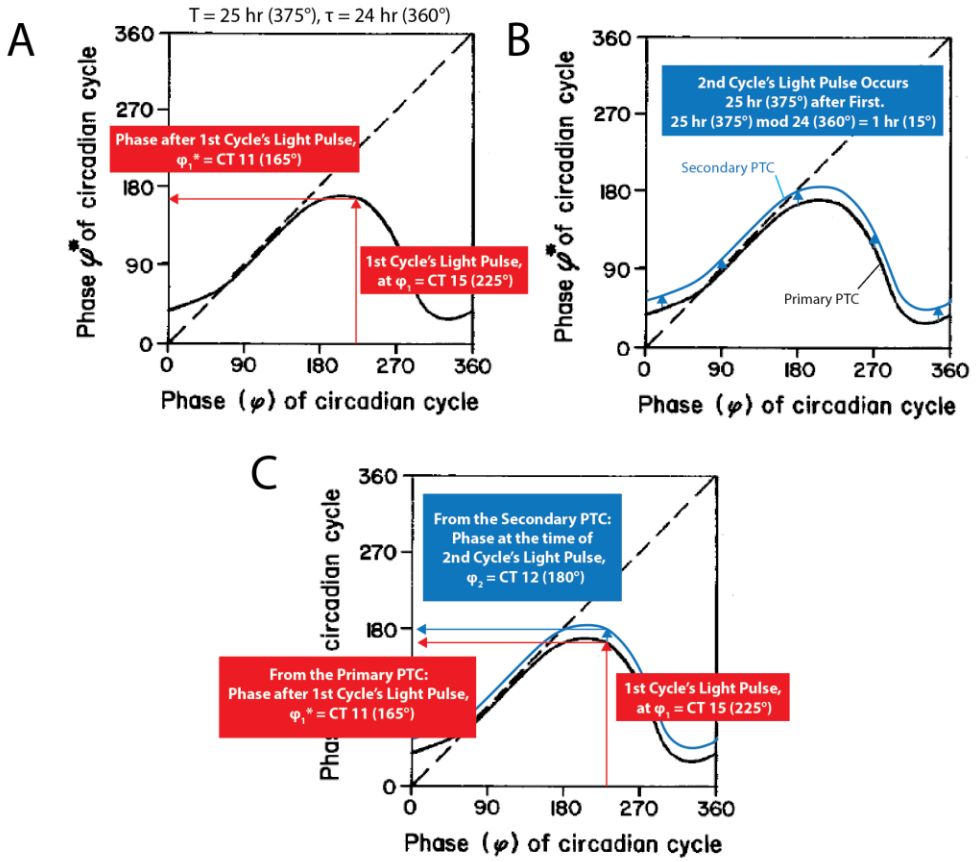

Figure A-2. The secondary PTC incorporates the time between cycles in order to show the phase of the pacemaker at the time of the second cycle's pulse. A, A primary PTC shows the phase of the pacemaker immediately after a phase-shifting light pulse (ϕ^*_n) at a particular initial phase (ϕ_n). In this example, a light pulse at ϕ_1 = CT 15 (225°) causes -4 hour phase shift, resulting in a new phase ϕ^*_1 of CT 11 (165°). B, While the primary PTC shows the new phase ϕ^*_n after a phase shift, the secondary PTC incorporates the time between cycles to show the phase of the pacemaker by the time the next cycle's pulse occurs (ϕ_{n+1}). The secondary PTC's vertical location along the axis is shifted according to how long after the first pulse the second pulse occurs. In this case, the second pulse occurs 25 hours after the first. If it occurred 24 hours after the first, it would overlap the original, primary PTC. Because it occurs one hour later than this, we plot it shifted 15° or 1 hour up from the primary PTC. C, In this example, we plot the same phase shifting pulse as in A, occurring at the initial phase ϕ_1 of CT 15 (225°). Now, using the primary PTC we see the new phase following the pulse (ϕ^*_n) of CT 11 (165°) and using the secondary PTC we see the phase at the time of the second pulse ϕ_2 is CT 12 (180°).

but is easily obtained from the PTC by assessing the slope of the PTC at the point of its intersection with the y = x diagonal line (i.e., the candidate phase for stable entrainment). Because the circadian pacemaker is a biological system, its period and thus its phase on a cycle-by-cycle basis is subject to biological variability. After a particular deviation from the predicted phase of the next pulse δ_1, we can apply the same strategy used to identify stability candidates to determine if the next cycle's deviation δ_2 will have increased or decreased relative to the first. It follows that in a scenario where $\delta_2 < \delta_1$, the deviations will trend back toward the equilibrium point, while if $\delta_2 > \delta_1$, the deviations will increase from cycle to cycle and equilibrium will be lost. To phrase this another way, while individual phases may be theoretically stable (the slope of the PTC is equal to 45° at that phase), real stability is determined by whether the phases immediately surrounding this "candidate" phase lead to shifts that trend back towards the stability candidate in the following cycles or propagate the deviation and move away from the candidate stability point. Paper II mathematically determines in this context that δ_2 will be less than δ_1 when the instantaneous slope of the PTC at any particular candidate phase for stable entrainment is less than 45°.

From this newly-described requirement, we can observe any family of secondary PTCs, identify candidates for stable entrainment, and then assess the stability of each of these candidates by measuring the slope of the curve at that instant. Looking at the family of PTCs plotted for *Drosophila pseudoobscura* in Figure 3 of Paper II, we can see that for T cycles of 19-29 hours there are stable candidates, while outside of that range the slope of the PTC is too high (>45°) at each candidate phase to allow stable entrainment.

The same principle can be applied to two-pulse Zeitgeber cycles. To do so, a PTC can be plotted for the alternating odd (P_1) and even (P_2) pulses in the same way that a secondary PTC is created for the single-pulse system in Figure A-2. The progression of phases can be determined by finding the new phase ϕ^*_n that occurs after the n^{th} pulse using the primary PTC

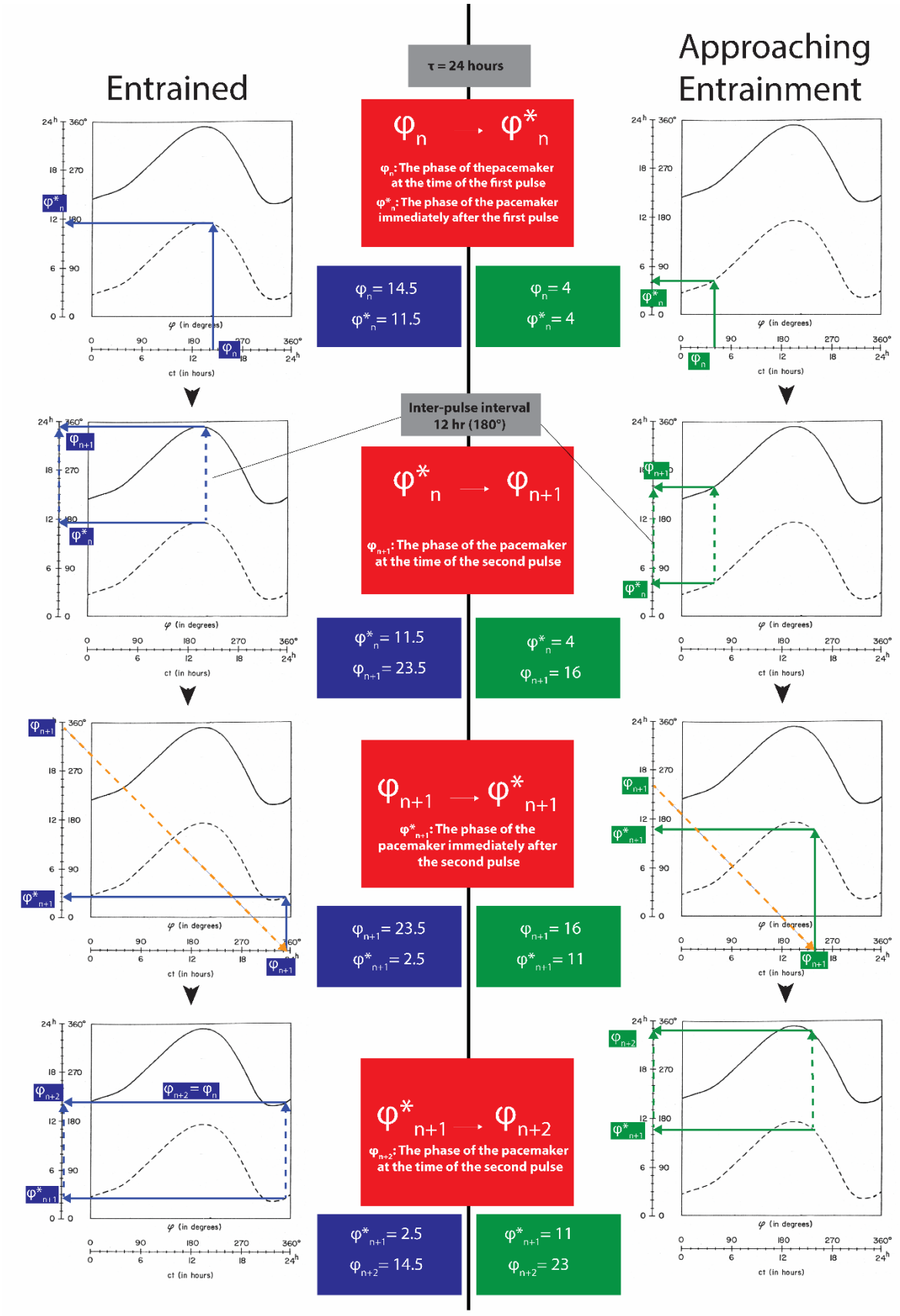
Entrained
Approaching Entrainment
τ = 24 hours
$\varphi_n \rightarrow \varphi^*_n$
φ_n: The phase of thepacemaker at the time of the first pulse
φ^*_n: The phase of the pacemaker immediately after the first pulse
$\varphi_n = 14.5$
$\varphi^*_n = 11.5$
$\varphi_n = 4$
$\varphi^*_n = 4$
Inter-pulse interval 12 hr (180°)
$\varphi^*_n \rightarrow \varphi_{n+1}$
φ_{n+1}: The phase of the pacemaker at the time of the second pulse
$\varphi^*_n = 11.5$
$\varphi_{n+1} = 23.5$
$\varphi^*_n = 4$
$\varphi_{n+1} = 16$
$\varphi_{n+1} \rightarrow \varphi^*_{n+1}$
φ^*_{n+1}: The phase of the pacemaker immediately after the second pulse
$\varphi_{n+1} = 23.5$
$\varphi^*_{n+1} = 2.5$
$\varphi_{n+1} = 16$
$\varphi^*_{n+1} = 11$
$\varphi^*_{n+1} \rightarrow \varphi_{n+2}$
φ_{n+2}: The phase of the pacemaker at the time of the second pulse
$\varphi^*_{n+1} = 2.5$
$\varphi_{n+2} = 14.5$
$\varphi^*_{n+1} = 11$
$\varphi_{n+2} = 23$
φ (in degrees)
ct (in hours)

Figure A-3 (previous page). Repeatedly using a single primary and secondary PTC to determine two-pulse entrainment. Primary and secondary PTCs can be used to determine how a pacemaker in a two-pulse skeleton photoperiod, in which two separate pulses per cycle simulate a particular photoperiod length, may reach entrainment. From top to bottom, these panels show the progression of the pacemaker's phases through the first three pulses of a two-pulse system (one and a half cycles- from original phase at the time of the first pulse ϕ_n to the phase at the time of the third pulse ϕ_{n+2}). In the left set, the pacemaker is already entrained, and so the phase of the pacemaker at the time of the third pulse (ϕ_{n+2}) is equal to the phase of the pacemaker at the time of the first pulse (ϕ_n). In the right set, the pacemaker is approaching entrainment. Given the first light pulse (ϕ_n), the immediate change in the pacemaker (ϕ^*_n) is shown as the intersection with the primary PTC (top row, dotted black line). The time of the pacemaker at the second pulse (ϕ_{n+1}) is found by creating a secondary PTC (second row, solid black line) that is shifted up according to the time between the pulses (12 hours in this case). The phase of the pacemaker at the time of the third pulse, ϕ_{n+1} (which is first determined using the y-axis, second row), is then translated to the x-axis (orange dashed line) to begin the process again.

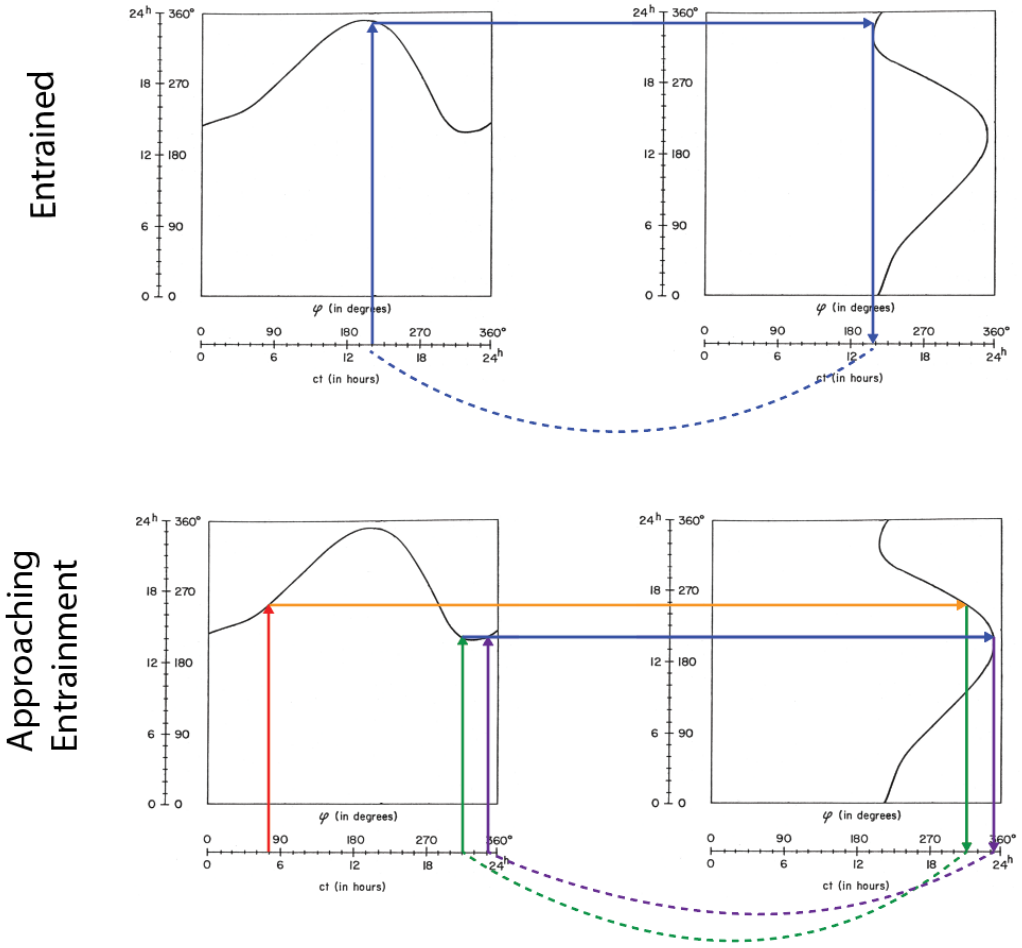

Figure A-4. Using a rotated, mirrored even-pulse PTC along with the odd-pulse PTC to determine stable two-pulse entrainment. The process of using primary and secondary PTCs to determine two-pulse photoperiod entrainment is simplified by omitting primary PTCs and using one set of secondary PTCs for the odd pulses and another set for the even pulses. By mirroring the even-pulse PTC and rotating it 90°, the y-axis for the odd-pulse PTC and the x-axis of the even-pulse PTC match, allowing for easy visual tracing of the phase transitions from odd to even pulse. In the top panel, an already-entrained pacemaker is shown, and in the bottom, a pacemaker as it entrains. As in Figure S3, the time of the first pulse is found on the x-axis and its intersection with the secondary PTC (solid black line is found). This intersection is then traced across to the second graph (right panel), where its intersection with the even-pulse PTC is used to determine the phase at the time of the second pulse. The process is then repeated for the third pulse and beyond.

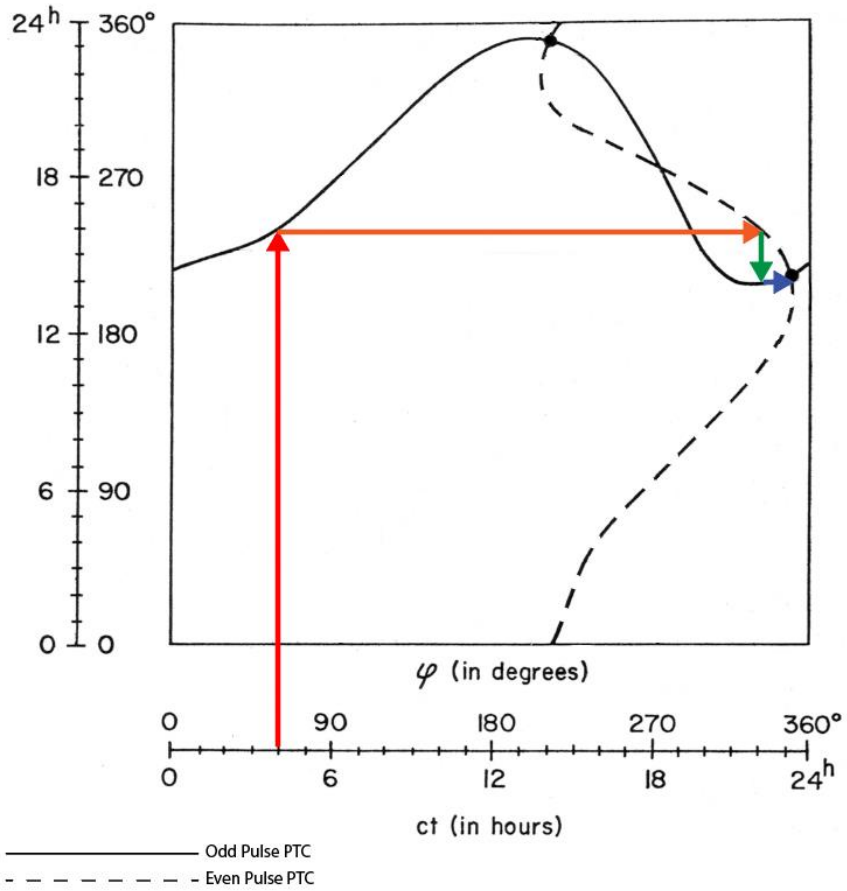

Figure A-5. Combing the odd- and even-pulse PTCs into a single graph. The last simplification is made by combining the odd and even pulse PTCs into the same Figure. In this case, the phase of the pacemaker at the time of the second pulse is found by tracing a line from the x-axis up to the odd-pulse PTC (red line), then the phase of the pacemaker at the time of the third pulse is found by tracing to the even-pulse PTC (orange line), then back to the odd-pulse PTC (green line) and so on. In doing so, the progression of phases will spiral towards stable entrainment if entrainment is possible under that set of conditions. Each intersection of the two PTCs is a candidate for stable entrainment, but only points at which both PTCs have slopes less than 45° will result in entrainment (see Figure S6-7 and Paper II, Figure 5).

(Figure A-3, top, dashed line PTC), followed by the phase at the time of the second pulse ϕ_{n+1} using the secondary PTC (Figure A-3, top, solid line PTC), and then repeating to find ϕ^*_{n+1}, ϕ_{n+2}, ϕ^*_{n+2}, and so on.

This can be simplified by using the PTC graph to determine the effect of the odd pulses and a second PTC graph that is the mirror image of the first PTC, rotated 90°, showing the effects of the even pulses (Figure A-4). Now, instead of repeatedly using the same PTC for both odd and even pulses, the progression of phase transitions can be mapped in a spiral-like pattern between the graphs to determine likely candidates for stable entrainment.

The last simplification can be made by now recombining the two PTCs, preserving the mirror-imaging and 90° rotation (Figure A-5). By doing so, the progression of phases is easily plotted and the candidates for stable entrainment are easily identifiable as intersections between the two PTCs. We can use Figure 6 of Paper II as an example. A pulse at $\phi_n = 120°$ or CT 8 shifts the pacemaker's phase. By drawing a vertical line from the x-axis at $\phi_n = 120$ up to the odd-pulse PTC (intersection 1' in the Figure), we can determine that the phase of the pacemaker at the second pulse, ϕ_{n+1}, is about 300°. Connecting this point (1') to the even-pulse PTC, we find that the phase of the pacemaker at the third pulse ϕ_{n+2} is about 225° (2' in the Figure). Moving again to the odd-pulse PTC (2' to 3'), we see that the phase of the pacemaker at the fourth pulse ϕ_{n+3} is 330°, continuing on as follows:

Cycle	Odd Pulse	Even Pulse
1	(n) 120°	(n+1) 300°
2	(n+2) 225°	(n+3) 330°
3	(n+4) 210°	(n+5) 345°
4	(n+5) 210°	(n+6) 345°
5	(n+7) 210°	(n+7) 345°

We therefore see how the phases of the pacemaker at each of the two pulses begin to converge upon consistent values (e.g., 210° and 345° in this example).

The same logic dictating which candidates are stable and which are unstable discussed above applies here, and Figure A-6 visually demonstrates why pulses near certain intersection points spiral away and towards other, stable intersection points. One of the major achievements of this manuscript is the determination of the mathematical criteria for stable entrainment points. Figure 5 of the Paper II depicts how the slopes of the two intersecting PTCs at their intersection can be compared and used to predict whether a particular candidate for stable entrainment (i.e., any intersection of the PTCs) is truly stable. Simplified, the requirement is that the slope of the odd-pulse PTC, shown in the Figure as a dotted line, must be less steep than that of the slope of the even-pulse PTC. In Figure A-7, the 12:12 skeleton photoperiod PTC shows how the tangent slope lines can be used to differentiate unstable and stable candidates for entrainment.

As mentioned previously, two major flaws of the non-parametric model in its early stages were the failure to correctly predict the limits of entrainment and the cumbersome approach to predicting bistability. The above criteria for identifying candidates for stable entrainment and determining which are truly stable satisfy the first insufficiency, and we can now more easily predict and explain bistability, satisfying the second insufficiency. Figure 6 of Paper II uses an example of a two-pulse Zeitgeber (i.e., a skeleton photoperiod) with the first pulse at phase 120° of the pacemaker and tracks its path toward stable entrainment. This Figure also demonstrates the phenomenon of bistability and how it can arise, if we plot the same process for the first pulse occurring at phase 30°. Though the pulses are still 12 hours apart, a different stable equilibrium is achieved. Figure 7 of Paper II demonstrates how this effect is seen in skeleton cycles of 11:13 to 13:11, but disappears outside that range (10:14 and 14:10, and beyond. As mentioned previously, when two stable equilibrium points exist, the critical factor remains the phase of the pacemaker at the time of the first pulse, and which inter-pulse interval occurs first. Outside of

this zone of bistability but within the limits of entrainment, there is only one stable phase relationship between pacemaker and environmental cycle, and therefore the system will trend towards (and lock onto) that relationship alone.

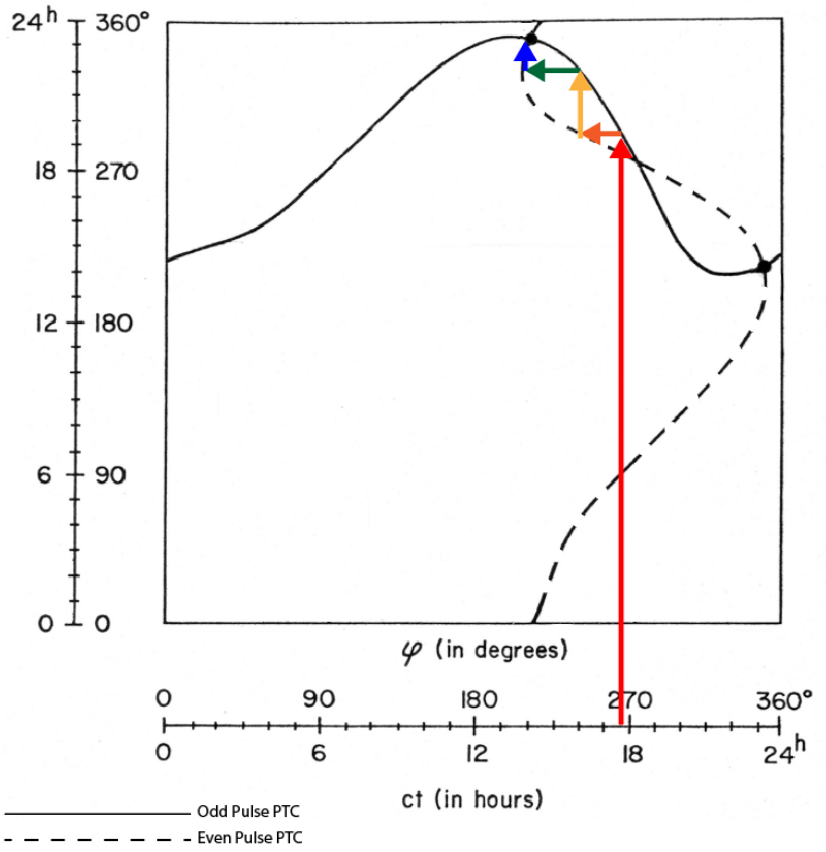

Figure A-6. Not all intersections between the odd- and even-pulse PTCs are stable. As an example of how not all intersections of the odd- and even-pulse PTCs are suitable for stable entrainment, two sets of pulses are given, each with initial pulses occurring very close to the intersection point at 270°. Though the PTCs cross here, the slope of the odd-pulse PTC at that point is greater than that of the even-pulse PTC, and as such the progression of phases spirals away from that crossing point and toward another.

Conclusion

Though many of the concepts and results included in the two manuscripts introduced here eventually made their way into the circadian literature in the years after the manuscripts were written, the full documents allow us to examine more fully the thinking behind these works. The process was clearly an evolution, given the fact that Pittendrigh (and his co-authors in the case of Paper II) continued to update these manuscripts, possibly for as long as ten years.

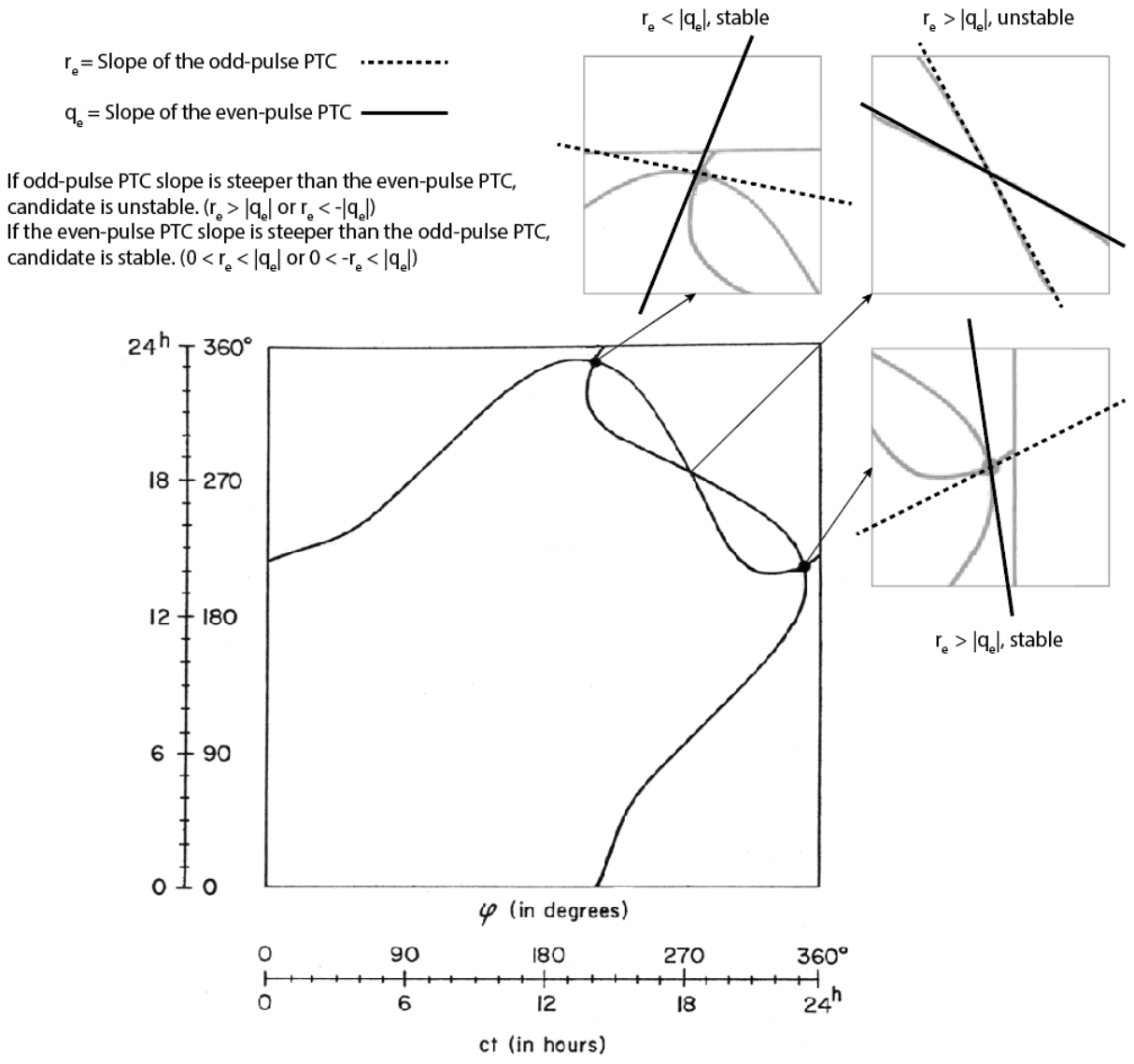

Figure A-7. Slopes of the tangent lines at the intersection points can be used to determine stability of each candidate for stable entrainment. The comparison between the slopes of the tangent line at the intersection of the two PTCs can be used to determine whether a particular crossing point will actually be stable. When the slope of the odd-pulse PTC (dotted line, r_e) is less steep than the slope of the even-pulse PTC (solid line, q_e), the crossing point is stable. If r_e is more steep than q_e, the crossing point is not stable. The three crossing points of the 12:12 skeleton PTC are shown enlarged and with their tangent lines drawn.

Appendix Bee: Disruption of Circadian Clock Timing by Neonicotinoid Pesticide

Michael C. Tackenberg, Manuel A. Giannoni-Guzmán, Caleb A. Doll, José L. Agosto-Rivera, Kendal Broadie, Darrell Moore and Douglas G. McMahon

Note: The data presented in the following appendix were collected and analyzed over a set of seasons ranging from 2014 to 2016. These experiments were performed at 25°C. After the completion of these trials, we began to employ 35°C temperatures for honey bee experiments. Data collected and analyzed after 2016, not presented here, reflect that temperature change.

Widespread losses of domestic honey bees and wild pollinators have generated extensive inquiries into causative factors. While likely a multifactorial problem, pollinator loss is characterized by impaired foraging behavior and immunity, and linked to environmental exposure to neonicotinoid pesticides[152–154]. The daily (circadian) clock is a key regulator of both foraging behavior and immunity in insects[155,156], and the mode of action of neonicotinoids is predicted to disrupt cholinergic light entrainment of the circadian clock[157,158]. Here, we have tested whether chronic ingestion of environmental levels of a commonly used neonicotinoid pesticide disrupts circadian timing in both honey bees and fruit flies.

Honey bees are highly dependent on the circadian clock for foraging, to enable sun compass orientation and “time memory” required to locate food resources in time and space, and to navigate back to the hive[43,159–163]. Disrupted circadian timing impairs orientation[164,165], with neonicotinoids compromising honey bee navigation at sub-lethal doses[166,167]. Neonicotinoids target cholinergic neurotransmission[168], a physiological basis by which light input synchronizes circadian clocks to local time. This mechanism is best studied in the *Drosophila* fruit fly model system[157,158]. Therefore, we tested whether neonicotinoids disrupt circadian timing

in bees and flies through interference with light cycle signals that synchronize the circadian clock to local time.

We first tested environmental levels of the neonicotinoid thiamethoxam on honey bee circadian clock function. We captured honey bee foragers from colonies maintained on the Vanderbilt campus, and housed them individually in activity monitors with food (bee candy) and water available *ad libitum*[169]. Thiamethoxam was added to bee candy at concentrations from 6.25 to 25 ng/g, in line with the concentration range reported in flower nectar and pollen encountered by foraging bees, and in hive honey stores[170–173]. There was no increase in the mortality of bees dosed with up to 25 ng/g thiamethoxam compared to control bees fed undosed bee candy (Materials and Methods, Figure B-S1).

Entrained locomotor activity rhythms were assayed in 12hr:12hr light-dark (LD) cycles. In wild-caught control foragers, activity began a few hours after lights on, peaked at mid-day, and terminated at or near lights off (Figure B-1A, C). Activity continued as free-running endogenous circadian rhythms in constant darkness (DD; Figure B-1A, C), similar to published reports[174]. Thiamethoxam feeding caused dose-dependent alterations in day-night partitioning of LD locomotor activity, the timing of endogenous rhythms relative to the previous light cycle, and in the period of endogenous DD rhythms (Figure B-1B, D-H). Thiamethoxam-dosed bees in LD were more active at night (control, 0.1351±0.012; 25 ng/g, 0.2024±0.018; p = 0.0041; Figure B-1E), reducing activity in the late day (control, 0.542±0.016; 25 ng/g, 0.489±0.018; p = 0.0094) and extending activity into the early night (control, 0.102±0.009; 25 ng/g, 0.147±0.014, p = 0.0318; Figure B-1F).

Thiamethoxam altered the synchronization of the circadian clock with the light cycle. In dosed bees, locomotor activity was 2.3 hours earlier relative to lights on, as projected from the onset of DD free-running rhythms (mean phase angle of entrainment: control, -5.538±0.69 hours; 25 ng/g, -3.24±0.70 hours; p = 0.0186; Figure B-1G). Moreover, thiamethoxam lengthened the intrinsic period of the circadian clock by 1.2 hours in DD following LD (control,

22.2±0.2 hours; 25 ng/g, 23.4±0.9 hours; p = 0.0016; Figure B-1H). Importantly, honey bee foragers that ingested thiamethoxam in constant darkness only (DD alone), rather than being exposed to pesticide during LD entrainment and then continuing in DD, did not display a significant difference in period (Figure B-S2). This result suggested a causative interaction on the honey bee circadian clock of environmental light exposure and thiamethoxam feeding.

To test whether light and thiamethoxam have synergistic effects on circadian activity, we assayed drug effects under different light conditions, categorizing each bee as arrhythmic (no rhythm), short period (<24 hours) or long period (>24 hours). In DD alone, 17% of bees were arrhythmic, 77% had short periods and 6% had long periods (Figure B-2A). In constant light (LL), we found the proportion of arrhythmic and long period activity increased with light intensity. Low intensity (60 lux, LL60), caused 27% arrhythmic bees, 36% with short periods and 36% with long periods. At moderate intensity (LL150), 65% of bees were arrhythmic, 6% had short periods and 27% had long periods (Figure B-2A). High intensity (LL2600) further increased the proportion of arrhythmic bees to 83%. Interestingly, increasing the thiamethoxam dosage while the light intensity remained dim caused the proportion of arrhythmic and long period bees to increase (LL60 + 25 ng/g thiamethoxam: 50% arrhythmic, 0% short period, 50% long period; Figure B-2B).

The additive effects of light and thiamethoxam on honey bee circadian rhythms suggest the pesticide aberrantly stimulates light input pathways. However, little is known about the circuits for light regulation of the honey bee circadian clock, so we turned to *Drosophila* where well-defined cholinergic processes mediate light input on circadian clock neurons[157,158], through nicotinic acetylcholine receptors (*6*). Overall, honey bees exhibit cholinergic neural signaling similar to *Drosophila*[168]. To verify that neonicotinoids affect circadian clock neurons we measured the response of *Drosophila* clock neurons to clothianidin, the active metabolite of thiamethoxam[175]. Intact whole-brain explants with genetically encoded, PDF-driven GCaMP5G Ca^{2+} indicator were analyzed for Ca^{2+}-dependent changes in fluorescence intensity upon

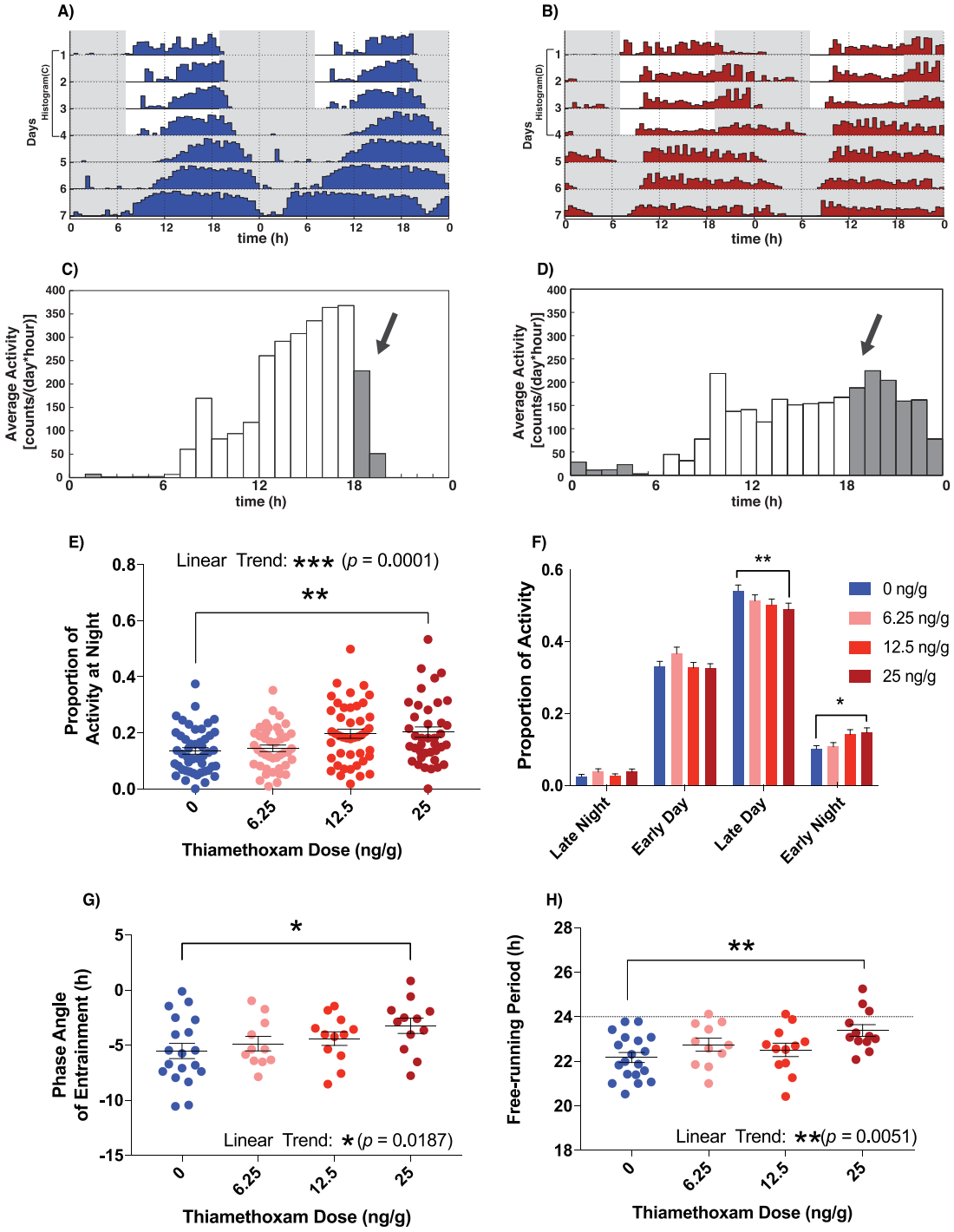

Figure B-1. Effects of Thiamethoxam on Honey bee Locomotor Rhythms. A-B, representative actograms showing activity in LD followed by DD. C-D, the matched LD average activity profile histograms for control bee (C) and bee dosed with 25-ng/g thiamethoxam (D). Arrows point to differences in activity near light offset. E-H, proportion of total activity occurring within the dark phase of the LD cycle (E), average activity profile of bees binned into 6-hour epochs (F), phase angle of entrainment (G), and free-running period (H). Averages represent the median with error bars showing the standard error of the mean. * indicates $p < 0.05$, ** $p < 0.01$, *** $p < 0.001$.

exposure to either clothianidin or vehicle (Materials and Methods). Exposure to clothianidin resulted in a ~350% increase in Ca^{2+} fluorescence in the PDF^{+} clock neurons (ΔF/F, vehicle, -0.01±0.04, cloth, 3.62±0.47, $p < 0.0001$, Figure B-3A, B, C).

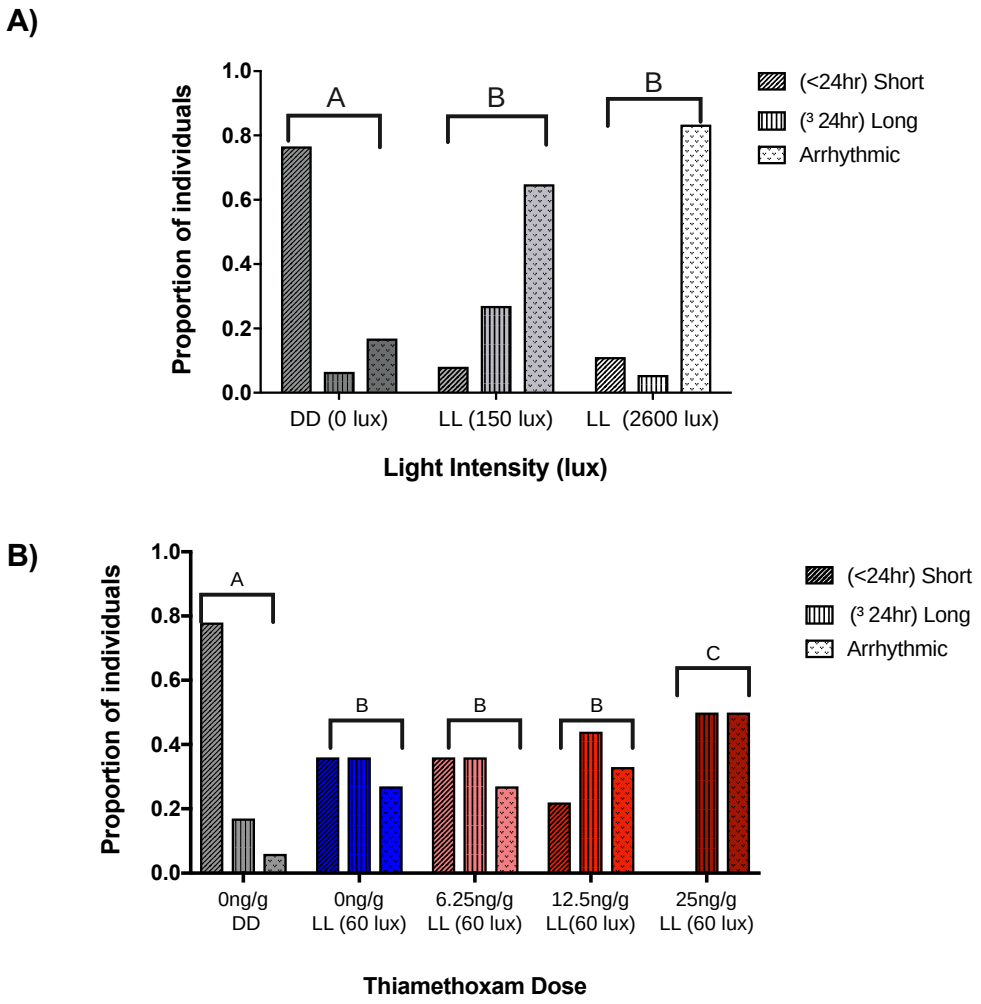

Figure B-2. Synergistic Effects of Thiamethoxam and Light on Honey Bee Locomotor Circadian Rhythms. A-B, proportion of bees that had short free-running periods (less than 24 hours, diagonal striped bars), long free-running periods (greater than 24 hours, vertical striped bars), or were arrhythmic (stippled bars). **A**, the proportions of short, long, and arrhythmic bees in constant darkness (DD) was significantly different from constant light (LL) at two different intensities 150 and 2600 lux (Pearson Chi Square, X2=85.46, p<0.0001). Comparison of the 150 and 2600 cohort did not reveal significant differences (Pearson Chi Square, X2=3.49, p=0.1743). **B**, the proportions short, long, and arrhythmic bees in constant darkness (DD) and in dim constant light (LL 60 lux) across different doses of thiamethoxam pesticide and in controls revealed significant differences between the following groups: 0ng/g DD vs 12.5 ng/g LL (Pearson Chi Square, X2=8.04, p=0.0180); 0ng/g DD vs 25ng/g LL (Pearson Chi Square, X2=18.10, p=0.0001): and 0ng/g LL vs 25ng/g LL (Pearson Chi Square, X2=7.25, p=0.0267).

With the confirmation that neonicotinoids excite fly clock neurons we then tested whether the circadian behavioral effects of thiamethoxam in flies are similar to bees. Individual flies in activity monitors were provided *ad libitum* food with and without thiamethoxam (Materials and Methods, Figure B-S3). Undosed flies in LD exhibited temporal patterning typical of *Drosophila* entrained circadian locomotor behavior[176,177], with distinct morning and evening peaks and a mid-day "siesta" in which activity was reduced (Figure B-4A, C). In DD, these rhythms continued to free-run with periods near 24 hours (Figure B-4).

Similar to honey bees, thiamethoxam feeding altered the partitioning of activity between day and night, clock timing relative to the light cycle, and free-running period (Figure B-4A-H). Dosed flies were proportionally more active at night (proportion of total activity occurring in the dark: control, 0.1324±0.012; 500 ng/g, 0.2324±0.020; p = 0.0002; Figure B-4E). The overall difference in day/night partitioning of activity was similarly due to a relative reduction in the activity of dosed flies in the late day and a relative increase in activity of dosed flies in the early night (late day, $p<0.0001$; early night, $p<0.001$, Figure B-4F). In dosed flies the timing of the circadian clock for locomotor activity was similarly shifted 2.5 hours later relative to lights on (phase angle of entrainment: control, 1.44±0.27; 500 ng/ml, -0.671±0.27; $p < 0.0001$; Figure B-4G). Likewise, the intrinsic period of the circadian clock in DD was significantly lengthened by thiamethoxam, from 24.0±0.2 to 24.6±0.2 hours (p = 0.0291; Figure B-4H). Thus, thiamethoxam alters behavioral timing and clock period in flies, with the overall effects on circadian activity rhythms in flies similar to effects seen in bees.

Taken together, the results show thiamethoxam alters both timing and intrinsic period of the honey bee circadian clock at concentrations occurring in nectar, pollen and honey in the field[170–173]. The circadian effects of thiamethoxam are largely conserved in *Drosophila*. A critical action of thiamethoxam is to shift the timing of the internal clock in bees and flies relative to environmental time, creating a disparity between internal time and local time. The >2 hour shift would significantly degrade honey bee clock-controlled orientation[164,165]. Timing shifts induced

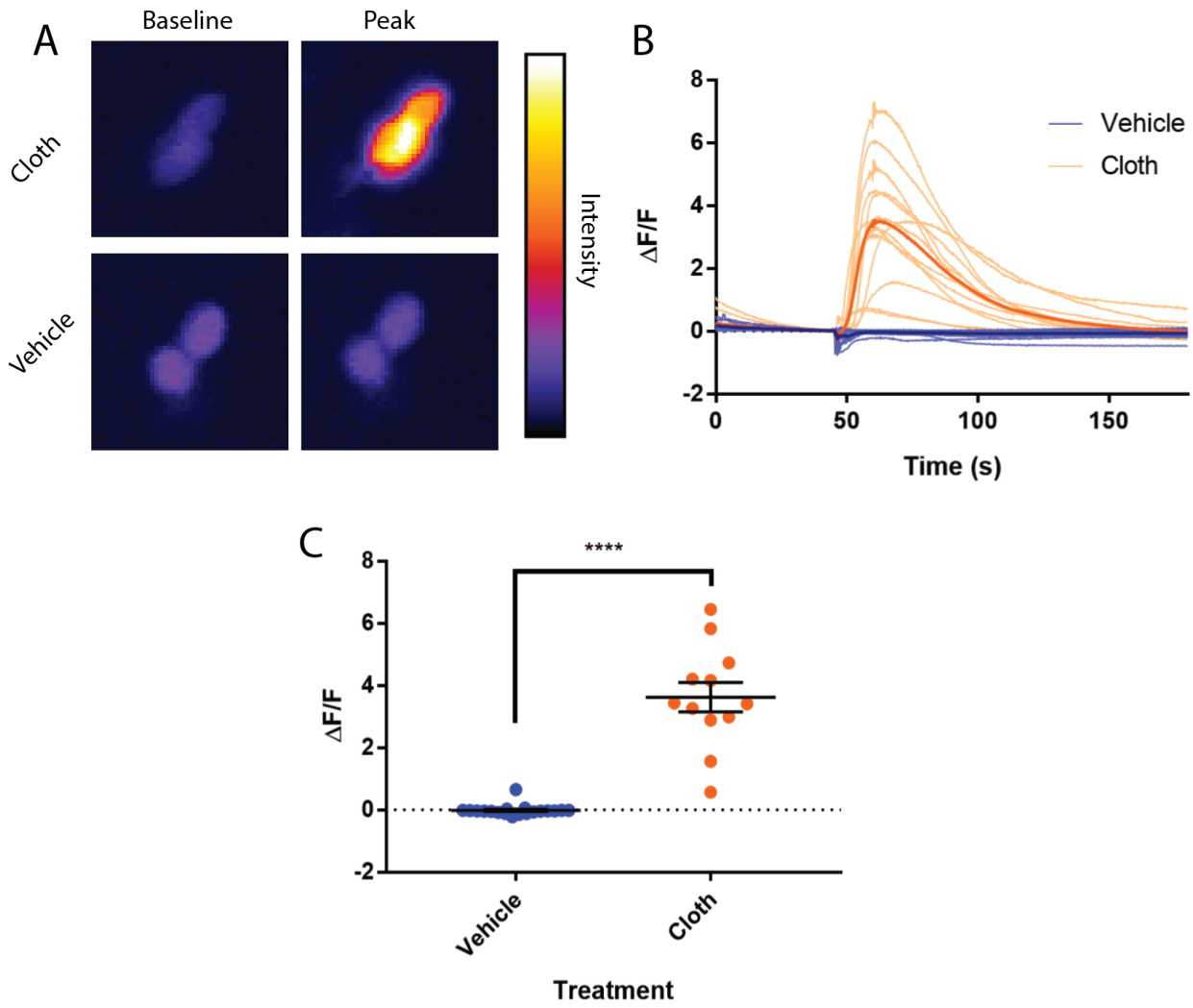

Figure B-3 Clothianidin induces excitatory increases in [Ca2+]i in Drosophila PDF+ clock neurons. A, representative images showing the baseline and peak fluorescence in *Drosophila* PDF^{+} neurons expressing GCaMP5G fluorescent calcium indicator, in response to 4.1 ng/ml clothianidin (cloth, top) or vehicle (bottom). B, fluorescence intensity traces showing individual responses of *Drosophila* PDF^{+} neurons to clothianidin (pale orange) or vehicle (pale blue). Averaged traces are shown for explants exposed to clothianidin (orange) and vehicle (blue). C, average peak fluorescence responses of cells in explants exposed to vehicle (blue) or clothianidin (orange). Error bars represent SEM. **** indicates $p < 0.0001$.

by anesthesia produce orientation errors of ~15 degrees per hour difference from local time[164]. Thus, the thiamethoxam-induced shift in circadian timing we observed in our experiments would result in orientation errors of ~35 degrees, or ~600 meters per kilometer traveled, resulting in the loss of foragers failing to return to the hive.

Thiamethoxam effects on the circadian clock are increased with environmental light intensity. Entrainment to light cycles in the presence of thiamethoxam potentiated the period lengthening in constant darkness, and ingestion of thiamethoxam during exposure to dim light increased both period lengthening and the degree of disruption of locomotor rhythms. This suggests that chronic low neonicotinoid exposure mediates a chemical signal to the circadian clock similar to continuous dim light. The thiamethoxam-induced increase in dark activity we observed in both diurnal insect species is consistent with this conclusion. In *Drosophila*, it is well established that light input via cholinergic signaling entrains circadian clock neurons[157,158] . Nicotinic receptors mediate light input from the lateral eyes and Hofbauer-Buchner eyelets[157,158], as well as synchronous rhythmic input to circadian clock neurons[178]. We have shown here that neonicotinoids excite clock neurons. This provides a mode of action to explain the light-dependence of thiamethoxam exposure on circadian behavior.

Thiamethoxam affects circadian rhythms similarly in flies and bees – more activity at night, altered circadian timing of activity and period lengthening – suggesting that the effects of thiamethoxam in bees may be similarly due to aberrant stimulation of cholinergic inputs of circadian photoreception. However, the direction of the circadian timing change was opposite in these insect species; the timing of bee activity was advanced, whereas fly timing was delayed. This may be due to the molecular differences in circadian clock organization in the two species. Flies express a type 1 *cryptochrome* in clock neurons that is photosensitive[179], and light synchronization of the fly clock is due to interactions of this intrinsic clock neuron photosensitivity with cholinergic inputs from photoreceptors[158]. In contrast, honey bees express

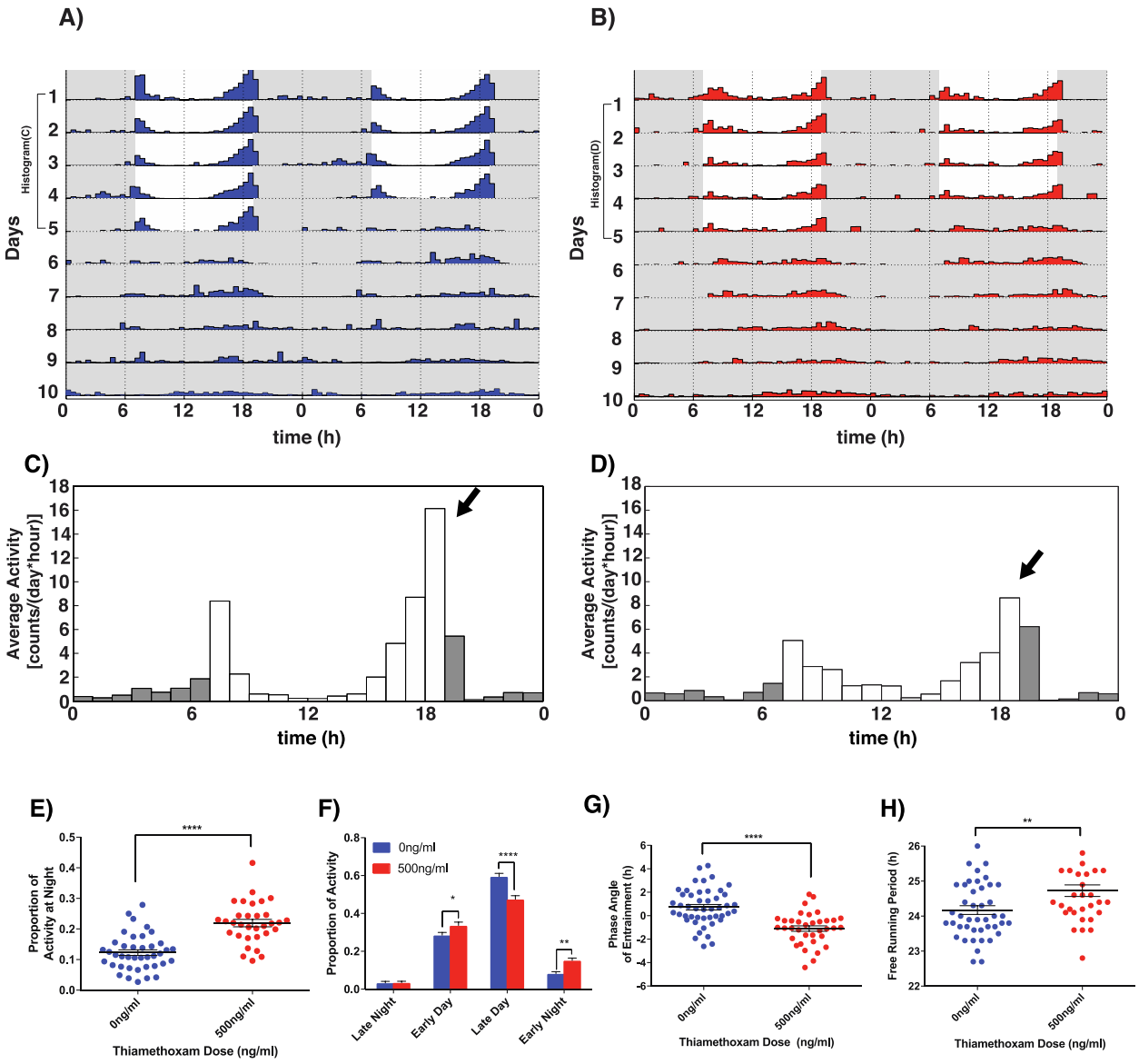

Figure B-4. Effects of Thiamethoxam on Fruit Fly Locomotor Circadian Rhythms. A-B, population average actograms showing activity in LD followed by DD. C-D the matched LD average activity profile histograms for control flies (C) and flies dosed with 500 ng/mL thiamethoxam (D). Arrows point to difference in activity near light offset. E-H, proportion of total activity occurring within the dark phase of the LD cycle (E), average activity profiles of flies binned into 6 hour epochs (F), phase angle of entrainment (G), free-running period (H). Averages shown represent median with error bars showing standard error of the mean. * indicates $p < 0.05$, ** $p < 0.01$, **** $p < 0.0001$.

a non-photosensitive type 2 *cryptochrome*[180] and therefore presumably rely solely on neural signals from photoreceptors for environmental light entrainment.

How might thiamethoxam-induced changes impact honey bee colonies that exist as eusocial “superorganisms”, in which multiple castes perform different functions? Forager bees that are directly exposed to ambient light cycles and neonicotinoids are likely to be more affected than nurse bees that exist within the dark hive, and provide brood care across all times of day[181]. However, nurse bees have functional circadian clocks revealed upon removal from the constant hive environment[182,183], and might also be subject to circadian disruption when exposed to neonicotinoids in hive pollen and honey stores[172]. In addition, the dominant signal for synchronization of nurse bee clocks are social cues from foragers[184], suggesting that the circadian disruption we have observed in foragers would be propagated throughout the hive. Finally, both contaminated hive food stores and altered social entrainment signals may affect the development of circadian clock function, the onset of which occurs within 48 hours of emergence and requires exposure to the hive environment[185].

In summary, chronic ingestion of sub-lethal doses of the neonicotinoid thiamethoxam perturbs both honey bee and *Drosophila* circadian clocks, likely via persistent stimulation of cholinergic light inputs to clock neurons. Such circadian disruption in bees, in which endogenous circadian rhythms are misaligned with local light cycles, will have detrimental impacts on behavior, physiology and immunity at multiple levels, much like jet-lag and shiftwork in humans[186]. In addition to sun-compass orientation, learning and memory is clock regulated[187], including time memory for temporally restricted food sources[188]. Therefore, neonicotinoid-induced clock disruption likely has deleterious effects on memory-dependent homing[167] and foraging efficiency[153]. Circadian disruption also decreases immunity and increase disease vulnerability[156]. Since the circadian system integrates behavior, metabolism and immunity with local time, clock disruption may represent a common cause for multiple facets of Colony Collapse Disorder.

Methods

Honey bee experiments

Honey bee experiments at Vanderbilt University were performed using commercially-obtained honey bees of the Italian sub-species (*Apis mellifera* ligustica L., Kelly Beekeeping, Clarkson, KY). Foragers were caught outside the hive entrance upon their return from foraging trips, confirmed by the presence of pollen on their hind legs. Foragers were individually housed in plastic tubes containing either dosed bee candy (ground white cane sugar and honey) containing a specified amount of thiamethoxam or control bee candy with no pesticide. Tubes were loaded into Locomotor Activity Monitors (LAMs, Trikinetics) and housed in an environmental room with a controlled LD 12:12 (12 h light alternating with 12 h dark) light:dark cycle, constant temperature of 25˚C. A filter paper wick supplied water from a reservoir to each tube. Data recording (infrared beam interruptions) began immediately after loading the monitors, and all data beginning with the first full day in LD were used for LD analysis. For DD analysis, bees were kept in LD for a specified number of days before the lights were turned off.

Experiments examining the effects of light intensity under constant light were performed in at the University of Puerto Rico Río Piedras using the local honey bee 39. Foragers were caught at the entrance of the hive and individually placed in LAMs. Circadian rhythms of locomotor activity were measured at either 0, 150 or 2600 lux of constant light and a constant temperature of 25˚C. The thiamethoxam LL experiment was performed in Vanderbilt University using Italian honey bee foragers. Bees were kept under dim constant light (~60 lux) L, with a constant temperature of 25˚C and provided bee candy with either a specific dose of thiamethoxam or vehicle and water ad libitum.

Drosophila experiments

All experiments were performed with male Drosophila melanogaster (strain Oregon-R). Flies were knocked out with CO2 and gently brushed into individual glass tubes. Each end of the tube was sealed with a 200-uL pipette tip. For each tube, one of these tips contained Drosophila food (sugar and agar), either dosed with a specified dose of thiamethoxam or control food containing no pesticide. Tubes were placed into Drosophila Activity Monitors (DAMs, Trikinetics) and each monitor was housed in an individual light/dark box with a LD 12:12 cycle matching their previous environmental chamber. Data recording began immediately after loading the monitors, and all data beginning with the first full day in LD was used for LD analysis. For DD analysis, flies were kept in LD for a specified number of days before the lights were turned off permanently.

Behavioral metrics

The proportion of activity occurring in the dark was calculated by dividing the number of infrared beam breaks recorded throughout the dark phase of a particular day by the number of beam breaks recorded throughout both the light and dark phases of that day. For each individual fly or bee, all days were then averaged and these values grouped together by treatment. Flies and bees were included in this analysis only if they survived throughout the entire LD portion of the experiment. Specific criteria for survival is detailed below.

Period (tau) was calculated using chi square periodogram provided by ClockLab (Actimetrics) in flies and using linear fit to computer-assisted identified onsets in honey bees. Bees or flies outside of 1.5 standard deviations of the mean were excluded from the analysis.

Phase angle of entrainment (psi) was calculated by fitting a line to the onsets (bees) or offsets (flies) during the DD portion of an experiment and tracing that line back to the last day of LD. The difference between that time and the time of lights-on (bees) or lights-off (flies) is reported. Bees or flies outside of 1.5 standard deviations of the mean were excluded from the analysis.

Calcium imaging

Calcium imaging was performed as previously described 40. Adult male flies (4-7 days post-eclosion) from the cross PDF-Gal4>20XUAS-IVS-GCamp5G 41 were immobilized on 300 mm petri dishes in 3 mL physiological saline containing 128 mM NaCl, 2 mM KCl, 4 mM MgCl2, 35.5 mM sucrose, 5 mM HEPES, and 1.8 mM Ca2+, pH 7.2. Labeled PDF soma were identified under halogen lamp illumination and allowed to rest for 2-3 minutes to photobleach soma prior to baseline recording. Soma were imaged with a 40x water-immersion objective with maximal pinhole aperture on a Zeiss LSM510Meta laser-scanning confocal microscope, using 256 x 256 resolution and a region of interest (ROI) box to achieve ~186 msec scans. Baseline fluorescence was recorded for 250 frames, followed by direct application of given drug, with a main recording for 1000 total frames. To confirm that explants were viable even when no response to treatment/vehicle was observed, 50 µL of 2.5M KCl was applied after 1000 frames to confirm a normal calcium response to high potassium.

Acknowledgements

This study was supported by an NSF Graduate Research Fellowship 0909667 and NIH F31 NS096813-02 to M.C.T., NIH R01 GM117650 and a Vanderbilt Discovery grant to D.G.M. The authors would like to thank Emma Rushton, Chad R. Jackson, Tugrul Giray, M. Wade Calcutt, R. Lane Coffee, and Heinrich J. Matthies for discussions, and Terry Jo Bichell and David Bichell for beekeeping.

Author contributions:

M.C.T. and D.G.M. conceived of the project. M.A.G.G. and M.C.T. performed pesticide/honey bee behavioral experiments. M.A.G.G. performed honey bee LL light intensity experiments. C.A.D, M.C.T., and M.A.G.G., performed *Drosophila* Ca^{2+} imaging experiments. M.C.T.

performed *Drosophila* behavioral experiments. M.C.T, M.A.G.G., C.A.D., D.M., and D.G.M. designed experiments. D.G.M., M.C.T., M.A.G.G., and K.B. wrote the paper. J.A.-R., K.B., and D.M. provided editing, comments, and experimental guidance.

Supplemental figures and tables

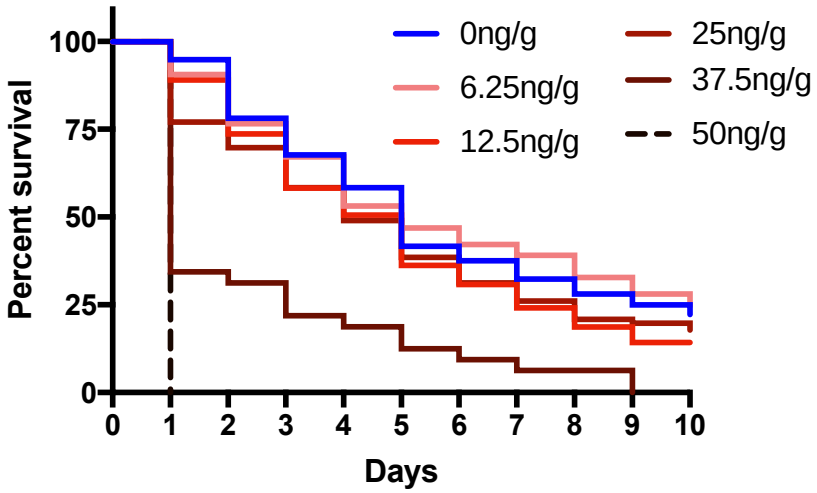

Figure B-S1. Honey Bee Survival Analysis. Survival curves showing the survival of honey bees fed bee candy containing 0- (blue), 6.25- (light red), 12.5- (red), 25-ng/g (dark red), 37.5 (brown), or 50 ng/g (dashed) thiamethoxam.

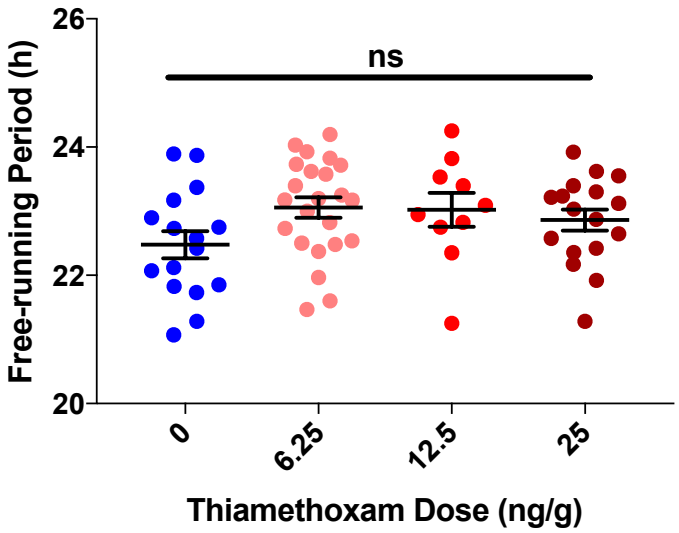

Figure B-S2. Free-Running Period of Honey Bees in DD Alone. Free-running period in honey bees fed bee candy with 0- (blue), 6.25- (light red), 12.5- (red), or 25-ng/g (dark red) thiamethoxam in DD alone.

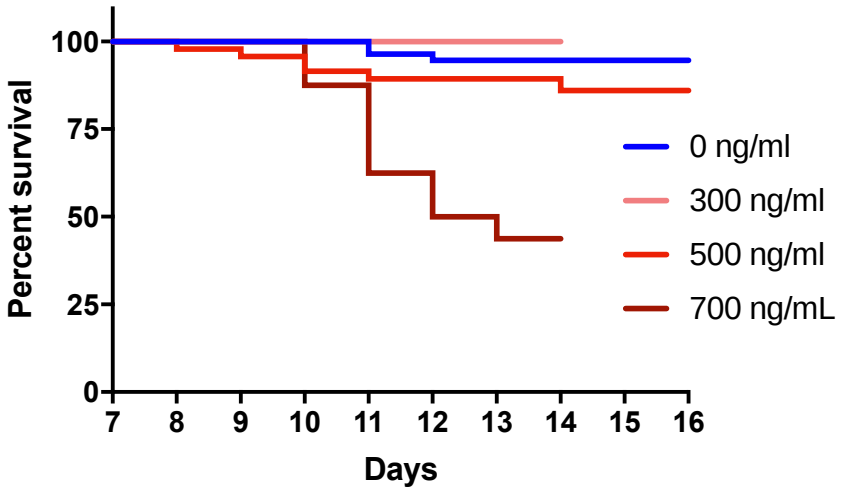

Figure B-S3. Fruit Fly Survival Analysis. Survival curves showing the survival of fruit flies fed fly food with 0- (blue), 300- (light red), 500- (red), or 700-ng/mL (dark red) thiamethoxam.

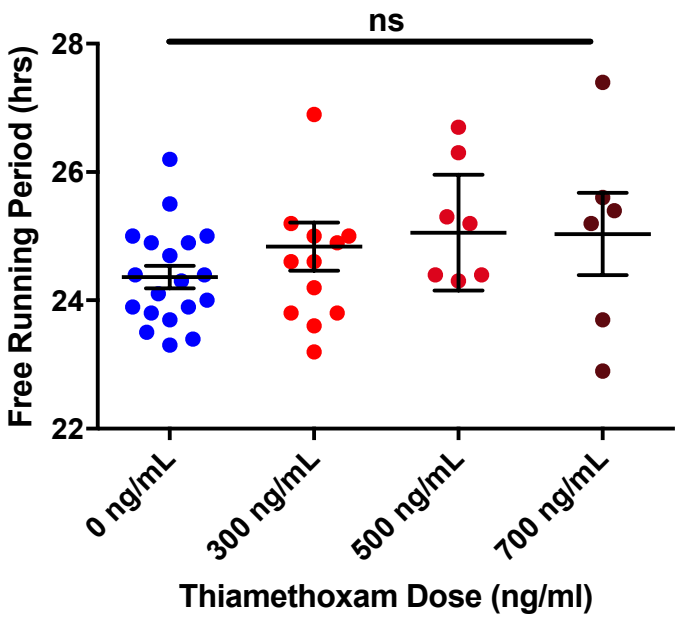

Figure B-S4. Dose Response for Thiamethoxam on Free Running Period in Fruit Flies. Free-running period in fruit flies fed fly food with 0- (blue), 300- (light red), 500- (red), or 700-ng/mL (dark red) thiamethoxam.

EXPERIMENT	FIGURE	DOSE (NG/G)	MEAN ± SEM	STATISTICAL TEST	*P* VALUE
PROPORTION OF ACTIVITY IN THE DARK	1E	0	0.1351±0.02	Kruskal-Wallis ANOVA with Dunn's Multiple Comparisons Test (0- vs. 25-ng/g) and test for Linear Trend*	0.0039 (ANOVA) 0.0041 (MC) 0.0001 (Linear Trend*)
		6.25	0.1444±0.01		
		12.5	0.1968±0.02		
		25	0.2024±0.02		
6-HOUR EPOCH ACTIVITY PROFILE	1F	[See Table 1B]		Repeated Measures Two-Way ANOVA with Dunnett's Multiple Comparisons Test (0- vs. 25-ng/g)	0.0268 (interaction) <0.0001 (time) <0.0001 (dose) 0.0094 (Late Day MC) 0.0318 (Early Night MC)
PHASE ANGLE OF ENTRAINMENT (PSI)	1G	0	-5.538±0.69	One-Way ANOVA with Sidak's Multiple Comparisons Test (0- vs. 25-ng/g) and Test for Linear Trend	0.1204 (ANOVA) 0.0186 (MC) 0.0187 (Linear Trend)
		6.25	-4.868±0.65		
		12.5	-4.403±0.62		
		25	-3.247±0.70		

FREE-RUNNING PERIOD (TAU)	1H	0	22.17±0.23	One-Way ANOVA with Sidak's Multiple Comparisons Test (0- vs. 25-ng/g) and Test for Linear Trend	0.0150 (ANOVA) 0.0016 (MC) 0.0051 (Linear Trend)
		6.25	22.74±0.29		
		12.5	22.51±0.31		
		25	23.38±0.26		
	S2	0	22.48±0.21	One-Way ANOVA with Test for Linear Trend	0.1295 (ANOVA) 0.1972 (Linear Trend)
		6.25	23.06±0.16		
		12.5	23.02±0.26		
		25	22.86±0.17		

*Kruskal-Wallis ANOVA was used for main analysis of variance. The post-hoc test for Linear Trend was performed after running an ordinary One-Way ANOVA (p = 0.0009).

Table B-S1A: Mean ± SEM for all values reported in the Figure B-1, with indicated statistical tests and p values.

	0	**6.25**	**12.5**	**25**
LATE NIGHT	0.025±0.006	0.038±0.008	0.028±0.005	0.038±0.007
EARLY DAY	0.331±0.014	0.367±0.018	0.327±0.015	0.326±0.013
LATE DAY	0.542±0.016	0.514±0.016	0.503±0.016	0.489±0.018
EARLY NIGHT	0.102±0.009	0.108±0.012	0.142±0.013	0.147±0.014

Table B-S1B. Mean ± SEM values for the 6-hour Epoch activity profile shown in Figure B-1F.

EXPERIMENT	FIGURE	DOSE (NG/G)	MEAN ± SEM	STATISTICAL TEST	*P* VALUE
PROPORTION OF ACTIVITY IN THE DARK	4E	0	0.1324±0.01	Unpaired t-test with Welsh's correction	0.0002
		500	0.2324±0.02		
PHASE ANGLE OF ENTRAINMENT (PSI)	4G	0	1.44±0.27	Mann-Whitney U-Test	<0.0001
		500	-0.67±0.27		
FREE-RUNNING PERIOD (TAU)	4H	0	24.03±17	Unpaired t-test with Welsh's correction	0.0291
		500	24.59±0.18		
	S4	0	24.36±0.17	Kruskal-Wallis ANOVA	0.4741 (ANOVA)
		300	24.84±0.38		
		500	25.05±0.90		
		700	23.5±1.6		

Table B-S2. Mean ± SEM for all values reported in the Figure B-4, with indicated statistical tests and *p* values.

References

1. Johnson, C. H., Golden, S. S. & Kondo, T. Adaptive significance of circadian programs in cyanobacteria. *Trends in Microbiology* (1998). doi:10.1016/S0966-842X(98)01356-0

2. DeCoursey, P. J., Walker, J. K. & Smith, S. a. A circadian pacemaker in free-living chipmunks: essential for survival? *J. Comp. Physiol. A.* **186,** 169–180 (2000).

3. Ananyev, G. M., Kim, Y.-I., Dismukes, G. C., Vinyard, D. J. & Golden, S. S. Oxidized quinones signal onset of darkness directly to the cyanobacterial circadian oscillator. *Proc. Natl. Acad. Sci.* (2012). doi:10.1073/pnas.1216401109

4. Katayama, M., Kondo, T., Xiong, J. & Golden, S. S. ldpA encodes an iron-sulfur protein involved in light-dependent modulation of the circadian period in the cyanobacterium Synechococcus elongatus PCC 7942. *J. Bacteriol.* **185,** 1415–22 (2003).

5. Pattanayak, G. & Rust, M. J. The cyanobacterial clock and metabolism. *Current Opinion in Microbiology* (2014). doi:10.1016/j.mib.2014.02.010

6. Emery, P., So, W. V., Kaneko, M., Hall, J. C. & Rosbash, M. Cry, a Drosophila clock and light-regulated cryptochrome, is a major contributor to circadian rhythm resetting and photosensitivity. *Cell* (1998). doi:10.1016/S0092-8674(00)81637-2

7. Emery, P. *et al.* Drosophila CRY is a deep brain circadian photoreceptor. *Neuron* (2000). doi:10.1016/S0896-6273(00)81181-2

8. Somers, D. E., Devlin, P. F. & Kay, S. A. Phytochromes and cryptochromes in the entrainment of the Arabidopsis circadian clock. *Science (80-.).* (1998). doi:10.1126/science.282.5393.1488

9. Pittendrigh, C. S. & Minis, D. H. The Entrainment of Circadian Oscillations by Light and Their Role as Photoperiodic Clocks. *Am. Nat.* **98,** 261–294 (1964).

10. Chandi~ashekai~ai~, M. ~ & Chandrashekaran, M. K. Studies on phase-shifts in endogenous rhythms - I. Effects of light pulses on the eclosion rhythms in Drosophila pseudoobscura. *Z. Vgl. Physiol.* **56,** 154–162 (1967).

11. Tackenberg, M. C., Johnson, C. H., Page, T. L. & Daan, S. Revealing Oft-cited but Unpublished Papers of Colin Pittendrigh and Coworkers. *J. Biol. Rhythms* **32,** 291–294 (2017).

12. Ralph, M., Foster, R., Davis, F. & Menaker, M. Transplanted suprachiasmatic nucleus determines circadian period. *Science* **247,** 975–978 (1990).

13. Rusak, B. & Boulos, Z. PATHWAYS FOR PHOTIC ENTRAINMENT OF MAMMALIAN CIRCADIAN RHYTHMS. *Photochem. Photobiol.* (1981). doi:10.1111/j.1751-1097.1981.tb08996.x

14. Schwartz, W., Gainer, H., Davis, F. & Menaker, M. Suprachiasmatic nucleus: use of 14C-labeled deoxyglucose uptake as a functional marker. *Science (80-.).* **197,** 1089–1091 (1977).

15. Stephan, F. K. & Zucker, I. Circadian Rhythms in Drinking Behavior and Locomotor

Activity of Rats Are Eliminated by Hypothalamic Lesions (suprachiasmatic and medial preoptic nuclei/retino-hypothalamic projection). *Proc.Natl.Acad.Sci.* (1972).

16. Green, D. J. & Gillette, R. Circadian rhythm of firing rate recorded from single cells in the rat suprachiasmatic brain slice. *Brain Res.* (1982). doi:10.1016/0006-8993(82)90361-4

17. Groos, G. & Hendriks, J. Circadian rhythms in electrical discharge of rat suprachiasmatic neurones recorded in vitro. *Neurosci. Lett.* (1982). doi:10.1016/0304-3940(82)90189-6

18. Sawaki, Y., Nihonmatsu, I. & Kawamura, H. Transplantation of the neonatal suprachiasmatic nuclei into rats with complete bilateral suprachiasmatic lesions. *Neurosci. Res.* (1984). doi:10.1016/0168-0102(84)90031-2

19. Abrahamson, E. E. & Moore, R. Y. Suprachiasmatic nucleus in the mouse: retinal innervation, intrinsic organization and efferent projections. *Brain Res* **916,** 172–191 (2001).

20. Nakamura, W., Yamazaki, S., Takasu, N. N., Mishima, K. & Block, G. D. Differential response of Period 1 expression within the suprachiasmatic nucleus. *J Neurosci* **25,** 5481–5487 (2005).

21. Freedman, M. S. *et al.* Regulation of mammalian circadian behavior by non-rod, non-cone, ocular photoreceptors. *Science (80-.).* (1999). doi:10.1126/science.284.5413.502

22. Jiang, G., Provencio, I., De Grip, W. J., Hayes, W. P. & Rollag, M. D. Melanopsin: An opsin in melanophores, brain, and eye. *Proc. Natl. Acad. Sci.* (2002). doi:10.1073/pnas.95.1.340

23. Panda, S. *et al.* Melanopsin (Opn4) requirement for normal light-induced circadian phase shifting. *Science (80-.).* (2002). doi:10.1126/science.1076848

24. Hattar, S., Liao, H. W., Takao, M., Berson, D. M. & Yau, K. W. Melanopsin-containing retinal ganglion cells: Architecture, projections, and intrinsic photosensitivity. *Science (80-.).* (2002). doi:10.1126/science.1069609

25. Ko, C. H. & Takahashi, J. S. Molecular components of the mammalian circadian clock. *Hum. Mol. Genet.* **15 Spec No,** R271-7 (2006).

26. Colwell, C. S. Linking neural activity and molecular oscillations in the SCN. *Nat. Publ. Gr.* **12,** 553–569 (2011).

27. Garner, W. W. & Allard, H. A. Effect of the Relative Length of Day and Night and Other Factors of the Environment on Growth and Reproduction in Plants. *Mon. Weather Rev.* **48,** 415 (1920).

28. Bünning, E. Die endonome Tagesrhythmik als Grundlage der photoperiodischen Reaktion. *Ber. Dtsch. Bot. Ges.* **54,** 590–607 (1936).

29. Bunning, E. Circadian Rhythms and the Time Measurement in Photoperiodism. *Cold Spring Harb. Symp. Quant. Biol.* **25,** 249–256 (1960).

30. Pittendrigh, C. S. Circadian oscillation in Drosophila pseudoobscura pupae-a model for photoperiodic clock. *Zeitschrift fur Pflanzenphysiologie* **54,** 275–307 (1966).

31. Gwinner, E. Circannual rhythms in bird migration: control of temporal patterns and interactions with photoperiod. *Bird Migr. Physiol. Ecophysiol.* 257–268 (1990).

32. Saunders, D. S., STELL, C. G. H., Vafopoulou, X. & Lewis, R. D. Photoperiodism and seasonal cycles of development. *Insect Clocks* **271298,** (2002).

33. Beck, S. D. *Insect photoperiodism*. (Elsevier, 2012).

34. Halle, S. & Stenseth, N. C. *Activity patterns in small mammals: an ecological approach*. **141,** (Springer, 2012).

35. Wehr, T. A. Photoperiodism in humans and other primates: Evidence and implications. *Journal of Biological Rhythms* (2001). doi:10.1177/074873001129002060

36. Rajajärvi, E. *et al.* The effect of seasons and seasonal variation on neuropsychological test performance in patients with bipolar I disorder and their first-degree relatives. *J. Affect. Disord.* **127,** 58–65 (2010).

37. Koorengevel, K. M., Beersma, D. G. M., den Boer, J. a & van den Hoofdakker, R. H. Mood regulation in seasonal affective disorder patients and healthy controls studied in forced desynchrony. *Psychiatry Res.* (2003). doi:http://dx.doi.org/10.1016/S0165-1781(02)00305-0

38. Oh, E. Y. *et al.* Global breast cancer seasonality. *Breast Cancer Res. Treat.* (2010). doi:10.1007/s10549-009-0676-7

39. Pyter, L. M., Reader, B. F. & Nelson, R. J. Short photoperiods impair spatial learning and alter hippocampal dendritic morphology in adult male white-footed mice (Peromyscus leucopus). *J Neurosci* **25,** 4521–4526 (2005).

40. Basnet, S. *et al.* Seasonal variations in mood and behavior associate with common chronic diseases and symptoms in a population-based study. *Psychiatry Res.* (2016). doi:10.1016/j.psychres.2016.02.023

41. Meyer, C. *et al.* Seasonality in human cognitive brain responses. *PNAS Proc. Natl. Acad. Sci. United States Am.* **113,** 3066–3071 (2016).

42. Mouritsen, H. & Ritz, T. Magnetoreception and its use in bird navigation. *Curr Opin Neurobiol* **15,** 406–414 (2005).

43. Lindauer, M. Time-compensated sun orientation in bees. *Cold Spring Harb Symp Quant Biol* **25,** 371–377 (1960).

44. Reppert, S. M., Gegear, R. J. & Merlin, C. Navigational mechanisms of migrating monarch butterflies. *Trends Neurosci.* **33,** 399–406 (2010).

45. Hut, R. A., Barnes, B. M. & Daan, S. Body temperature patterns before, during, and after semi-natural hibernation in the European ground squirrel. *J. Comp. Physiol. B Biochem. Syst. Environ. Physiol.* **172,** 47–58 (2002).

46. Ruby, N. F., Ibuka, N., Barnes, B. M. & Zucker, I. Suprachiasmatic nuclei influence torpor and circadian temperature rhythms in hamsters. *Am J Physiol* **257,** R210-5 (1989).

47. Grahn, D. A., Miller, J. D., Houng, V. S. & Heller, H. C. Persistence of circadian rhythmicity in hibernating ground squirrels. *Am. J. Physiol.* **266,** 1251–1258 (1994).

48. Kortner, G. & Geiser, F. The temporal organization of daily torpor and hibernation: Circadian and circannual rhythms. *Chronobiol. Int.* **17,** 103–128 (2000).

49. Dodd, A. N. Plant Circadian Clocks Increase Photosynthesis, Growth, Survival, and

Competitive Advantage. *Science (80-.).* **309,** 630–633 (2005).

50. Dodd, A. N., Belbin, F. E., Frank, A. & Webb, A. A. R. Interactions between circadian clocks and photosynthesis for the temporal and spatial coordination of metabolism. *Front. Plant Sci.* **6,** (2015).

51. Hennessey, T. L. & Field, C. B. Circadian rhythms in photosynthesis. *Plant Physiol.* **96,** 831–836 (1991).

52. Sumova, A., Travnickova, Z., Peters, R., Schwartz, W. J. & Illnerova, H. The rat suprachiasmatic nucleus is a clock for all seasons. *Proc Natl Acad Sci U S A* **92,** 7754–8 (1995).

53. Sumová, A., Trávníčková, Z. & Illnerová, H. Memory on long but not on short days is stored in the rat suprachiasmatic nucleus. *Neurosci. Lett.* **200,** 191–194 (1995).

54. Schwartz, W. J., de la Iglesia, H. O., Zlomanczuk, P. & Illnerova, H. Encoding le quattro stagioni within the mammalian brain: photoperiodic orchestration through the suprachiasmatic nucleus. *J Biol Rhythm.* **16,** 302–311 (2001).

55. Mrugala, M., Zlomanczuk, P., Jagota, A. & Schwartz, W. J. Rhythmic multiunit neural activity in slices of hamster suprachiasmatic nucleus reflect prior photoperiod. *Am J Physiol Regul Integr Comp Physiol* **278,** R987-94 (2000).

56. Takahashi, J. S., Hong, H. K., Ko, C. H. & McDearmon, E. L. The genetics of mammalian circadian order and disorder: implications for physiology and disease. *Nat Rev Genet* **9,** 764–775 (2008).

57. Quintero, J. E., Kuhlman, S. J. & McMahon, D. G. The biological clock nucleus: a multiphasic oscillator network regulated by light. *J. Neurosci.* **23,** 8070–6 (2003).

58. Okamura, H. Integration of mammalian circadian clock signals: from molecule to behavior. *J Endocrinol* **177,** 3–6 (2003).

59. Schaap, J., Pennartz, C. M. & Meijer, J. H. Electrophysiology of the circadian pacemaker in mammals. *Chronobiol Int* **20,** 171–188 (2003).

60. Groos, G., Mason, R. & Meijer, J. Electrical and pharmacological properties of the suprachiasmatic nuclei. *Fed Proc* **42,** 2790–2795 (1983).

61. Kuhlman, S. J., Silver, R., Le Sauter, J., Bult-Ito, A. & McMahon, D. G. *Phase resetting light pulses induce Per1 and persistent spike activity in a subpopulation of biological clock neurons*. *J Neurosci* **23,** 1441–1450 (2003).

62. Miyake, S. *et al.* Phase-dependent responses of Per1 and Per2 genes to a light-stimulus in the suprachiasmatic nucleus of the rat. *Neurosci Lett* **294,** 41–44 (2000).

63. Messager, S., Hazlerigg, D. G., Mercer, J. G. & Morgan, P. J. Photoperiod differentially regulates the expression of Per1 and ICER in the pars tuberalis and the suprachiasmatic nucleus of the Siberian hamster. *Eur J Neurosci* **12,** 2865–2870 (2000).

64. Steinlechner, S. *et al.* Robust circadian rhythmicity of Per1 and Per2 mutant mice in constant light, and dynamics of Per1 and Per2 gene expression under long and short photoperiods. *J Biol Rhythm.* **17,** 202–209 (2002).

65. Lincoln, G., Messager, S., Andersson, H. & Hazlerigg, D. Temporal expression of seven clock genes in the suprachiasmatic nucleus and the pars tuberalis of the sheep: evidence

for an internal coincidence timer. *Proc Natl Acad Sci U S A* **99,** 13890–13895 (2002).

66. Sumova, A., Bendova, Z., Sladek, M., Kovacikova, Z. & Illnerova, H. Seasonal molecular timekeeping within the rat circadian clock. *Physiol Res* **53 Suppl 1,** S167-76 (2004).

67. Sumova, A., Jac, M., Sladek, M., Sauman, I. & Illnerova, H. Clock gene daily profiles and their phase relationship in the rat suprachiasmatic nucleus are affected by photoperiod. *J Biol Rhythm.* **18,** 134–144 (2003).

68. Schaap, J. *et al.* Heterogeneity of rhythmic suprachiasmatic nucleus neurons: Implications for circadian waveform and photoperiodic encoding. *Proc. Natl. Acad. Sci. U. S. A.* **100,** 15994–9 (2003).

69. VanderLeest, H. T. *et al.* Seasonal Encoding by the Circadian Pacemaker of the SCN. *Curr. Biol.* **17,** 468–473 (2007).

70. Inagaki, N., Honma, S., Ono, D., Tanahashi, Y. & Honma, K. Separate oscillating cell groups in mouse suprachiasmatic nucleus couple photoperiodically to the onset and end of daily activity. *Proc Natl Acad Sci USA* **104,** 7664–7669 (2007).

71. Ciarleglio, C. M., Axley, J. C., Strauss, B. R., Gamble, K. L. & McMahon, D. G. Perinatal photoperiod imprints the circadian clock. *Nat Neurosci* **14,** 25–27 (2011).

72. Ohta, H., Yamazaki, S. & McMahon, D. G. Constant light desynchronizes mammalian clock neurons. *Nat. Neurosci.* **8,** 267–9 (2005).

73. Kováčiková, Z. *et al.* Ontogenesis of photoperiodic entrainment of the molecular core clockwork in the rat suprachiasmatic nucleus. *Brain Res.* **1064,** 83–89 (2005).

74. Cambras, T. & Díez-Noguera, A. Evolution of rat motor activity circadian rhythm under three different light patterns. *Physiol. Behav.* **49,** 63–68 (1991).

75. Cambras, T., Canal, M. M., Torres, A., Vilaplana, J. & Diez-Noguera, A. Manifestation of circadian rhythm under constant light depends on lighting conditions during lactation. *Am J Physiol* **272,** R1039-46 (1997).

76. Canal-Corretger, M. M., Cambras, T., Vilaplana, J. & Díez-Noguera, a. Bright light during lactation alters the functioning of the circadian system of adult rats. *Am. J. Physiol. Regul. Integr. Comp. Physiol.* **278,** R201–R208 (2000).

77. Canal-Corretger, M. M., Vilaplana, J., Cambras, T. & Díez-Noguera, a. Functioning of the rat circadian system is modified by light applied in critical postnatal days. *Am. J. Physiol. Regul. Integr. Comp. Physiol.* **280,** R1023–R1030 (2001).

78. Farajnia, S., Meijer, J. H. & Michel, S. Photoperiod Modulates Fast Delayed Rectifier Potassium Currents in the Mammalian Circadian Clock. *ASN Neuro* **8,** 175909141667077 (2016).

79. Yamaguchi, S. *et al.* Synchronization of cellular clocks in the suprachiasmatic nucleus. *Science (80-.).* **302,** 1408–1412 (2003).

80. Shigeyoshi, Y. *et al.* Light-induced resetting of a mammalian circadian clock is associated with rapid induction of the mPer1 transcript. *Cell* **91,** 1043–1053 (1997).

81. Reddy, a B., Field, M. D., Maywood, E. S. & Hastings, M. H. Differential resynchronisation of circadian clock gene expression within the suprachiasmatic nuclei of mice subjected to experimental jet lag. *J. Neurosci.* **22,** 7326–30 (2002).

82. Jac, M., Sumova, A. & Illnerova, H. c-Fos rhythm in subdivisions of the rat suprachiasmatic nucleus under artificial and natural photoperiods. *Am J Physiol Regul Integr Comp Physiol* **279,** R2270-6 (2000).

83. Brown, T. M. & Piggins, H. D. Spatiotemporal Heterogeneity in the Electrical Activity of Suprachiasmatic Nuclei Neurons and their Response to Photoperiod. *J. Biol. Rhythms* **24,** 44–54 (2009).

84. Jac, M., Kiss, A., Sumova, A., Illnerova, H. & Jezova, D. Daily profiles of arginine vasopressin mRNA in the suprachiasmatic, supraoptic and paraventricular nuclei of the rat hypothalamus under various photoperiods. *Brain Res* **887,** 472–476 (2000).

85. Evans, J. A., Leise, T. L., Castanon-Cervantes, O. & Davidson, A. J. Intrinsic regulation of spatiotemporal organization within the suprachiasmatic nucleus. *PLoS One* **6,** e15869 (2011).

86. Naito, E., Watanabe, T., Tei, H., Yoshimura, T. & Ebihara, S. Reorganization of the Suprachiasmatic Nucleus Coding for Day Length. *J. Biol. Rhythms* **23,** 140–149 (2008).

87. Hazlerigg, D. G., Ebling, F. J. P. & Johnston, J. D. Photoperiod differentially regulates gene expression rhythms in the rostral and caudal SCN. *Current Biology* **15,** (2005).

88. Sosniyenko, S., Hut, R. A., Daan, S. & Sumová, A. Influence of photoperiod duration and light-dark transitions on entrainment of Per1 and Per2 gene and protein expression in subdivisions of the mouse suprachiasmatic nucleus. *Eur. J. Neurosci.* **30,** 1802–1814 (2009).

89. Buijink, M. R. *et al.* Evidence for weakened intercellular coupling in the mammalian circadian clock under long photoperiod. *PLoS One* **11,** (2016).

90. Pittendrigh, C. S. & Daan, S. A functional analysis of circadian pacemakers in nocturnal rodents (V). *J. Comp. Physiol. ? A* **106,** 333–355 (1976).

91. Yoshikawa, T. *et al.* Localization of photoperiod responsive circadian oscillators in the mouse suprachiasmatic nucleus. *Sci. Rep.* **7,** (2017).

92. Evans, J. A., Leise, T. L., Castanon-Cervantes, O. & Davidson, A. J. Dynamic interactions mediated by nonredundant signaling mechanisms couple circadian clock neurons. *Neuron* **80,** 973–983 (2013).

93. Albus, H., Vansteensel, M. J., Michel, S., Block, G. D. & Meijer, J. H. *A GABAergic mechanism is necessary for coupling dissociable ventral and dorsal regional oscillators within the circadian clock*. *Curr Biol* **15,** 886–893 (2005).

94. Farajnia, S., van Westering, T. L. E., Meijer, J. H. & Michel, S. Seasonal induction of GABAergic excitation in the central mammalian clock. *Proc. Natl. Acad. Sci.* **111,** 9627–9632 (2014).

95. Myung, J. *et al.* GABA-mediated repulsive coupling between circadian clock neurons in the SCN encodes seasonal time. *Proc. Natl. Acad. Sci.* **112,** E3920–E3929 (2015).

96. Lucassen, E. A. *et al.* Role of vasoactive intestinal peptide in seasonal encoding by the suprachiasmatic nucleus clock. *Eur. J. Neurosci.* **35,** 1466–1474 (2012).

97. Goldman, B. D. Mammalian Photoperiodic System: Formal Properties and Neuroendocrine Mechanisms of Photoperiodic Time Measurement. *J. Biol. Rhythms* **16,**

283–301 (2001).

98. Goldman, B. D. & Darrow, J. M. The pineal gland and mammalian photoperiodism. *Neuroendocrinology* **37,** 386–396 (1983).

99. Elliott, J. A. & Goldman, B. D. in *Neuroendocrinology of reproduction* 377–423 (Springer, 1981).

100. Bartness, T. J., Goldman, B. D. & Bittman, E. L. SCN lesions block responses to systemic melatonin infusions in Siberian hamsters. *Am J Physiol* **260,** R102-12 (1991).

101. Goldman, B. D., Darrow, J. M. & Yogev, L. Effects of timed melatonin infusions on reproductive development in the Djungarian hamster (Phodopus sungorus). *Endocrinology* **114,** 2074–2083 (1984).

102. Goldman, B. D. Parameters of the circadian rhythm of pineal melatonin secretion affecting reproductive responses in Siberian hamsters. *Steroids* **56,** 218–225 (1991).

103. Pickard, G. E. & Turek, F. W. The hypothalamic paraventricular nucleus mediates the photoperiodic control of reproduction but not the effects of light on the circadian rhythm of activity. *Neurosci Lett* **43,** 67–72 (1983).

104. Bittman, E. L., Bartness, T. J., Goldman, B. D. & DeVries, G. J. Suprachiasmatic and paraventricular control of photoperiodism in Siberian hamsters. *Am J Physiol* **260,** R90-101 (1991).

105. Bartness, T. J. & Wade, G. N. Photoperiodic control of body weight and energy metabolism in syrian hamsters (mesocricetus auratus): Role of pineal gland, melatonin, gonads, and diet. *Endocrinology* **114,** 492–498 (1984).

106. Mercer, J. G., Moar, K. M., Ross, A. W., Hoggard, N. & Morgan, P. J. Photoperiod regulates arcuate nucleus POMC, AGRP, and leptin receptor mRNA in Siberian hamster hypothalamus. *Am. J. Physiol. Regul. Integr. Comp. Physiol.* **278,** R271-81 (2000).

107. Green, N. H., Jackson, C. R., Iwamoto, H., Tackenberg, M. C. & McMahon, D. G. Photoperiod programs dorsal raphe serotonergic neurons and affective behaviors. *Curr Biol* **25,** 1389–1394 (2015).

108. Uchiwa, T., Takai, Y., Tashiro, A., Furuse, M. & Yasuo, S. Exposure of C57BL/6J mice to long photoperiod during early life stages increases body weight and alters plasma metabolomic profiles in adulthood. *Physiol. Rep.* **4,** e12974 (2016).

109. Otsuka, T. *et al.* Photoperiod regulates corticosterone rhythms by altered adrenal sensitivity via melatonin-independent mechanisms in fischer 344 rats and C57BL/6J mice. *PLoS One* **7,** (2012).

110. Sosniyenko, S., Parkanová, D., Illnerová, H., Sládek, M. & Sumová, A. Different mechanisms of adjustment to a change of the photoperiod in the suprachiasmatic and liver circadian clocks. *Am. J. Physiol. Regul. Integr. Comp. Physiol.* **298,** R959-71 (2010).

111. Jackson, C. R., Capozzi, M., Dai, H. & McMahon, D. G. Circadian perinatal photoperiod has enduring effects on retinal dopamine and visual function. *J. Neurosci.* **34,** 4627–4633 (2014).

112. Ohta, H., Mitchell, A. C. & McMahon, D. G. Constant light disrupts the developing mouse biological clock. *Pediatr Res* **60,** 304–308 (2006).

113. Boland, M. R., Shahn, Z., Madigan, D., Hripcsak, G. & Tatonetti, N. P. Birth month affects lifetime disease risk: a phenome-wide method. *J. Am. Med. Informatics Assoc.* **22,** 1042–1053 (2015).

114. Terman, M. & Terman, J. S. Light therapy for seasonal and nonseasonal depression: efficacy, protocol, safety, and side effects. *CNS Spectr* **10,** 647–63; quiz 672 (2005).

115. Watanabe, S. *et al.* Designing Artificial Environments for Preterm Infants Based on Circadian Studies on Pregnant Uterus. *Front. Endocrinol.* **4,** 113 (2013).

116. Rosenthal, N. E. *et al.* Seasonal Affective Disorder. 74–80 (1984).

117. Daan, S. The Colin S. Pittendrigh Lecture. Colin Pittendrigh, Jürgen Aschoff, and the natural entrainment of circadian systems. *J. Biol. Rhythms* (2000). doi:10.1177/074873040001500301

118. Bartness, T. J., Elliott, J. A. & Goldman, B. D. Control of torpor and body weight patterns by a seasonal timer in Siberian hamsters. *Am. J. Physiol. Integr. Comp. Physiol.* (1989). doi:10.1152/ajpregu.1989.257.1.R142

119. Tackenberg, M. C. & McMahon, D. G. Photoperiodic Programming of the SCN and Its Role in Photoperiodic Output. *Neural Plast.* **2018,** 1–9 (2018).

120. Rosenthal, N. E. & Wehr, T. A. Seasonal Affective Disorders. *Psychiatr. Ann.* **17,** 670–674 (1987).

121. Refinetti, R. Compression and expansion of circadian rhythm in mice under long and short photoperiods. *Integr. Physiol. Behav. Sci.* (2002). doi:10.1007/BF02688824

122. Gu, C., Rohling, J. H. T., Liang, X. & Yang, H. Impact of dispersed coupling strength on the free running periods of circadian rhythms. *Phys. Rev. E* **93,** 032414 (2016).

123. Pittendrigh, C. S. & Daan, S. A functional analysis of circadian pacemakers in nocturnal rodents (IV). *J. Comp. Physiol. A* **106,** 291–331 (1976).

124. Houben, T., Deboer, T., Van Oosterhout, F. & Meijer, J. H. Correlation with behavioral activity and rest implies circadian regulation by scn neuronal activity levels. *J. Biol. Rhythms* (2009). doi:10.1177/0748730409349895

125. An, S., Tsai, C., Ronecker, J., Bayly, A. & Herzog, E. D. Spatiotemporal distribution of vasoactive intestinal polypeptide receptor 2 in mouse suprachiasmatic nucleus. *J. Comp. Neurol.* (2012). doi:10.1002/cne.23078

126. Colwell, C. S. *et al.* Disrupted circadian rhythms in VIP- and PHI-deficient mice. *Am J Physiol Regul Integr Comp Physiol* **285,** R939-49 (2003).

127. Harmar, A. J. *et al.* The VPAC2 receptor is essential for circadian function in the mouse suprachiasmatic nuclei. *Cell* (2002). doi:10.1016/S0092-8674(02)00736-5

128. Aton, S. J., Colwell, C. S., Harmar, A. J., Waschek, J. & Herzog, E. D. Vasoactive intestinal polypeptide mediates circadian rhythmicity and synchrony in mammalian clock neurons. *Nat. Neurosci.* (2005). doi:10.1038/nn1419

129. Ciarleglio, C. M. *et al.* Population encoding by circadian clock neurons organizes circadian behavior. *J. Neurosci.* **29,** 1670–1676 (2009).

130. Jones, J. R., Simon, T., Lones, L. & Herzog, E. D. SCN VIP neurons are essential for

normal light-mediated resetting of the circadian system. *J. Neurosci.* (2018). doi:10.1523/JNEUROSCI.1322-18.2018

131. Jones, J. R., Tackenberg, M. C. & Mcmahon, D. G. Manipulating circadian clock neuron firing rate resets molecular circadian rhythms and behavior. *Nat. Neurosci.* **18,** 373–377 (2015).

132. Hughes, M. E., Hogenesch, J. B. & Kornacker, K. JTK-CYCLE: An efficient nonparametric algorithm for detecting rhythmic components in genome-scale data sets. *J. Biol. Rhythms* (2010). doi:10.1177/0748730410379711

133. Sokolove, P. G. & Bushell, W. N. The chi square periodogram: Its utility for analysis of circadian rhythms. *J. Theor. Biol.* **72,** 131–160 (1978).

134. Refinetti, R., Cornélissen, G. & Halberg, F. Procedures for numerical analysis of circadian rhythms. *Biological Rhythm Research* (2007). doi:10.1080/09291010600903692

135. Dowse, H. B. Maximum entropy spectral analysis for circadian rhythms: theory, history and practice. *J. Circadian Rhythms* **11,** 6 (2013).

136. Leise, T. L. & Harrington, M. E. Wavelet-based time series analysis of Circadian rhythms. *J. Biol. Rhythms* **26,** 454–463 (2011).

137. Dowse, H. B. Analyses for physiological and behavioral rhythmicity. *Methods Enzymol.* **454,** 141–74 (2009).

138. Levine, J. D., Funes, P., Dowse, H. B. & Hall, J. C. Signal analysis of behavioral and molecular cycles. *BMC Neurosci.* **3,** 1 (2002).

139. Leise, T. L. Wavelet analysis of circadian and ultradian behavioral rhythms. *J. Circadian Rhythms* **11,** 5 (2013).

140. Comas, M., Beersma, D. G. M., Spoelstra, K. & Daan, S. Phase and Period Responses of the Circadian System of Mice (Mus musculus) to Light Stimuli of Different Duration. *J. Biol. Rhythms* **21,** 362–372 (2006).

141. Pittendrigh, C. S. & Daan, S. A functional analysis of circadian pacemakers in nocturnal rodents (I). *J. Comp. Physiol. A* **106,** 223–252 (1976).

142. Pittendrigh, C. S. Circadian systems: entrainment. *Handb. Behav. Neurobiol.* **4,** 95–124 (1981).

143. Berens, P. CircStat : A MATLAB Toolbox for Circular Statistics. *J. Stat. Softw.* **31,** (2009).

144. Azzi, A. *et al.* Circadian behavior is light-reprogrammed by plastic DNA methylation. *Nat. Neurosci.* **17,** 377–382 (2014).

145. Fernandez, D. C. *et al.* Light Affects Mood and Learning through Distinct Retina-Brain Pathways. *Cell* (2018). doi:10.1016/j.cell.2018.08.004

146. Hastings, J. W. & Sweeney, B. M. a Persistent Diurnal Rhythm of Luminescence in Gonyaulax Polyedra. *Biol. Bull.* **115,** 440–458 (1958).

147. DeCoursey, P. J. Phase Control of Activity in a Rodent. *Cold Spring Harb. Symp. Quant. Biol.* **25,** 49–55 (1960).

148. Daan, S. The Colin S. Pittendrigh Lecture. Colin Pittendrigh, Jurgen Aschoff, and the

natural entrainment of circadian systems. *J Biol Rhythm.* **15,** 195–207 (2000).

149. Aschoff, J. & Wever, R. Beginn und Ende der täglichen Aktivität freilebender Vögel. *J. für Ornithol.* **103,** 2–27 (1962).

150. Aschoff, J. Comparative Physiology: Diurnal Rhythms. *Annu. Rev. Physiol.* **25,** 581–600 (1963).

151. Chandrashekaran, M. K. Studies on phase-shifts in endogenous rhythms. *Z. Vgl. Physiol.* **56,** 154–162 (1967).

152. Vanengelsdorp, D. *et al.* Colony collapse disorder: a descriptive study. *PLoS One* **4,** e6481 (2009).

153. Feltham, H., Park, K. & Goulson, D. Field realistic doses of pesticide imidacloprid reduce bumblebee pollen foraging efficiency. *Ecotoxicology* **23,** 317–323 (2014).

154. Goulson Elizabeth Nicholls, Cristina Botías, Ellen L. Rotheray, D. Bee declines driven by combined\rstress from parasites, pesticides, and\rlack of flowers. *Science (80-.).* **347,** 1255957 (2015).

155. Moore, D. Honey bee circadian clocks: Behavioral control from individual workers to whole colony rhythms. *J. Insect Physiol.* **47,** 843–857 (2001).

156. Shirasu-Hiza, M. M., Dionne, M. S., Pham, L. N., Ayres, J. S. & Schneider, D. S. Interactions between circadian rhythm and immunity in Drosophila melanogaster. *Curr. Biol.* **17,** R353–R355

157. Lelito, K. R. & Shafer, O. T. Reciprocal cholinergic and GABAergic modulation of the small ventrolateral pacemaker neurons of Drosophila's circadian clock neuron network. *J. Neurophysiol.* **107,** 2096–2108 (2012).

158. Schlichting, M. *et al.* A Neural Network Underlying Circadian Entrainment and Photoperiodic Adjustment of Sleep and Activity in Drosophila. *J. Neurosci.* **36,** 9084–9096 (2016).

159. Forel, A. *Das Sinnesleben der Insekten : eine Sammlung von experimentellen und kritischen Studien ueber Insektenpsychologie*. (Reinhardt, 1910).

160. Beling, I. Über das Zeitgedächtnis der Bienen. *Z. Vgl. Physiol.* **9,** 259–338 (1929).

161. Renner, M. Neue Versuche Über den Zietsinn der Honigbiene. *Z. Vgl. Physiol.* **40,** 85–118 (1957).

162. Renner, M. Über die Haltung von Bienen in geschlossenen, künstlich beleuchteten Räumen. *Naturwissenschaften* **42,** 539–540 (1955).

163. Beier, W. & Lindauer, M. Der Sonnenstand als Zeitgeber für die Biene. *Apidologie* (1970).

164. Cheeseman, J. F. *et al.* General anesthesia alters time perception by phase shifting the circadian clock. *Proc Natl Acad Sci USA* **109,** 7061–7066 (2012).

165. Cheeseman, J. F. *et al.* Way-finding in displaced clock-shifted bees proves bees use a cognitive map. *Proc. Natl. Acad. Sci.* **111,** 8949–8954 (2014).

166. Henry, M. *et al.* A common pesticide decreases foraging success and survival in honey bees. *Science (80-.).* **336,** 348–350 (2012).

167. Fischer, J. *et al.* Neonicotinoids interfere with specific components of navigation in honeybees. *PLoS One* **9,** e91364 (2014).

168. Dupuis, J., Louis, T., Gauthier, M. & Raymond, V. Insights from honeybee (Apis mellifera) and fly (Drosophila melanogaster) nicotinic acetylcholine receptors: from genes to behavioral functions. *Neurosci. Biobehav. Rev.* **36,** 1553–1564 (2012).

169. Giannoni-Guzmán, M. A. *et al.* Measuring individual locomotor rhythms in honey bees, paper wasps and other similar-sized insects. *J. Exp. Biol.* **217,** 1307–1315 (2014).

170. Stewart, S. D. *et al.* Potential exposure of pollinators to neonicotinoid insecticides from the use of insecticide seed treatments in the mid-southern United States. *Env. Sci Technol* **48,** 9762–9769 (2014).

171. Botias, C. *et al.* Neonicotinoid Residues in Wildflowers, a Potential Route of Chronic Exposure for Bees. *Env. Sci Technol* **49,** 12731–12740 (2015).

172. Codling, G., Al Naggar, Y., Giesy, J. P. & Robertson, A. J. Concentrations of neonicotinoid insecticides in honey, pollen and honey bees (Apis mellifera L.) in central Saskatchewan, Canada. *Chemosphere* **144,** 2321–2328 (2016).

173. Krupke, C. H., Hunt, G. J., Eitzer, B. D., Andino, G. & Given, K. Multiple routes of pesticide exposure for honey bees living near agricultural fields. *PLoS One* **7,** (2012).

174. Moore, D. & Rankin, M. A. Circadian locomotor rhythms in individual honeybees. *Physiol. Entomol.* **10,** 191–197 (1985).

175. Nauen, R., Ebbinghaus-Kintscher, U., Salgado, V. L. & Kaussmann, M. Thiamethoxam is a neonicotinoid precursor converted to clothianidin in insects and plants. *Pestic. Biochem. Physiol.* **76,** 55–69 (2003).

176. Helfrich-Förster, C. Differential control of morning and evening components in the activity rhythm of Drosophila melanogaster - Sex-specific differences suggest a different quality of activity. *J. Biol. Rhythms* **15,** 135–154 (2000).

177. Engelmann, W. & Mack, J. Different oscillators control the circadian rhythm of eclosion and activity in Drosophila. *J. Comp. Physiol. □ A* **127,** 229–237 (1978).

178. McCarthy, E. V *et al.* Synchronized bilateral synaptic inputs to Drosophila melanogaster neuropeptidergic rest/arousal neurons. *J. Neurosci.* **31,** 8181–93 (2011).

179. Stanewsky, R. *et al.* The cryb mutation identifies cryptochrome as a circadian photoreceptor in Drosophila. *Cell* **95,** 681–692 (1998).

180. Rubin, E. B. *et al.* Molecular and phylogenetic analyses reveal mammalian-like clockwork in the honey bee (Apis mellifera) and shed new light on the molecular evolution of the circadian clock. *Genome Res.* **16,** 1352–1365 (2006).

181. Moore, D., Angel, J. E., Cheeseman, I. M., Fahrbach, S. E. & Robinson, G. E. Timekeeping in the honey bee colony: integration of circadian rhythms and division of labor. *Behav Ecol Sociobiol* **43,** 147–160 (1998).

182. Shemesh, Y., Cohen, M. & Bloch, G. Natural plasticity in circadian rhythms is mediated by reorganization in the molecular clockwork in honeybees. *FASEB J.* **21,** 2304–2311 (2007).

183. Shemesh, Y., Eban-Rothschild, A., Cohen, M. & Bloch, G. Molecular Dynamics and

Social Regulation of Context-Dependent Plasticity in the Circadian Clockwork of the Honey Bee. *J. Neurosci.* **30,** 12517–12525 (2010).

184. Fuchikawa, T., Eban-Rothschild, A., Nagari, M., Shemesh, Y. & Bloch, G. Potent social synchronization can override photic entrainment of circadian rhythms. *Nat. Commun.* **7,** 11662 (2016).

185. Eban-Rothschild, A., Shemesh, Y. & Bloch, G. The colony environment, but not direct contact with conspecifics, influences the development of circadian rhythms in honey bees. *J. Biol. Rhythms* **27,** 217–225 (2012).

186. Bedrosian, T. A., Fonken, L. K. & Nelson, R. J. Endocrine Effects of Circadian Disruption. *Annu. Rev. Physiol.* **78,** 109–131 (2016).

187. Lehmann, M., Gustav, D. & Galizia, C. G. The early bee catches the flower - circadian rhythmicity influences learning performance in honey bees, Apis mellifera. *Behav. Ecol. Sociobiol.* **65,** 205–215 (2011).

188. Moore, D., Van Nest, B. N. & Seier, E. Diminishing returns: the influence of experience and environment on time-memory extinction in honey bee foragers. *J Comp Physiol A Neuroethol Sens Neural Behav Physiol* **197,** 641–651 (2011).